Universidade de Aveiro
2021

ANDRÉ FILIPE DIAS LIMA

HIDROGÉIS À BASE DE LISADOS DE PLAQUETAS COMO PLATAFORMAS 3D DE CULTURA DE CÉLULAS PARA REGENERAÇÃO CARDÍACA

PLATELET LYSATES-BASED HYDROGELS AS 3D CELL CULTURE PLATFORMS FOR CARDIAC REGENERATION

Universidade de Aveiro
2021

ANDRÉ FILIPE DIAS LIMA

HIDROGÉIS À BASE DE LISADOS DE PLAQUETAS COMO PLATAFORMAS 3D DE CULTURA DE CÉLULAS PARA REGENERAÇÃO CARDÍACA

Dissertação apresentada à Universidade de Aveiro para cumprimento dos requisitos necessários à obtenção do grau de Mestre em Bioquímica, realizada sob a orientação científica da Doutora Catarina de Almeida Custódio, Investigadora auxiliar do Departamento de Química da Universidade de Aveiro, e do Professor Doutor João Filipe Colardelle da Luz Mano, Professor Catedrático do Departamento de Química da Universidade de Aveiro

The present work was financially supported by the Portuguese Foundation for Science and Technology (FCT) with the project Beat (PTDC/BTM-MAT/30869/2017), and by the European Research Council (ERC) for project ATLAS (ERC-2014-ADG-669858). The work was also partially supported by the European Union (EU) Horizon 2020 for the project InterLynk, Grant agreement: H2020-NMBP-TR-IND-2020, Project ID: 953169.

This work was developed within the scope of the project CICECO-Aveiro Institute of Materials, FCT Ref. UID/CTM/50011/2019, financed by national funds through the FCT/MCTES.

Aos meus pais

o júri

presidente	Prof. Doutor Brian James Goodfellow professor auxiliar da Universidade de Aveiro
vogal - orientador	Doutora Catarina de Almeida Custódio investigadora auxiliar da Universidade de Aveiro
vogal - arguente principal	Doutor José Eduardo Marques Bragança professor associado com agregação da Universidade do Algarve

agradecimentos

Primeiramente, gostaria de agradecer ao Prof. Dr. João Mano pela oportunidade de desenvolver este projeto no COMPASS Research Group. Obrigado pela orientação científica prestada ao longo do mesmo.

À Dr. Catarina Custódio, o meu agradecimento pelo acompanhamento e disponibilidade que demonstrou desde o primeiro dia. Obrigado pelo apoio e ajuda que me permitiram ultrapassar as dificuldades encontradas.

Um muito obrigado à Cátia Monteiro por toda orientação e ajuda desde o início, sem a qual não seria possível a realização deste trabalho. Obrigado pela paciência e por todas as ideias que me permitiram melhorar e aperfeiçoar o meu trabalho.

Por fim, agradecer a todos os membros do COMPASS Research Group por me acolherem tão bem e por todo o companheirismo e amizade prestados ao longo deste projeto que foram um incentivo para o desenvolvimento deste.

palavras-chave

Enfarte do miocárdio, regeneração cardíaca, plataformas de cultura 3D, lisado de plaquetas, plataformas de cultura 3D, esponjas liofilizados, pensos cardíacos com esferóides

resumo

As doenças cardiovasculares são a principal causa de morte no mundo com o enfarte do miocárdio conduzindo à insuficiência cardíaca e morte das vítimas. Uma vez que os tratamentos atuais não restauram a função do tecido cardíaco, a engenharia de tecidos visa criar pensos cardíacos para promover uma melhor regeneração cardíaca. Neste estudo, abordagens acelulares e celulares foram escolhidas para produzir adesivos cardíacos. Na abordagem acelular, lisados de plaquetas modificados com grupos metacrílicos (PLMA) foram usados para fabricar hidrogéis reidratados formados por liofilização que foram avaliados para aplicação como pensos cardíacos e para observar o impacto do processo de liofilização nas propriedades do hidrogel. As propriedades mecânicas dos hidrogéis aumentaram com a liofilização, não apenas em termos de módulo de Young, tensão e deformação finais, mas também em durabilidade. Embora a porosidade da superfície superior não seja diferente para todas as concentrações de PLMA usadas, as esponjas de PLMA mostraram uma alta razão de absorção, que diminui ao longo do tempo devido à libertação de proteína da matriz, um valor condutividade na mesma ordem de grandeza do coração humano e capacidade para serem transportadas em cateteres. Para avaliar estas matrizes como uma plataforma de cultura 3D, células endoteliais de veia umbilical humana (HUVECs) foram cultivadas em hidrogéis de PLMA com a concentração de proteína que melhor desempenho obteve (15% de concentração de PLMA), mostrando, juntamente com os resultados de propriedades físicas, resultados promissores para o uso desses hidrogéis reidratados como adesivos cardíacos para regeneração cardíaca pós-enfarte do miocárdio. Para a abordagem celular, a ideia seria criar um sistema capaz de produzir hidrogéis de PLMA incorporados com os esferoides de cardiomiócitos numa disposição quadrada e usando poços de tamanho controlado. Para otimizar este sistema, células MG-63 foram usadas devido à facilidade de formarem esferoides. Para uma caracterização mais física, os hidrogéis de PLMA foram avaliados quanto às propriedades para aplicação biomédica e para o tecido cardíaco mais especificamente. As propriedades mecânicas dos hidrogéis mostraram um aumento no módulo de elasticidade com o aumento da concentração de PLMA presente nos hidrogéis e os testes de conteúdo de água demonstraram que todos os hidrogéis usados apresentavam um alto teor de água. Usando a células MG-63, depois de 7 dias o sistema apresentava a formação de alguns esferoides, embora o sistema não tenha funcionado de forma correta. Os resultados obtidos demonstram que os hidrogéis da PLMA têm boas características para aplicação biomédica e cardíaca e que a otimização deste sistema pode ser capaz de formar esferóides de cardiomiócitos. Em conclusão, os resultados atuais sugerem que ambas as abordagens podem atuar como pensos cardíacos devido às características do hidrogéis e compatibilidade celular para este fim, apesar de ser ainda possível obter resultados interessantes para suportar esta afirmação.

keywords

Myocardial infarction, cardiac regeneration, cardiac patches, 3D culture platforms, platelet lysates, freeze dried scaffolds, cardiac patches with spheroids

abstract

Cardiovascular diseases are the leading cause of death in the world with myocardial infarction leading to heart failure and death of the victims. Since the current treatments do not restore the function of the cardiac tissue, tissue engineering aims to create cardiac patches to promote a better cardiac regeneration. In this study, two approaches of acellular and cellular strategies were chosen to produce cardiac patches for cardiac regeneration. On the acellular approach, platelet lysates modified with methacrylic groups (PLMA) were used to fabricate rehydrated scaffolds formed by freeze drying and were evaluated for cardiac patch application and to observe the impact of the freeze drying process on the hydrogel properties. The mechanical properties of the hydrogels increase with the freeze drying, not only in terms of Young's modulus, ultimate stress and ultimate strain, but also in durability. Although the top surface porosity wasn't different for all the PLMA concentrations used, PLMA scaffolds showed a high swelling ration, that decreases due to the liberation of protein from the scaffold matrix, a conductivity preliminary value on the same order of magnate of the human heart and capacity for being transported in a catheter. To evaluate this scaffold as a 3D culture platform, a successfully HUVECs assay was performed with the best performing PLMA concentration of 15%, showing, together with the physical properties results, promising results towards the use of this rehydrated hydrogels as cardiac patches for myocardial infarction regeneration. For the cellular approach, the idea was to build a system that could produce PLMA hydrogels incorporated with cardiomyocyte's spheroids in a square feature and using size-controlled wells. To optimize this system, MG-63 cells were used since they can easily form spheroids. For a more physical characterization, PLMA hydrogels were also evaluated for important properties for biomedical application and for the cardiac tissue more specific. Mechanical properties of the hydrogels showed the increases in the elasticity modulus when increasing the PLMA concentration present in the hydrogels and water content tests demonstrated that all used PLMA concentration hydrogels had a high content of water. Using MG-63 cells, after 7 days the system had formed a few spheroids although the system did not work properly. The obtained results showed that PLMA hydrogels have good characteristics for biomedical and cardiac application and that the optimizing of this system might be able to form cardiomyocyte's spheroids. In conclusion, the current results suggest these approaches can act as cardiac patches due to their hydrogel characteristics and cellular compatibility for this end, besides more interesting results can be obtained to support this outcome.

Contents

Tables

Figures

scaffolds for the conditions of 10%, 15%, 20% and 30% (w/v) of PLMA. Statistical analysis through one-way ANOVA analysis with Tukey's multiple comparison test. Data is presented as mean ± standard deviation (n≥3).

Figure IV.4. (B) Swelling capacity of PLMA-based scaffolds for the conditions of 10%, 15%, 20% and 30% (w/v) of PLMA thought out a period of 24 hours (A) with a close up of the first 30 minutes. Data is presented as mean ± standard deviation (n≥3).

Figure IV.5. Transportation of a 15% (w/v) PLMA rehydrated scaffold with a coronary micro-guide catheter.

Figure IV.6. Fluorescence microscopy images of live/dead staining of the established HUVECs seeded on the top surface of rehydrated PLMA scaffolds. The green and red channels represent the Calcein-AM and PI staining of live and dead cells, respectively. The blue and red channels at day 14 represents DAPI/Phalloidin staining, respectively.

Figure V.1. (A) Young's modulus, (B) ultimate stress and (C) ultimate strain obtained for PLMA hydrogels at 10%, 15%, 20% and 30% (w/v). Statistical analysis through two-way ANOVA with Tukey's multiple comparison test (*p<0.05, **p<0.005, ***p<0.0005, ****p<0.0001). Data is presented as mean ± standard deviation (n≥3).

Figure V.2. Water absorption capacity of PLMA-based hydrogels of 10%, 15%, 20% and 30% PLMA after 16 hours. Statistical analysis through one-way ANOVA with Tukey's multiple comparison test. (**p<0.005, ****p<0.0001). Data is presented as mean ± standard deviation (n≥3).

Figure V.3. 15% (w/v) PLMA hydrogel grafted with PLMA to a chicken heart.

Figure V.4. Fluorescence microscopy images of live/dead staining of the established MG-63 spheroids on the 15% (w/v) PLMA hydrogel. The green and red channels represent the Calcein-AM and PI staining of live and dead cells, respectively.

Abbreviations

2D - Two-dimensional
3D - Three-dimensional
ADHF - Acute decompensated heart failure
ADSC - Adipose-derived stem cell
AF - Atrial fibrillation
AHF - Acute heart failure
ATDPC - Adipose tissue-derived progenitor cell
CABG - Coronary artery bypass graft
CAD - Coronary artery disease
CEC - Competent Ethics Committee
CF - Cardiac fibroblast
CHF - Chronic heart failure
CM - Cardiomyocyte
CPC - Cardiac progenitor cell
CSC - Cardiac stem cell
DAMP - Danger-associated molecular pattern
DAPI - 4',6'-diamino-2-fenil-indol
DMSO - Dimethyl sulfoxide
EC - Endothelial cell
ECM - Extracellular matrix
EF - Ejection fraction
EIS - Electrochemical Impedance Spectroscopy
ePTFE - Expanded Polytetrafluoroethylene
ESC - Embryonic stem cell
FBS - Fetal bovine serum
FDA - Food and Drug Administration
Gal-3 - Galectin-3
GCSF - Granulocyte colony-stimulating factor
GelMA - Gelatin methacryloyl
GFP - Green fluorescent protein
GNR - Gold nanorod

HA - Hyaluronic acid

HCAEC - Human coronary artery endothelial cell

HF - Heart failure

HUVEC - Human umbilical vein endothelial cell

I/R - Ischaemia-reperfusion

IHD - Ischemic heart disease

IL - Interleukin

iPSC - Induced pluripotent stem cell

IRAK - Interleukin-1 receptor associated kinase

Islet-1 - Insulin gene enhancer protein binding protein-1

LV - Left ventricle

MA - Methacrylic anhydride

MAAP - Magnesium L-ascorbic acid 2 phosphate

MCP-1 - Monocyte chemoattractant protein-1

MeCol - Methacrylated collagen

MI - Myocardial infarction

MMP - Matrix metalloproteinase

MSC - Mesenchymal stem cell

P(3HO) - Poly(3-hydroxyoctanoate)

PBS - Phosphate buffered saline

PCL - Polycaprolactone

PDGF - Platelet-derived growth factor

PDMS - Polydimethylsiloxane

PECUU - Poly(ester carbonate urethane) urea

PEG - Poly(ethylene glycol)

PELA - Poly(ethylene glycol)-poly(DL-lactide)

PEO - Polyethylene oxide

PEUU - Poly(ester urethane urea)

PGS - Poly(glycerol sebacate)

PI - Propidium iodide

PL - Platelet lysates

PLA - Poly(lactic acid)

PLGA - Poly(lactic-co-glycolic) acid

PLLA - Poly(L-lactic acid)

PLMA - Methacryloyl platelet lysates

POE - Polyoxyethylene

PU - Poly(urethane)

PVCL - Polyδ-valerolactone-cε-caprolactone

ROS - Reactive oxygen species

RT - Room temperature

SCA1 - Stem cell antigen 1

SEM - Scanning electron microscope

SOEA - Soybean oil epoxidized acrylate

TE - Tissue engineering

Th2 - T helper type 2

TIMP - Tissue inhibitors of metalloproteinase

TLR - Toll-like receptor

TNF - Tumour necrosis factor

UV - Ultraviolet

VEGF - Vascular endothelial growth factor

α-MEM - Minimum Essential Medium Alpha

Chapter I

Background

Background

Abstract

Myocardial infarction is one of main causes of death in the world due to the poor regeneration capacity of the cardiac tissue that leads to heart failure. Current treatments for this event cannot restore the cardiac function and this is where tissue engineering and cardiac patches aim to act by recapitulating the *in vivo* conditions and improving the cardiac healing. Throughout the years, the use of cells in cardiac patches has been an important point of research due to the benefits they can bring in terms of regeneration and maintenance of appropriate cell behaviour. With this, approaches have been developed: cellular cardiac patches, that relies on the incorporation of cells within the biomaterials, and acellular cardiac patches, where cells are not present but the patch have the biochemical properties that allow its engraftment into the tissue. In terms of biomaterials, the common research focusses on synthetic and animal origin materials that have disadvantages related with cellular interaction, toxicity and immune response. This is where platelet lysates can be an alternative and, after being chemically modified, used to produce hydrogels with a very simple protocol. The aim of this work is to investigate the use of these hydrogels as cardiac patches for cellular and acellular approaches and evaluate their characteristics for cardiac regeneration.

1. Introduction

Cardiovascular diseases are the leading cause of death in the world.[1] Ischemic heart disease (IHD) is the main contributor for this statistic and the incidence of IDH increases after the fourth decade of life due to aged risk factors.[2] In most scenarios, IDH is responsible for causing myocardial infarction (MI), leading to heart failure (HF) and death.[3] Therefore, urgent need for therapies to prevent HF is a strong topic in clinical research.

The composition of the heart is divided in epicardium, myocardium and endocardium.[4] Epicardium is the outer protective layer of the heart, being essential for heart regeneration after injury by providing paracrine factors and progenitor/stem cells that contribute to regeneration of cardiomyocytes (CMs), vascular smooth muscle cells, and endothelial cells (ECs).[5] On the other hand, endocardium is a three inner layer lining the

heart wall and is composed by vascular endothelium, fibroelastic tissue and subendocardial connective tissue. Myocardium, the thickest middle layer of the heart wall composed of CMs, enables continuous contraction and relaxation to pump blood throughout the human body.[4] Upon MI, myocardium ceases to function properly due to the death of CMs and extremely low healing capacity of this tissue.[6] This is accompanied by a cardiac remodelling process, formation of scar tissue and degradation of extracellular matrix (ECM), indicating progressive worsening of heart function, finally leading to HF.[7]

Various pharmaceutical and surgical techniques have been exploited to slow down the progression of HF but, unfortunately, these therapies do not restore function of the damaged myocardium.[8] Heart transplantation is the only option to fully treat HF but is severely restricted due to the shortage of donor organs.[9] Thus, innovative therapeutic strategies should be developed to restore the function of infarcted myocardium.[4] This is where cardiac patches emerge as an innovate therapeutical approach using tissue engineering (TE). Cardiac TE aims to recreate the heart microenvironment in order to facilitate cell assembly and build of functional tissue with the goal of providing replacement for damaged tissue after MI. This is done by recapitulation of the conditions occurring during *in vivo* development and combining the expertise of multiple fields such as engineering, biology, medicine, biochemistry and pharmacology, in order to create suitable tissue replacements capable of restoring function and improving quality of life.[8]

2. Cellular and acellular cardiac patches

The incorporation or not of cells into cardiac patches have been widely intriguing for researchers. Cells have the ability to address limitations in scaffold thickness and the potential to be more readily vascularized by the host circulatory system which contributes for better cardiac regeneration.[10] But these patches can also face several limitations that may contribute to inconsistencies in efficacy. Problems including fragile cellular cargo, limited long-term stability, extensive production times and costs and the presence of undifferentiated cells contributing to uncontrolled cell growth or tumorgenicity following transplantation are the main concerns with cellular cardiac patches. To address these limitations, acellular cardiac patches approaches have been explored to keep the benefits of cells while eliminating most of problems associated with them.[11]

Cells can open a huge space of opportunity to increase regeneration capacity due to the different cell types and technologies available, existing already substantial *in vitro* and *in vivo* data. Overall, the main requisites for functional cardiac patches with successful cardiac tissue improvements are the alignment of CMs (and stem cells) with the synchronous electromechanical contractile force and healing process, the generation of functional microvasculature to provide adequate nutrient and oxygen delivery for cells on the patch and on native tissue, the absence of immunogenic response on the host and suitable degree of cell maturation.[8]

The development of acellular patches, and the possibility to incorporate molecular factors involved in cardiac function, has been demonstrated as a viable strategy to address cellular patches disadvantages and optimize tissue regeneration. In both cases this can partial overcome cells limitations in an easier way for commercialization, although the same results in terms of regeneration are not normally achieve. Apart from cell integration, requisites for acellular patches are similar to cellular patches with the scaffolds matching native heart elasticity, being mechanically stable, provide nutrient and oxygen diffusion and being nonimmunogenic to support tissue function and regeneration.[12]

3. Platelet lysates as a biomaterial

In terms of biomaterials, synthetic materials normally show good mechanical proprieties but have limitations at biochemical levels and the opposite is found in natural materials where suitable biochemical properties are present but do not offer good mechanically capability.[13]

Synthetic polymers advantages rely on mechanical properties such as their strength and durability over natural polymers.[14] The support offered by them can enable restoration of damaged or diseased tissue structure and function and can exhibit similar physicochemical and mechanical characteristics to biological tissues. Although, normally these type of materials lack cell adhesion motifs, requiring chemical modifications to enhance cell adhesion.[15] Besides, their toxicity is also a concern, especially in the case of biodegradable materials, which can release potentially harmful byproducts of degradation into the body.[14]

In the case of natural biomaterials, they can derive from native tissues of autogenic (same individual), allogenic (same-species donor) or xenogenic (animal) sources.

Autologous biomaterials, derived from and used for the same patient, is the current gold standard due to its superior functionality and nonimmunogenicity. The supply of tissues needed and health status of the patient are the major hindrances to obtain autologous tissue. The next best choice is allogenic biomaterials or biomaterials derived from tissues of organisms of the same species. Unfortunately, human donor tissues needed for treating cardiovascular disease are in very limited supply.[14] So, xenogenic biomaterials derived from tissues of animals have helped to fill this need.[16]

Immune response is of particular concern with allogenic and xenogenic biomaterials. With allogenic human donor biomaterials, immunosuppressive drugs must be taken by the patient, and even then it may still be rejected.[17] In the case of xenogenic biomaterials, they are decellularized before use in patients which increases the necessary labour and costs to produce these type of biomaterials.[18] Mostly ECM materials such as collagens and proteins remain after decellularization. In cardiovascular applications, bovine (cow), porcine (pig) and equine (horse) tissue sources have become quite popular for their compatibility to humans.[14]

In order to find a solution for cell progression on synthetic materials and immune response and time-consuming procedures on animal origin materials, new sets of biomaterials have been developed. One of the alternatives is platelet lysates (PL). PL are an autologous source of grown factors, cytokines and several other proteins[19–21] that can locally promote wound[22–24] and tissue healing[25]. This material is obtained by a process of freeze/thaw cycles of platelet concentrates harvest from whole blood. As previously reported, chemically modified PL with methacrylic anhydride (MA) can form hydrogels by covalent photocrosslinking using UV light irradiation in the presence of a photoinitiator.[26] These hydrogels of methacryloyl platelet lysates (PLMA) have good mechanical and biochemical properties, supporting the adhesion and proliferation of encapsulated cells/spheroids while being an animal-free product approach for cell culture and biomedical applications.[27,28]

4. Objectives

Taking in count the current research on cellular and acellular cardiac patches and the known problems with synthetic and animal origin biomaterials, this work was focus on

validate PLMA hydrogels, a human origin biomaterial, for potential cardiac patch application. The objective is to evaluate the use of PLMA hydrogels as cardiac patches through acellular and cellular approaches (**Figure I.1**). As an acellular patch, PLMA scaffolds will be produced using freeze drying. Our study aims to validate this strategy for the cardiac use and evaluate the effects of this process on the physical characteristics of the hydrogel. As a cellular patch, PLMA hydrogels will incorporate squared feature wells of precise dimensions. The goal is to create a platform that is able to form and control the position of spheroids on the hydrogel, that can potentially be made of CMs. In both cases, hydrogels needed similar characteristics to correspond to the cardiac tissue and to mimic it in the best way possible, and also support cellular adhesion and proliferation, most importantly CMs.

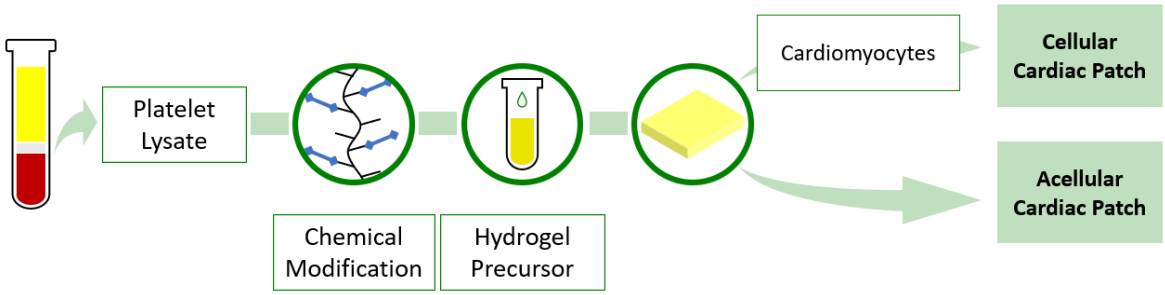

Figure I.1. PLMA hydrogels fabrication for acellular and cellular cardiac patch approach.

References

1. Virani, S. S. *et al.* Heart Disease and Stroke Statistics -2020 Update: A Report From the American Heart Association. *Circulation* **141**, e139–e596 (2020).
2. Khan, M. A. *et al.* Global Epidemiology of Ischemic Heart Disease: Results from the Global Burden of Disease Study. *Cureus* **12**, e9349 (2020).
3. Bui, A. L., Horwich, T. B. & Fonarow, G. C. Epidemiology and risk profile of heart failure. *Nat Rev Cardiol* **8**, 30–41 (2011).
4. He, L. & Chen, X. Cardiomyocyte Induction and Regeneration for Myocardial Infarction Treatment: Cell Sources and Administration Strategies. *Adv. Healthc. Mater.* **9**, 2001175 (2020).
5. Zhou, B. *et al.* Epicardial progenitors contribute to the cardiomyocyte lineage in the developing heart. *Nature* **454**, 109–113 (2008).

6. Bergmann, O. *et al.* Evidence for cardiomyocyte renewal in humans. *Science* **324**, 98–102 (2009).
7. Cohn, J. N., Ferrari, R. & Sharpe, N. Cardiac remodeling--concepts and clinical implications: a consensus paper from an international forum on cardiac remodeling. Behalf of an International Forum on Cardiac Remodeling. *J. Am. Coll. Cardiol.* **35**, 569–582 (2000).
8. Thavandiran, N., Nunes, S. S., Xiao, Y. & Radisic, M. Topological and electrical control of cardiac differentiation and assembly. *Stem Cell Res. Ther.* **4**, 14 (2013).
9. Stehlik, J. *et al.* The Registry of the International Society for Heart and Lung Transplantation: Twenty-eighth Adult Heart Transplant Report--2011. *J Hear. Lung Transpl.* **30**, 1078–1094 (2011).
10. Zhang, J., Liu, Y., Walker, W. B., Dong, S. L. & Wang, G. R. Identification and localization of two sensory neuron membrane proteins from Spodoptera litura (Lepidoptera: Noctuidae). *Insect Sci.* **22**, 399–408 (2015).
11. Tang, J. N. *et al.* Concise Review: Is Cardiac Cell Therapy Dead? Embarrassing Trial Outcomes and New Directions for the Future. *Stem Cells Transl. Med.* **7**, 354–359 (2018).
12. Domenech, M., Polo-Corrales, L., Ramirez-Vick, J. E. & Freytes, D. O. Tissue Engineering Strategies for Myocardial Regeneration: Acellular Versus Cellular Scaffolds? *Tissue Eng. - Part B Rev.* **22**, 438–458 (2016).
13. Jang, Y., Park, Y. & Kim, J. Engineering biomaterials to guide heart cells for matured cardiac tissue. *Coatings* **10**, 925 (2020).
14. Lam, M. T. & Wu, J. Biomaterial applications in cardiovascular tissue repair and regeneration. *Expert Rev Cardiovasc Ther* **10**, 1039–1049 (2012).
15. Reddy, M. S. B., Ponnamma, D., Choudhary, R. & Sadasivuni, K. K. A comparative review of natural and synthetic biopolymer composite scaffolds. *Polymers (Basel).* **13**, 1105 (2021).
16. Dalmau, M. J. *et al.* Hemodynamic performance of the Medtronic Mosaic and Perimount Magna aortic bioprostheses: five-year results of a prospectively randomized study. *Eur. J. Cardiothorac. Surg.* **39**, 844–52 (2011).
17. Hodges, A. M. *et al.* Late antibody-mediated rejection after heart transplantation following the development of de novo donor-specific human leukocyte antigen

antibody. *Transplantation* **93**, 650–656 (2012).

18. Byrne, G. W. & McGregor, C. G. A. Cardiac xenotransplantation: progress and challenges. *Curr. Opin. Organ Transplant.* **17**, 148–154 (2012).
19. Altaie, A., Owston, H. & Jones, E. Use of platelet lysate for bone regeneration - are we ready for clinical translation? *World J Stem Cells* **8**, 47–55 (2016).
20. Wang, H. & Avila, G. Platelet Rich Plasma: Myth or Reality? *Eur J Dent* **1**, 192–194 (2007).
21. Araki, J. *et al.* Optimized preparation method of platelet-concentrated plasma and noncoagulating platelet-derived factor concentrates: Maximization of platelet concentration and removal of fibrinogen. *Tissue Eng. - Part C Methods* **18**, 176–185 (2012).
22. Gentile, P., Scioli, M. G., Bielli, A., Orlandi, A. & Cervelli, V. The Use of Adipose-Derived Stromal Vascular Fraction Cells and Platelet Rich Plasma in Regenerative Plastic Surgery. *Stem Cells* **35**, 117–134 (2017).
23. Backly, R. El *et al.* Platelet lysate induces in vitro wound healing of human keratinocytes associated with a strong proinflammatory response. *Tissue Eng. - Part A* **17**, 1787–1800 (2011).
24. Picard, F., Hersant, B., Bosc, R. & Meninguad, J.-P. Should we use platelet-rich plasma as an adjunct therapy to treat 'acute wounds', 'burns' and 'laser therapies': a review and a proposal of a quality criteria checklist for further studies. *Wound Repair Regen* **23**, 163–170 (2015).
25. Haleem, A. M. *et al.* The clinical use of human culture-expanded autologous bone marrow mesenchymal stem cells transplanted on platelet-rich fibrin glue in the treatment of articular cartilage defects: A pilot study and preliminary results. *Cartilage* **1**, 253–261 (2010).
26. Santos, S. C., Custódio, C. A. & Mano, J. F. Photopolymerizable Platelet Lysate Hydrogels for Customizable 3D Cell Culture Platforms. *Adv. Healthc. Mater.* **7**, e1800849 (2018).
27. Monteiro, C. F., Custódio, C. A. & Mano, J. F. Bioengineering a humanized 3D tri-culture osteosarcoma model to assess tumor invasiveness and therapy response. *Acta Biomater.* **134**, 204–214 (2021).
28. Monteiro, C. F., Santos, S. C., Custódio, C. A. & Mano, J. F. Human Platelet Lysates-

Based Hydrogels: A Novel Personalized 3D Platform for Spheroid Invasion Assessment. *Adv. Sci.* **7**, 1902398 (2020).

Chapter II

Materials and Methods

Materials and Methods

1. Synthesis of methacryloyl platelet lysates

Platelet lysates (PL) are an autologous source of grown factors, cytokines and several other proteins[1–3] that can locally promote wound[4–6] and tissue healing[7]. This material is obtained by a process of freeze/thaw cycles of platelet concentrates harvest from whole blood.[1–3] Although PL has been used as an alternative culture supplement to animal-derived serum, it has also been showed as a promising biomaterial for three-dimensional (3D) culture platforms.[8]

Over the years, stimuli-responsive hydrogels have gain an increasing scientific interest.[9,10] From all the stimulus, light is considered easy to control in terms of time, space and wavelength usage.[11,12] The use of photopolymerization via chemical modification of proteins with methacryloyl groups is one of the strategies that allows the fabrication of hydrogels by covalent photocrosslinking through light irradiation in the presence of a photoinitiator.[13]

PL (STEMCELL Technologies, Canada) stored at -20 ºC and thawed at 37 ºC was chemically modified with methacrylic anhydride 94% (MA) (Sigma-Aldrich, USA) to form methacryloyl platelet lysates (PLMA) of low-degree of modification (PLMA100) for the purpose of this work.[14] Briefly, the reaction pH was maintained between 6 and 8 using 5 M sodium hydroxide (AkzoNobel, USA) solution to prevent protein precipitation, at room temperature (RT) and under constant stirring. The synthetized PLMA100 was then purified by dialysis with Float-A-Lyzer G2 Dialysis Device 3.5-5 kDa (Spectrum, USA) in deionized water for 24 hours, sterilized with a low protein retention 0.2 µm filter (Enzymatic S. A., Portugal), frozen in liquid nitrogen, freeze dried (LyoQuest Plus Eco, Telstar, Spain) and stored at 4 °C.

2. PLMA hydrogel formation

As explain previously, photopolymerization is one of the most used strategies for photocrosslinking and, with the modification of PL to PLMA, this method can be used for hydrogel formation in this work.

The combination of 10%, 15%, 20% or 30% (w/v) of lyophilized PLMA100 with 0.5% (w/v) 2-hydroxy-4'-(2-hydroxyethoxy)-2-methylpropiophenone (Sigma-Aldrich) in phosphate buffered saline (PBS) (Sigma-Aldrich) create a PLMA precursor solution that was pipetted to polydimethylsiloxane (PDMS) (Dow Corning, USA) molds with different shape and sizes. In both works, the hydrogels had an hight of 1 mm, approximately, and photopolimerazation occur within 60 seconds of exposure to ultraviolet (UV) radiation at 2.45 w/cm^2 in an 8 cm distance between the solution and the UV lamp. Hydrogels were placed at 4 ºC overnight in 5 mL PBS to achieve maximum absorption capacity and used in this state in all experiments. The shape and sizes of hydrogels used in the different experiments is specified in each one of them bellow.

3. PLMA hydrogel freeze drying

Freeze drying is the process that removes water or other solvents present in samples though sublimation. In the case of water, this will pass directly from liquid to gas using controlled low temperatures and low pressure.[15] When hydrogels are freeze dried, a porous scaffold is formed and the covalent network matrix of the biomaterial is maintained in a sponge form.[16]

The prepared PLMA hydrogels were placed in Mr. Frosty^{TM} Freezing Container (ThermoFisher Scientific) for a cooling rate of -1 ºC/minute, to avoid damaging the hydrogels upon rapid cooling, at - 80 ºC for 2 hours. After that time, the frozen hydrogels where freeze dried (LyoQuest Plus Eco, Telstar, Spain) overnight and rehydrated in 5 mL of PBS also overnight to achieve maximum absorption capacity.

4. PLMA hydrogel characterization

4.1 Mechanical properties

In tissue engineering, the mechanical properties of biomaterials are one of the most important parameters for medical applications since they can interfere with cell behaviour. When mimicking the original cell environment, the better hydrogels can fulfill the

extracellular matrix (ECM) of the cells they are supporting, the better these will adapt, organize and proliferate.[17]

The elasticity behaviour of PLMA hydrogels was tested using a Universal Mechanical Testing Machine Shimadzu MMT-101N (Shimadzu Scientific Instruments, Kyoto, Japan) equipped with a load cell of 100 N. To this end, a unidirectional tensile test was performed at RT on rectangular shaped hydrogels with a length of 2.5 cm, a width of 0.5 cm and using 75 µL of PLMA precursor solution. Samples of all four concentrations, from both freeze dried and non-freeze dried hydrogels, were used with an extension rate of 1 mm/minute. The Young's modulus was defined as the slope of the linear region of the strain/stress curve, corresponding from 0 to 45% strain. Ultimate stress and ultimate strain values were taken as the point where failure of the hydrogel occurred.

Preliminary cyclic tensile tests were also performed using the same spectrum of samples and equipment at a rate of 15.75 cm/minute for 45% of strain to replicate the 70 bpm of the human heart using this percentage of strain. The total cycle number obtained was the number of cycles each hydrogel support until failure and the maximum stress value was taken in count the of stress at 45% of strain within cycle number 5 to cycle number 10, the 5 cycles at half total cycle number and also the last 5 cycles discarding the last 5 total cycles obtained. The medium of these 15 cycles was the maximum stress value. All the samples were kept hydrated through all the tests.

4.2 Scanning electron microscopy

Scanning electron microscopy (SEM) analysis was obtained in a Hitachi TM4000 plus (Japan) equipment in order to analyse the scaffolds' structure and the surface porosity of the hydrogels for all concentrations by measuring the medium pore size using Image J software.

4.3 Swelling ratio

Porous scaffolds have the ability of swell when put in contact with a thermodynamically compatible solvent due to the polar groups present on their matrix. This

event can be particularly affected by pore size and type of porous structure present on the sponge.[18]

The sweeling capacity of PLMA sponges of all concentrations was evaluated over time for a period of 24 hours with several time points (30 seconds, 1 minute, 2 minutes, 3 minutes, 4 minutes, 5 minutes, 10 minutes, 15 minutes, 20 minutes, 25 minutes, 30 minutes, 1 hour, 2 hours, 3 hours, 4 hours, 5 hours, 6 hours, 12 hours and 24 hours) in circular scaffolds with 0.6 cm in diameter using 16.9 µL of PLMA precursor solution. Hydrogels were freeze dried and the value of the dry weight (W_d) was measure in this state. The scaffolds were then placed to hydrate in 10 mL of deionized water and, at the times mentioned above, the hydrated scaffolds were taken out from the deionized water, have the exceed water removed with filter paper (Fisher Scientific, USA) and the value for the wet weight of that time point measured (W_t). With the W_d and the W_t, the swelling ratio for that specific time point was calculated using the following equation (**Equation 1**) and the process repeated for all time points:

$$Swelling\ Ratio = \frac{W_t - W_d}{W_t} \quad \textbf{(Equation 1)}$$

4.4 Conductivity

The conductivity analysis of hydrogels was performed in partnership with Dr. Paula Barbosa of CICECO – Aveiro Institute of Materials. One of the methods to evaluate the capacity of conductivity of materials is electrochemical impedance spectroscopy (EIS) which can study the behavior of a system in ion mass transport though an electrolyte and associated electrode processes. A variable in time electrical sinusoidal tension (V(ω,t)) is applied with an amplitude (V_0) and a frequency (ω)[19] which results in electrical current (I) in the sample that propagates in a certain angle (ϕ). The reason between the tension and the current has a behavior of sinusoidal type that is defined as impedance (Z) with the help of the Ohm law, following **Equation 2-4**:[19]

$$V(\omega, t) = V_0\ sen(\omega t) \quad \textbf{(Equation 2)}$$

$$I(\omega, t) = I_0\ sen\ (\omega t + \emptyset) \quad \textbf{(Equation 3)}$$

$$Z(\omega, t) = \frac{V_0\, sen(\omega t)}{I_0\, sen\,(\omega t + \emptyset)} = \frac{sen(\omega t)}{sen\,(\omega t + \emptyset)} \quad \textbf{(Equation 4)}$$

The values of impedance can also be represented as complex numbers, based on Equation 5:

$$Z(i\omega) = Z'(\omega) + iZ''(\omega) \quad \textbf{(Equation 5)}$$

In **Equation 5**, Z' and Z'' are the real and imaginary components, respectively, with the real part being the real component of the material and the imaginary part a function of the capacity phenomenon. The values of Z measured in a certain break of frequency from mHz to MHz and the resultant graphic has a semicircle appearance that, when performed to obtain the through plane conductivity, the value of the resistant (R) of the material is given by the value of Z' at the minimum Z''. With the resistance, the conductivity of the material is obtained by the following equation (**Equation 6**), where L is the distance between the in-plane silver stripes and A is the cross-section area of the membranes, which normalizes the resistance to the sample geometry:[20]

$$\sigma = L(RA)^{-1} \quad \textbf{(Equation 6)}$$

For this work, a preliminary through plane electrical conductivity of membranes was determined by impedance spectroscopy using an Agilent E4980A Precision LCR meter with measurements carried at 37 °C and 95% relative humidity after 20 minutes, in a climatic chamber (ACS DY 110). The impedance spectra was collected between 20 Hz and 2 MHz with a test signal amplitude of 100 mV. The electrodes were applied on a sample with an area of approximately 1.1 cm^2 by using a circular hydrogel with 0.6 cm in diameter, that was prepared from 16.9 µL of 20% (w/v) PLMA precursor solution, with 0.12 cm of thickness. The current collection was ensured by separate platinum wires for voltage and current. The sample holder is designed to ensure stable electrical contact while fully exposing the membrane surface to the surrounding atmosphere. The spectra was analyzed with ZView (Version 2.6b, Scribner Associates) to assess the ohmic R and the conductivity of the PLMA calculated using the last above-mentioned equation (**Equation 6**).

4.5 Catheter patch transportation

In order to look for alternatives to minimize the invasiveness of cardiac patch implantation, deliver cardiac patches with catheters can be an interesting medical procedure if the cardiac patch is able to reach the target while maintaining integrity. A preliminary evaluation of the patch integrity when transported throw a catheter was performed using a rectangular shaped rehydrated scaffold with a length of 2.5 cm, a width of 0.5 cm and applying 75 µL of solution of 15% (w/v) PLMA precursor solution using a FineCross® micro-guide microcatheter (Terumo, Japan). The construct was pulled in and out while submerse on PBS solution used to achieve the maximum absorption capacity throughout the catheter extension and, after five rounds of transportation, the visual aspect of the rehydrated scaffold was access to see if there was any visible damage.

4.6 Water content

Water is an important part of hydrogels since they can absorb large amounts of this solvent.[21] Like scaffolds, this extensive capacity comes from polar groups on the polymeric chain and their porous nature.[22] To evaluate this capacity, hydrogels of all concentrations in a circular shape with 0.6 cm in diameter, using 16.9 µL of PLMA precursor solution, were hydrated for 16 hours in 5 mL of deionized water at 4º C and 2 more hours at RT before the wet weight (W_w) was measured. After freeze drying of these hydrogels, the dry weight (W_d) was also measured and compared with the initial W_w using the following equation (**Equation 7**) that presents the water content value in percentage:

$$Water\ Content\ (\%) = \frac{W_w - W_d}{W_w} \times 100 \quad \textbf{(Equation 7)}$$

4.7 Cardiac patch implantation

In order to recapitulate a cardiac patch implantation and evaluate *in vitro* if the cardiac patch is able to keep the integrity in a mechanical hostile environment similar to the heart constant movement, a chicken heart, removed at the time of the chicken death and

frozen at -20 ºC until defrost for use, was used to attach a square shaped hydrogel with a length and width of 0.5 cm and using 30 µL of solution of 15% (w/v) PLMA precursor solution. The hydrogel was fixed to the heart using 10 µL of the same prepared solution to reticulate the hydrogel pipetted around the limits of this and using the same protocol of photopolimerazation. The heart with the attached hydrogel was then submerse on 50 mL of PBS in a cup and placed at 350 rpm overnight in order to do a preliminary test to the hydrogel integrity but also to the capacity of PLMA to hold the hydrogel to the heart.

5. Cell culture

5.1 Scaffold seeding

Human umbilical veins endothelial cells (HUVECs) were isolated from human umbilical cord vein of newborn babies, under the approval of the Competent Ethics Committee (CEC), COMPASS Research Group and Hospital Infante D. Pedro, Aveiro, established a cooperation agreement to collect the human tissue. The consent declaration was obtained from all subjects and the handling of received human tissues was made in accordance with CEC guidelines. The samples were collected to a container with PBS supplemented with 1% (v/v) antibiotic/antimycotic (Thermo Fisher Scientific) and kept at 4°C until isolation procedure initiation. The samples were transferred to the laboratory within 24h after collection and immediately processed. Vein washing was performed with PBS, placing a catheter extender with side shunt (Vygon, Portugal) into the vein hole at one end of umbilical cord. The endothelial cells were released from vein walls by enzymatic digestion using 0.1% (w/v) collagenase type IA (MP Biomedicals, USA), under 37 °C for 20-25 minutes. The HUVECs suspension was obtained rising the vein walls with M199 medium (Sigma-Aldrich) supplemented with 1% (v/v) of Endothelial Cell Growth Supplement (40 mg/mL, Merck, Germany), 10% (v/v) of Heparin (100 mg/mL, Sigma-Aldrich), 20% heat-inactivated fetal bovine serum (FBS, Thermo Fisher Scientific) and 1% antibiotic/antimycotic. The resultant cell suspension was plated in cell culture flasks previously coated with gelatin (0.7% (w/v), porcine skin type A, Sigma-Aldrich) for 20 minutes at 37 °C. Flow cytometry was then performed to confirm the successful isolation of HUVECs. HUVECs phenotypic profile was analyzed regarding CD31-APC (BioLegend,

USA) positive surface marker and CD34-FITC (BioLegend) and CD90-Alexa Fluor 647 (BioLegend) negative surface markers for endothelial cells. The cells were harvested by TrypLE™ Express solution (Thermo Fisher Scientific) at 37 °C for 5 min, centrifuged and resuspended in a PBS solution containing 2% (w/v) BSA and 0.1% (w/v) sodium azide (TCI Chemicals, Belgium). The antibodies were added at the dilutions recommended by the manufacture and incubated at 4 °C for 45 minutes, in the dark. After that, cell suspensions were washed with the above-mentioned PBS/BSA/sodium azide solution, centrifuged, fixed in another PBS solution containing 1% (v/v) formaldehyde (Sigma-Aldrich) and 0.1% (w/v) sodium azide and then analyzed in a flow cytometer (Flow Citometer BD Accuri C6 Plus, BD Biosciences).

HUVEC cells were cultured in M199 medium (Sigma-Aldrich) supplemented with 1% (v/v) of Endothelial Cell Growth Supplement (40 mg/mL, Merck, Germany), 10% (v/v) of Heparin (100 mg/mL, Sigma-Aldrich), 20% (v/v) heat-inactivated FBS and 1% (v/v) antibiotic/antimycotic in T-flasks, maintained under 5% CO_2 atmosphere at 37 °C (standard cell culture conditions) and passaged at about 80% confluence. The medium was replaced every 2 to 3 days. Cells were detached with 0.25% trypsin/EDTA solution (Gibco, Thermo Fisher Scientific, USA) and resuspended in the same culture medium for application.

The ability of PLMA rehydrated scaffolds to be a 3D culture platform was assessed by seeding HUVECs, respectively, on the top surface of a scaffold with a circular shape of 0.6 cm in diameter prepared from 16.9 µL of 15% (w/v) PLMA precursor solution. A 20 µL cell suspension containing 40 000 cells of HUVECs was applied on the top of the hydrogels and the cells were allowed to adhere for 4 hours. The culture was maintained for 14 days also in the described medium.

5.2 Preparation of micro-well PLMA hydrogels and spheroid encapsulation

In order to test the system for spheroid formation, MG-63 (European Collection of Authenticated Cell Cultures, ECACC) tumour cell line was used because of its great ability for spheroid formation.[23] MG-63 cell line was cultured in Minimum Essential Medium Alpha (α-MEM, Thermo Fisher Scientific, USA) supplemented with 2.2 g/L sodium bicarbonate (Sigma-Aldrich), 10% (v/v) heat-inactivated FBS and 1% (v/v) antibiotic/antimycotic in T-flasks, maintained under 5% CO_2 atmosphere at 37 °C (standard

cell culture conditions) and passaged at about 80% confluence. The medium was replaced every 2 to 3 days and cells were detached with 0.25% trypsin/EDTA and resuspended in the same culture medium for application.

At hydrogel formation, a PDMS mold was used to imprint 100 wells in a 1 cm length and 1 cm width hydrogel using 110 µL of 15% (w/v) PLMA precursor solution. The wells had 500 µm in diameter and 250 µm height arranged in a squared formation of 10 per 10 with a spacing between wells of 500 µm and 250 µm between the external wells and the limit of the hydrogel, respectively. This hydrogel was placed at another PDMS mold to support it for centrifugation at 500 G for 10 minutes with a MG-63 cell suspension of 150 µL containing 100 000 cells. This process is used to distribute in the most equally way the cells through all the wells in other to obtain 10 000 cells/well, approximately. The hydrogel culture was maintained for 7 days also in the described medium.

5.3 Cell viability

Cell viability is assessed through a live/dead assay followed by fluorescence imaging. Briefly, live cells can internalize the acetomethoxy derivate of calcein (Calcein AM), a non-fluorescent dye, and convert it to calcein, a green fluorescent dye that can be used to visualize these cells. In the case of dead cells, propidium iodide (PI) can penetrate the cells cytoplasmatic and nuclear membranes and intercalate with the nucleic acids, being visualized in the red channel.

The live/dead assay of the rehydrated scaffolds was made at days 3, 7 and 14 of culture in a solution of 1:500 of Calcein AM 4mM solution in dimethyl sulfoxide (DMSO) (Life Technologies, Thermo Fisher Scientific) and 1:1000 of 1 mg/mL PI (Thermo Fisher Scientific) in PBS at standard cell culture conditions (5% CO_2 at 37 °C) for 30 minutes. After three times washing with PBS, the samples were observed under a fluorescence microscope (Fluorescence Microscope Zeiss, Axio Imager 2, Zeiss, Germany), maintaining the same imaging parameters throughout all samples. For the MG-63 spheroids, the live/dead assay was performed after 7 days in culture, in a solution of 1:500 of Calcein AM 4mM solution in DMSO and 1:1000 of 1 mg/mL PI in PBS at standard cell culture conditions (5% CO_2 at 37 °C) for 1 hour, with the next steps being the same as the mentioned above.

5.4 Cell morphology analysis

To evaluate the morphology of cells, more specific the actin filaments and DNA, cell staining with phalloidin and 4',6-diamidino-2-phenylindole (DAPI), respectively, can be performed to analyse cell organization in the culture conditions that is inserted.

After 14 days of culture with HUVECs in hydrated PLMA scaffolds, the samples were washed with PBS and fixed in a solution of 4% (v/v) formaldehyde (Sigma-Aldrich) in PBS during at least 2 hours. After that, a phalloidin solution (Flash Phalloidin™ Red 594, 300U, Biolegend, USA) was diluted 1:40 PBS and the samples were incubated at 37 ºC for 1 hour. After three PBS washes, a DAPI (Thermo Fisher Scientific) solution was diluted 1:1000 in PBS, applied to the samples and incubated at 37 ºC for 5 minutes. After three more washes with PBS, the samples were examined using a fluorescence microscope (Fluorescence Microscope Zeiss, Axio Imager 2, Zeiss, Germany).

6. Statistical analysis

All data were statistically analysed using the GraphPah Prism 8.4.2 software and, except for the preliminary tests, are expressed as mean ± standard deviation of at least 3 independent experiments. Statistical significance of unidirectional tensile test for both freeze dried and non-freeze dried samples was determined using two-way ANOVA analysis with Tukey's multiple comparison test and using one-way ANOVA analysis with Tukey's multiple comparison test for surface pore size, water content and unidirectional tensile test of non-freeze dried samples.

References

1. Altaie, A., Owston, H. & Jones, E. Use of platelet lysate for bone regeneration - are we ready for clinical translation? *World J Stem Cells* **8**, 47–55 (2016).
2. Wang, H. & Avila, G. Platelet Rich Plasma: Myth or Reality? *Eur J Dent* **1**, 192–194 (2007).
3. Araki, J. *et al.* Optimized preparation method of platelet-concentrated plasma and noncoagulating platelet-derived factor concentrates: Maximization of platelet

concentration and removal of fibrinogen. *Tissue Eng. - Part C Methods* **18**, 176–185 (2012).

4. Gentile, P., Scioli, M. G., Bielli, A., Orlandi, A. & Cervelli, V. The Use of Adipose-Derived Stromal Vascular Fraction Cells and Platelet Rich Plasma in Regenerative Plastic Surgery. *Stem Cells* **35**, 117–134 (2017).
5. Backly, R. El *et al.* Platelet lysate induces in vitro wound healing of human keratinocytes associated with a strong proinflammatory response. *Tissue Eng. - Part A* **17**, 1787–1800 (2011).
6. Picard, F., Hersant, B., Bosc, R. & Meninguad, J.-P. Should we use platelet-rich plasma as an adjunct therapy to treat 'acute wounds', 'burns' and 'laser therapies': a review and a proposal of a quality criteria checklist for further studies. *Wound Repair Regen* **23**, 163–170 (2015).
7. Haleem, A. M. *et al.* The clinical use of human culture-expanded autologous bone marrow mesenchymal stem cells transplanted on platelet-rich fibrin glue in the treatment of articular cartilage defects: A pilot study and preliminary results. *Cartilage* **1**, 253–261 (2010).
8. Robinson, S. T. & Brewster, L. P. Platelet Lysate to Promote Angiogenic Cell Therapies. in *Physiologic and Pathologic Angiogenesis - Signaling Mechanisms and Targeted Therapy* 365–383 (2017).
9. Sun, M. *et al.* Synthesis and Properties of Gelatin Methacryloyl (GelMA) Hydrogels and Their Recent Applications in Load-Bearing Tissue. *Polymers (Basel).* **10**, 1290 (2018).
10. Yuan, M., Bi, B., Huang, J., Zhuo, R. & Jiang, X. Thermosensitive and photocrosslinkable hydroxypropyl chitin-based hydrogels for biomedical applications. *Carbohydr. Polym.* **192**, 10–18 (2018).
11. Zhao, X. *et al.* Photocrosslinkable Gelatin Hydrogel for Epidermal Tissue Engineering. *Adv. Healthc. Mater.* **5**, 108–118 (2016).
12. Wang, R., Yang, Z., Luo, J., Hsing, I. M. & Sun, F. B12-dependent photoresponsive protein hydrogels for controlled stem cell/protein release. *Proc. Natl. Acad. Sci. U. S. A.* **114**, 5912–5917 (2017).
13. Custódio, C. A., Reis, R. L. & Mano, J. F. Photo-Cross-Linked Laminarin-Based Hydrogels for Biomedical Applications. *Biomacromolecules* **17**, 1602–1609 (2016).

14. Santos, S. C., Custódio, C. A. & Mano, J. F. Photopolymerizable Platelet Lysate Hydrogels for Customizable 3D Cell Culture Platforms. *Adv. Healthc. Mater.* **7**, e1800849 (2018).
15. Shukla, S. Freeze drying process: a review. *Int. J. Pharm. Sci. Res.* **2**, 3061–3068 (2011).
16. Qian, L. & Zhang, H. Controlled freezing and freeze drying: A versatile route for porous and micro-/nano-structured materials. *J. Chem. Technol. Biotechnol.* **86**, 172–184 (2011).
17. Chamkouri, H. & Chamkouri, M. A Review of Hydrogels, Their Properties and Applications in Medicine. *Am. J. Biomed. Sci. Res.* **11**, 485–493 (2021).
18. Ganji, F., Vasheghani-Farahani, S. & Vasheghani-Farahani, E. Theoretical description of hydrogel swelling: A review. *Iran. Polym. J.* **19**, 375–398 (2010).
19. Nahir, T. M. Impedance Spectroscopy: Theory, Experiment, and Applications, 2nd ed Edited by Evgenij Barsoukov (Texas Instruments Inc.) and J. Ross Macdonald (University of North Carolina, Chapel Hill). John Wiley & Sons, Inc.: Hoboken, NJ. 2005. xvii + 596 pp. $125. *J. Am. Chem. Soc.* **127**, 12431 (2005).
20. Almeida, T. Membranas poliméricas à base de fibroína para células de combustível. (University of Aveiro, 2018).
21. Chai, Q., Jiao, Y. & Yu, X. Hydrogels for Biomedical Applications: Their Characteristics and the Mechanisms behind them. *Gels* **3**, 6 (2017).
22. Ahmed, E. M. Hydrogel: Preparation, characterization, and applications: A review. *J. Adv. Res.* **6**, 105–121 (2015).
23. Monteiro, C. F., Santos, S. C., Custódio, C. A. & Mano, J. F. Human Platelet Lysates-Based Hydrogels: A Novel Personalized 3D Platform for Spheroid Invasion Assessment. *Adv. Sci.* **7**, 1902398 (2020).

Chapter III*

Cardiac patches for regeneration after myocardial infarction

* This chapter is based on the following publication:

A. F. Lima, C. A. Custódio, J. F. Mano, *Cardiac patches for regeneration after myocardial infarction*. (manuscript under preparation)

Cardiac patches for regeneration after myocardial infarction

Abstract

Myocardial infarction is a medical condition known for leading to heart failure by progress loss of function of the cardiac tissue due to poor regeneration capacity. Current available treatments only focus on infarct size reduction, therefore, researchers and clinicians working in cardiac regeneration have found in tissue engineered cardiac patches a possible solution. These scaffolds aim to mimic the complex environment of the heart and induce regeneration through mechanical support and biochemical interaction. This occurs via patch biomaterial and vehicle capacity to delivery cells and other components to promote regeneration. Improved cardiac function post myocardial infarction has already been reported with cardiac patches showing promising results in tissue regeneration. This review focus on the clinical significance of myocardial infarction, cardiac tissue regeneration and research on patches, with emphasis on the needed characteristics for cardiac application, patch biomaterials, most recent research on cellular and acellular scaffolds, influence of patch architecture on performance and cardiac patches in pre-clinical and clinical use.

1. Introduction

Cardiovascular diseases are the leading cause of death in the world.[1] Ischemic heart disease (IHD) is the main contributor for this statistic and the incidence of IDH increases after the fourth decade of life due to aged risk factors.[2] In most scenarios, IDH is responsible for causing myocardial infarction (MI) leading to heart failure (HF) and death.[3] Therefore, urgent need for therapies to prevent HF is a strong topic in clinical research.

The composition of the heart is divided in epicardium, myocardium and endocardium.[4] Epicardium is the outer protective layer of the heart, being essential for heart regeneration after injury by providing paracrine factors and progenitor/stem cells that contribute to regeneration of cardiomyocytes (CMs), vascular smooth muscle cells, and endothelial cells (ECs).[5] On the other hand, endocardium is a three inner layer lining the heart wall and is composed by vascular endothelium, fibroelastic tissue and subendocardial connective tissue. Myocardium, the thickest middle layer of the heart wall composed of

CMs, enables continuous contraction and relaxation to pump blood throughout the human body.[4] Upon MI, myocardium ceases to function properly due to the death of CMs and extremely low healing capacity of this tissue.[6] This is accompanied by a cardiac remodelling process, formation of scar tissue and degradation of extracellular matrix (ECM), indicating progressive worsening of heart function, finally leading to HF.[7]

Various pharmaceutical and surgical techniques have been exploited to slow down the progression of HF but, unfortunately, these therapies do not restore function of the damaged myocardium.[8] Heart transplantation is the only option to fully treat HF but is severely restricted due to the shortage of donor organs.[9] Thus, innovative therapeutic strategies should be developed to restore the function of infarcted myocardium.[4] This is where cardiac patches emerge as an innovate therapeutical approach using tissue engineering (TE). Cardiac TE aims to manipulate the heart microenvironment in order to facilitate cell assembly and build of functional tissue with the goal of providing replacement for damaged tissue after MI. This is done by recapitulation of the conditions occurring during *in vivo* development and combining the expertise of multiple fields such as engineering, biology, medicine, biochemistry and pharmacology, in order to create suitable tissue replacements capable of restoring function and improving quality of life.[8]

The present review focusses on the clinical outcomes of heart healing post-MI, main topics and current treatments on cardiac tissue regeneration and research on cardiac patches, with emphasis on the needed characteristics for cardiac application, used biomaterials, most recent constructs on cellular and acellular scaffolds, influence of patch architecture on performance and cardiac patches in pre-clinical and clinical use.

2. Ischemic heart disease

IHD is a pathophysiological condition caused by insufficient supply of oxygen to the myocardium.[10] The most frequently pathological process is coronary artery disease (CAD) or microvascular dysfunction. CAD appears due to atherosclerotic obstruction or spasm of the epicardial coronary arteries. Normally, IHD and CAD are used synonymously with IHD being associated with chronic and progressive disease that can translate or initiate, at any time, an unstable condition caused by plaque rupture or erosion called acute coronary thrombosis and cause partial or complete occlusion of the artery. The main consequences of

this event are vascular hypoperfusion and MI.[11] The risk factors of IDH differ from non-modifiable to modifiable since some risks can be eliminated or minimized.[12] The non-modifiable risks are male gender, age, family history incidents and co-morbidities (including kidney disease, hypercholesterolemia, type I and II diabetes, etc.)[13] and the modifiable risks are stress, alcohol, smoking and metabolic syndrome (including elevated glucose, hypertension, lipid disorders, etc.).[14]

The reduction in diameter of a coronary artery by 50% or more limits its maximum vasodilatory capacity, while reduction by 85% or more determines a reduction in flow, even at rest.[15] Since the nutrition of the myocardium depends on the oxygen capacity of the blood and on the coronary flow,[10] during an acute event the reduction of oxygen supply to the myocardium impairs oxidation of glucose and free fatty acids turning cytoplasmic anaerobic glycolysis the main source of energy of cells. This process can't follow the cells energy needs and accumulates lactates and hydrogen ions that reach toxic concentrations[16] causing loss of myocardial tissue, contractile force[17] and relaxation capability.[18] This leads to HF by myocardial systolic dysfunction. Classically, patients with IHD who develop HF have a clinical history of MI with atherosclerotic disease of epicardial arteries.[19]

The loss of function of the cardiac tissue that leads to HF is duo to mainly two mechanisms: inflammation and fibrosis. These processes alter the tissue architecture, electrical conduction, mechano-electrical coupling and have deleterious effects on force generation by CMs.[20,21]

2.1 Inflammation

Inflammation is a physiological defence mechanism of the body against injurious stimuli such as tissue damage and infection.[22] This is beneficious in terms that, the right and timely inflammatory response can facilitate healing after an injury but, when this response lasts, this leads to chronic inflammation, extended tissue destruction and progressive fibrosis.[23] The inflammatory response is complex and compromises several stages including vascular phase, cellular phase and resolution phase. Leukocytes have a major role through various mechanisms, several cytokines are important mediators,[24] the endothelial layer undergo activation and selective changes in permeability to allow cellular components to shift from intravascular to extravascular compartments,[25] osteopontin and versican mediate

leukocyte adherence and migration[26,27] and low molecular weight hyaluronic acid (HA) has an active role in proinflammatory response by monocytes, dendritic cells, lymphocytes and macrophages.[28]

2.2 Fibrosis

In the case of fibrosis, it is an essential component of tissue repair that follows tissue injury and is usually associated with inflammation.[22] The objective is to deposit connective tissue in order to preserve tissue architecture but progressive fibrosis reflets a pathologic state and results in scarring, impairment of function and organ damage.[29] The fibrosis mechanism has also the participation of several components. Myofibroblasts are cells with a huge role in ECM secretion that arise from cardiac fibroblasts (CFs) and other cells types[30] and macrophages participate in secretion of ECM components, remodelling and are major sources of matrix metalloproteinases (MMPs) and tissue inhibitors of metalloproteinases (TIMPs).[31] Macrophages are also involved in the phagocytosis of cellular debris and infectious agents with the phagocytosed particle and other chemical molecules influencing their phenotypic characteristics.[32] This cells assume a more fibrotic phenotype (M2) after ingesting apoptotic neutrophils[33] and with cytokines such as interleukin (IL)13 and IL4. M2 phenotype is characterized by reduced expression, secretion of inflammatory mediators, augmentation of cell survival and fibrotic signals[34] and endocytose collagen.[35] In resume, the fibrotic response is modulated by the communication between inflammatory cells, CFs and ECM.[36,37] Extensive cardiac fibrosis results in electro-mechanical disturbances and reduces nutrient supply toward the myocardium, perpetuating a vicious cycle of fibrosis, cell death and inflammation.[38]

2.3 From myocardium infarction to heart failure

Inflammation and fibrosis are two mechanisms that stimulate each other to a continuum of events within the framework of tissue defence, repair and regeneration after MI. This event is characterized by extensive necrosis of CMs which results in leakage of intracellular contents and accumulation of reactive oxygen species (ROS).[22] Danger-associated molecular patterns (DAMPs) and cytokine signals are released from the

neighbouring cells[39] but the infarcted area has limited or no vascularization and this prevents immune cells from gaining immediate access to the necrotic core. During these initial stages, cardiac myofibroblasts could potentially take over the phagocytic role of macrophages by actively engulfing dead cells[40] that is followed by an intense and transient inflammatory phase with infiltration of neutrophils and monocytes.[41] However, both resident cardiac cells (CMs, CFs, resident macrophages, mast cells) and recruited cells (leukocytes) contribute to the development of sterile inflammation post-MI.[41] The immune cells recognize the released alarmins and activate downstream inflammatory pathways. Inflammation is further sustained by upregulation of various proinflammatory cytokines (monocyte chemoattractant protein-1 (MCP-1), tumour necrosis factor (TNF)α and IL6) within the infarcted myocardium. MCP-1 is involved in the recruitment of monocytes while TNFα enhances adhesion and extravasation of leukocytes through the endothelium.[42–44] TNFα is an acute-phase protein involved in both post-MI inflammatory reaction and ischaemia-reperfusion (I/R) injury.[45,46] The role of IL6 in cardiac inflammation and remodelling is ambiguous. Enhanced IL6 expression could accentuate the inflammatory response and exacerbate the deleterious after-effects of MI.[47] However, knocking out IL6 confers no protective effect in a mouse model of MI[48] and IL6 receptor inhibition did not improve cardiac function after I/R in a recent study.[49] There are also changes in ECM around the necrotic area after MI. For instance, large polymers of HA are degraded to low molecular weight HA and together with fibronectin fragments initiate and sustain a multitude of inflammatory cascades.[50] Molecular stop signals of inflammation such as interleukin-1 receptor associated kinase (IRAK)-M in macrophages and CFs actively wean the post-MI inflammatory response by acting as a functional decoy to attenuate sustained inflammatory response and improve adverse post-infarction cardiac remodelling.[51] In the proliferative phase that follows, macrophages secrete several cytokine growth factors and activate mesenchymal reparative cells to deposit ECM.[41] Galectin-3 (Gal-3), a profibrotic protein produced predominantly by macrophages, is a major player in post-MI cardiac remodelling.[52] TGFβ, another key fibrotic cytokine, aids in repair by supressing inflammation and stimulating hypertrophic CM growth after MI. TGFβ also promotes ECM deposition by upregulating collagen and fibronectin synthesis and downregulating ECM degradation.[53] Crosstalk between M2 macrophages and CFs together with T helper type 2 (Th2) cells responses sustains the fibrotic response. Recent studies also suggest the indispensable role of proteoglycans such as syndecan-1 and 4 in post-MI remodelling and

fibrosis of the heart.[54,55] Apoptosis of the majority of reparative cells marks the end of the proliferative stage and infarct maturation occurs with the formation of cross-linked collagen. The extent of post-MI remodelling depends on the infarct size and the quality of cardiac repair. The infarct zone undergoes replacement fibrosis while the surrounding non-infarct zone displays perivascular and interstitial fibrosis.[56] The aim of the fibrotic response is to preserve structural integrity and to maintain the pump function of the heart by preventing dilatation, aneurysm formation or myocardial rupture.[57] However, failure of cardiac myofibroblasts to undergo apoptosis or persistence of profibrotic signalling could result in pathological remodelling of the heart.

Although most patients survive the primary cardiac event due to early detection and timely management, every cardiac insult decreases the cardiac contractile reserve and these patients have an increased risk of developing HF.[58] HF can be defined as the inability of the heart to adequately maintain cellular perfusion under normal cardiac filling pressure. While half of the patients with HF exhibit decreased ejection fraction (EF), the other half have a normal EF. Based on clinical presentation, HF can be classified as acute HF (AHF), when the patient presents with cardiac decompensation, and chronic HF (CHF), when the patient has impaired cardiac function but is compensated and stable, i.e. able to maintain tissue perfusion without assistance.[59] AHF is characterized by a systemic inflammatory response, with elevated proinflammatory cytokines.[60] Other triggers may be present that provoke inflammation: AHF is often accompanied by viral or bacterial infection and is usually preceded by MI or atrial fibrillation (AF). However, after the acute event has been treated, a chronic response develops, and such patients frequently develop CHF. Other concomitant factors such as hypertension can also contribute to the development of AHF and CHF. It is also important to note that CHF can itself be a predisposing factor for the development of future AHF, and the goal of CHF management is to maintain the patient in compensated HF state and prevent them from deteriorating into a state of acute decompensated HF (ADHF).[59] Inflammation in the setting of CHF can be very complex. Low-grade systemic inflammation can both be a cause and consequence of HF.[61,62] Moreover, chronic oxidative stress associated with HF can exacerbate the pre-existing inflammatory state.[63] It is hypothesised that the presence of co-morbidities might lead to increased inflammation and to HF.[64] There is also upregulation of toll-like receptor (TLR)4 in CMs during HF, suggesting the direct role of CMs in cardiac inflammation associated with HF.[65] Sustained activation of protective

neurohormonal mechanisms can also contribute to ongoing cardiac inflammation and fibrosis,[66,67] resulting in further loss of cardiac function and clinical deterioration up to the point of ADHF and death.

In resume, the myocardium responds to MI by formation of a fibrotic scar through a modest wound healing process that creates an hypertrophic remodeling.[57] The outcome of the wound healing process is a mechanically inferior cardiac muscle, with a rigid collagenous fibrotic scar to avoid cardiac rupture.[68] Unable to function correctly, these structural changes markedly increase the mechanical stress on the ventricular wall leading to HF.[69] Other pathologies, including valvular disease, hypertension, genetic cardiomyopathies or aging which cause slow functional cell loss over time, may also help the progression of HF.[70]

3. Myocardium regeneration

The human adult heart consists mostly of terminally differentiated CMs and a small population of cardiac stem cells (CSCs) involved in maintaining cellular homeostasis.[71] The main obstacle on the way to recovery from myocardial injury is the poor endogenous regenerative capacity of the adult heart since the majority of adult CMs do not proliferate. Shortly after birth, the human cardiac tissue mechanism of growth shifts from hyperplasia to hypertrophy, meaning cell enlargement.[72] A major aspect of this transition is that most CMs in the myocardium withdraw from the cell cycle and grow 30–40 times in mass.[73] Besides that, proliferating cell populations were found to present negligible turnover rates (< 1% per year and decreasing with age).[74] Even though there are evidences for cardiac progenitor cells (CPCs) or CSCs residing in the adult myocardium, these subpopulations are considered minuscule (approximately 1 cell per 13,000 myocytes).[71] These cell populations were observed to increase dramatically in number after MI, although 50% exhibited a senescent phenotype incapable of cycling and differentiating.[75] In addition, recruitment and activation of these cells is inadequate to lead to cardiac repair due to physical barriers and lack of appropriate signaling.[69] Overall, these attributes result in insufficient intrinsic regenerative potential, unable to compensate for extensive loss of heart muscle cells in MI.

3.1 Mechanisms for cardiac tissue regeneration

Considering the poor intrinsic capability of the adult heart to properly regenerate, there are key topics towards the best possible tissue regeneration. Achieving effective cardiac regeneration should include tissue recovery following injury (meaning cell survival), overturn or attenuation of tissue remodelling and fibrosis, and myocardium renewal via formation of new myocardium and blood vessels.[70] Therefore, the therapeutics strategies should take in count the following processes associated with MI:

- **Cardioprotection**

Myocardial preservation post-MI and throughout remodelling mitigate long-term damage and cardiac dysfunction.[76] Preservation of tissue and cellular function is imperative to maintain functionality of the heart by inhibition of apoptotic signalling pathways and/or induction of pro-survival signals.[77] CM survival is critical for the preservation of myocardium for ongoing hemodynamic performance and limitation of remodelling with a mechanism associated with inhibition of senescence, reduction of inflammation, allowing for generation of new myocytes, angiogenesis and vascularization.[78]

- **Inflammation reduction**

In response to ischemia, necrotic CM signalling initiates a proinflammatory response for remodelling and regeneration. The second phase includes an anti-inflammatory response, the purpose of which is to allow wound healing and scar formation. The shift between each of these responses is tightly regulated by multiple interactions between cellular myocardium components and the immune system.[70] Manipulation of the time frames of the pro/anti-inflammatory response after MI by changing the chemokine/cytokine profile or cellular responses may allow proper tissue repair to occur rather than the undesired results of an excessive inflammation, including cell death and scarring.[79]

- **Extracellular matrix remodelling and cardiac fibrosis**

Attenuation of the fibrotic response, meaning ECM composition changes and scar formation, by altering pro-fibrotic signalling pathways.[70] In order to reconstruct tissue organization and functionality, it is essential to supply the cells with appropriate mechanical

support, topographical guidance, and proper biochemical signalling to allow desired tissue organization, differentiation, and maturation *in situ*.[80]

- **Angiogenesis and vascularization**

Formation of new blood vessels to allow appropriate nutrient supply to the ischemic regions. This could be achieved by induction of pro-angiogenesis signals, including proteins, ECs recruitment, and altering inflammation and scarring.[81] Vessels deliver oxygen, metabolites and export waste products and new blood vessel formation is essential for recovery of tissue function after ischemia or tissue injury. Impaired circulatory flow correlates with a poor prognosis in patients cause depressed coronary flow reserve after acute MI.[82]

- **Cardiomyogenesis**

To fully restore cardiac function, it is essential that the infarct zone will be replaced by regenerated myocardium, which could involve proliferation of CPCs/CSCs, proliferation of adult CMs via induction of cell-cycle re-entry, and/or exogenous transplantation of CMs/CPCs.[83] Two primary hypotheses of sources that contribute to new CM formation are the resident stem and progenitor cell pool differentiation and the pre-existing CMs dedifferentiation followed by cell-cycle re-entry. By all accounts, resident CM mitotic activity remains a rare event in late postnatal and adult mice, and degree of myocardial regeneration from pre-existing CMs is functionally insignificant.[84,85]

- **Cell-to-cell communication**

Cell–cell communication within or between organs allows exchange of electric and chemical signals through gap junctions and secretome signalling.[86] Additional outside-in and inside-out signalling within tissue occurs between cells and the ECM to adjust myocardial mechanical force, thereby preserving cardiac function during homeostasis and in response to myocardial injury.[76] Interstitial cells residing between CMs are highly contributory to intercellular communication, response to environment, ECM, and remodelling stimuli.[87,88]

- **Cardiac Aging**

Cardiac aging is a heterogeneous process characterized by increased levels of ROS, genomic DNA damage, epigenetic modifications, and telomere shortening. Consequences of aging pursuant to these deleterious changes include defective protein homeostasis, progressive loss of quality control processes, and accumulation of dysfunctional organelles that directly impact CM, CFs, and stem cell populations. Such stochastic insults initiated by both extrinsic and intrinsic stimuli eventually lead to impaired contractile function, lower hemodynamic performance as well as defective regenerative responses to injury and stress stimuli.[76]

3.2 Myocardium infarction treatment

While current clinical interventions improve patient outcomes, many patients ultimately succumb to HF due to inability to reverse or prevent downstream left ventricle (LV) remodeling.[89] Moreover, some procedures are limited in eligibility due to prior surgeries and patient's medical conditions, which limit the ability to harvest autologous small diameter vessels.[90] Additionally, long-term outcomes associated with both autologous and synthetic graft options are limited due to thrombosis.[91] Finally, standard clinical interventions mainly restore macrovascular reperfusion following MI and fail to address microvascular perfusion deficits contributing to eventual HF.[89]

Currently, the only approved treatments for end-stage HF post-MI are LV assist devices and heart transplantation. The first is plagued by the complications of a chronic external assist device, which include bleeding, right ventricular failure, thromboembolism, primary device failure and infection.[92] And the second is a limited resource in which proper matching of the donor organ to the patient is a great challenge, limiting even further its use.[93] Several surgical approaches have been developed to improve patient survival and quality of life, and which can be an option for patients excluded from cardiac transplantation lists:

- **Ischemic tissue revascularization**

There is agreement that initial treatment is restoring blood flow to the ischemic area via tissue reperfusion. The main alternatives for reperfusion can be classified into pharmacologic, surgical or mechanical. The pharmacological breakdown of blood clots (thrombus) in stenotic coronary arteries is known as thrombolysis. The mechanical

alternative to reperfusion is known as primary percutaneous surgical alternative coronary intervention or primary coronary angioplasty where the occlusion is mechanically expanded to allow blood flow. The surgical alternative is known as coronary artery bypass graft (CABG) surgery, which when compared with angioplasty, is highly invasive (requiring open heart surgery) and requires extra surgery to obtain the vein graft. There are various pharmacological and non-pharmacological interventions used to reduce reperfusion injury. In the case of pharmacological interventions, the use of drugs such as cyclosporine-A, metoprolol and glucose modulators have shown some promising results, but a long list of failed examples makes them a weak alternative. In contrast, non-pharmacological interventions have focused on limiting the infarct size as means to reduce reperfusion injury.[93]

- **Left ventricular reconstruction**

After MI, the formation of scar tissue leads to changes in LV size, shape, structure and physiology through a process known as myocardial remodelling.[94] During this process there is thinning of the LV walls, with the elliptical LV becoming more spherical and dilated.[95] A number of different surgical techniques and modifications have been developed to restore LV shape and reduce its volume to improve LV function and are collectively known as LV reconstruction.[96,97] This is a specific surgical procedure developed for the management of HF with LV remodelling caused by coronary artery disease.[98] Despite its success, these procedures have not found general acceptance in the medical community.[93]

- **Cellular cardiomyoplasty**

Cell transplantation is an area of growing interest in clinical cardiology, as a potential means of treating patients after acute MI. Cellular cardiomyoplasty is a therapeutic strategy in which progenitor cells are used to repair regions of damaged or necrotic myocardium. The ability of transplanted progenitor cells to improve function within the failing heart has been shown in experimental animal models and in some human clinical trials.[99] The progenitor cells involved in these new therapeutic approaches include bone marrow or adipose tissue-derived mesenchymal stem cells (MSCs), hematopoietic precursor cells, endothelial progenitor cells, endogenous CSCs, skeletal muscle-derived cells, induced pluripotent stem cells (iPSCs) and embryonic stem cells (ESCs).[100,101] Three mechanisms have been proposed

to describe how cardiomyoplasty improves myocardial function: transdifferentiation of the administered stem cells into CMs, ECs and smooth muscle cells,[102,103] fusion between the stem cell and endogenous CMs,[104] and release of paracrine factors that stimulate endogenous cardiac repair mechanisms.[105,106] Conflicting results showing a lack of transdifferentiation have put into question its role in cardiomyoplasty and motivated the search of alternative hypotheses like fusion and paracrine signalling.[102,107] Further studies suggested that the lack of transdifferentiation shown was related to differences in experimental procedures but the exact mechanism remains unknown.[108] In addition, it has been consistently reported that the level of fusion between stem cells and CMs remains low[104] suggesting that additional mechanisms may be involved. Current results support paracrine signalling as the principal mechanism for the improvement of myocardial function. In it, stem cells release cytokines and chemokines to stimulate other cells into the regenerative process. In fact, MSCs have been shown to stimulate host myocardial precursor cells to amplify and differentiate into CMs *in vivo*.[109] The clinical application of cellular cardiomyoplasty for the treatment of the ischemic tissues after acute MI involves tissue revascularization, isolation of autologous stem cells from the patient, and implementation through repeat cardiac catheterization or intramyocardial injection.[110] A major limitation for the application of cellular cardiomyoplasty as a treatment option is stem cell retention and engraftment after intramyocardial implantation.[111] A significant proportion of the transplanted cells leak out through the needle track that is made by the puncturing needle or enter systemic circulation.[112] Cell retention is normally less than 10%, regardless of the delivery route within the first 24 hours.[113] Although it was initially thought that cell death by apoptosis was the reason for low engraftment,[114] it has been demonstrated that venous drainage and the contraction of the beating heart are the main reasons for cell loss.[115] Short-term cell retention is necessary for subsequent long-term engraftment and cardiac tissue functional improvement after acute MI. Other unresolved issues include cell delivery method and route, cell distribution, time transplantation, cell type, cell number and viability.[93]

There are new therapeutic approaches involving engineering culture systems, the use of novel biomaterials for mechanical support of the cells and for controlled release of therapeutics, and TE. These surgical techniques, and the use of non-bioactive materials as tissue replacements helped spark the interest in exploring innovative use of biomaterials and

TE constructs.[93] In this context, cardiac patches research and improvement are a solution to the current state of MI treatments.

4. Cardiac Patches

Cardiac patches are engineered constructs that aim to restore cardiac function.[116] There are certain specifications that cardiac patches can try to fulfil in order to promote a better regeneration and assimilation with the surrounding myocardium.

Physically, they can provide mechanical support to the tissue, electrophysiological communication and nutrient supply. A graft incorrectly integrated with the host heart tissue, both mechanically and electrically, could possibly lead to arrhythmia caused by unsynchronized electrophysiological signal transmission between the graft, the host myocardium, and the fibrotic interface in between.[117] Future designs must take into consideration not only the patch's own functionality, but also its assimilation with host myocardium and synchronization.

At a biochemistry level, cardiac patches can have some characteristics but they can also act as a vehicle to deliver therapeutic cargo to the ischemic tissue.[118] Even though cardiac patches improve cell viability and retention by itself, cells engrafted through such constructs or through intracardiac injection could still induce an immunogenic response, which ultimately will lead to allograft rejection.[119] In addition, transplantation not accompanied with suppression of the host immune system will limit transplanted cell survival rate and therefore will result in failing integration.[120] Expanding upon cardiac patch delivery alone, therapeutic cargo such as proteins, cytokines, and growth factors can be incorporated in the cardiac patch to further enhance the therapeutic benefit of this approach.[121,122] The designed scaffolds must try to be accessible for cell migration from areas close to the infarcted zones and allow the formation of blood vessels and nerves.[123] Later, these networks can integrate properly with those of the host.[124]

Cardiac TE aims to manipulate the microenvironment that cells interact with, to facilitate cell assembly and build functional tissue.[125] Engineered cardiac patch is fabricated to offer mechanical support and promote cell engraftment into the region of infarction (**Figure III.1**). Its application helps to limit LV remodelling, prevent dilatation and thinning of the infarct zone, enhance mechanical properties of ventricle, and reduce CM apoptosis.

Also, it aids to retain viable transplanted stem cells, which stimulate the formation of vasculature, myofibroblasts and CMs.[93] Hence, the optimal properties of a scaffold involve: high porosity, microenvironment similar to ECM, good mechanical properties, biodegradability, and biocompatibility.

In this review, a presentation about the most used and important biomaterials in cardiac patches and the use of cellular, acellular and architecture patches in recent years will be giving.

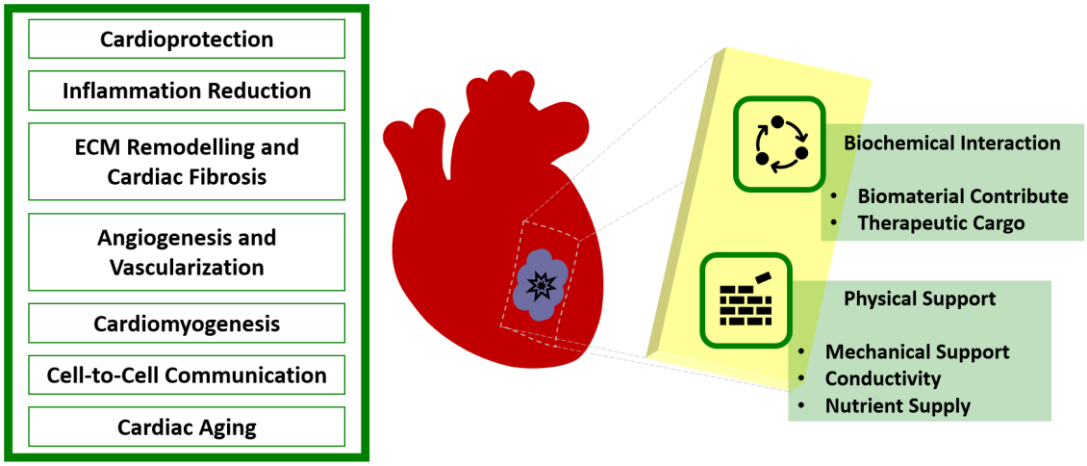

Figure III.1. Resume of needed characteristics for cardiac patches and key topics in cardiac regeneration.

5. Biomaterials

There are several types of biomaterials grouped in two different categories: natural and synthetic origin that have been explored for the preparation of cardiac patches. The combination of materials is also a common practise given rise to a new hybrid patch category, which can be formed by biomaterials from same or different origins. Biomaterials of synthetic and natural origin and some description of the fabricated hybrid patches are analysed in the next sections.

5.1 Synthetic origin

- **Polycaprolactone**

Polycaprolactone (PCL) is a biomaterial used due to its rapid availability, low price and high support capacity.[126] It can show poor nutrient flow but this problem can be overcome with different production techniques.[127,128] Cellular adhesion, function and proliferation on PCL are influenced mainly by material uniformity and, in less impact, by fiber size.[129] Fabrication methods for PCL scaffolds are widely variable, with most focusing on electrospinning as the primary fabrication method.[126] A linear relationship between compressive stiffness and material porosity was found in this material, which can be an important parameter in tissue regeneration and mechanical behaviour.[130]

- **Poly(glycerol sebacate)**

Poly(glycerol sebacate) (PGS) is a biomaterial with mechanical and degradation properties controlled by the ratio of glycerol and sebacic acid, showing a high degree of customization.[131] Its mechanical and structural properties assemble the ones of the myocardium.[132] Even tough, biomimic parameters can be improved by laser patterning modifications which incorporate anisotropic morphologies into the scaffold. The closer is the native cardiac tissue resemble, the more improved native cell alignment is obtained and better the mechanical properties.[133]

- **Poly(lactic-co-glycolic) acid**

Poly(lactic-co-glycolic) acid (PLGA) scaffolds are a popular block copolymer. This biomaterial is highly biodegradable, biocompatible, and easily customizable.[134] The effects already observed with the utilization of this biomaterial include cell proliferation and ventricular remodelling. The addiction of GFs and cells enhance its beneficial effects with better cardiac function obtained.[135]

- **Poly(urethane)**

Poly(urethane) (PU), specially poly(ester urethane urea) (PEUU), is another used biomaterial in cardiac patches. This material can show host CFs penetration and almost completely absorption indicating the patch is able to grow cells capable of withstanding pressure without additional structural support.[136] Another study utilizing this material verified the presence of connective tissue throughout the scaffolding and improved

angiogenesis as well.[137] Mechanical tests to PEUU patches exhibited a good degree of elasticity and had low deformation.[138]

- **Poly(lactic acid)**

Poly(lactic acid) (PLA) is a nontoxic compound that has been widely used in TE.[139] Ring-opening polymerization of lactide in presence of metal catalysts is the mostly used fabrication method, which also yields the production of racemic mixture of D-PLA and L-PLA (PLLA) and D,L-PLA.[140] PLA is biodegradable and the degradation rate depends on the isomer ratio, processing temperature and molecular weight. In comparison with other synthetic polymers, PLA has a high biocompatibility and processability but has poor toughness and an overall slow degradation rate.[141] PLLA cardiac patches can indicated proper cell differentiation and migration into the scaffold, providing evidence of integration into the patch.[142]

- **Poly(ethylene glycol)**

Poly(ethylene glycol) (PEG) is an especially hydrophilic polymer used in TE[143] and is called polyethylene oxide (PEO) or polyoxyethylene (POE) depending on its molecular weight.[144] This biomaterial, produced by the interaction of ethylene oxide and catalysts with water, can contain water to more than 95% of the total volume.[145] Because of this characteristic, PEG is highly permissible and enabling facile diffusion of nutrients. In addition, molecules such as drugs, proteins, and therapeutic vesicles can be attached to the polymer chain of PEG via covalent or noncovalent bonds by a process called PEGylation.[146]

5.2 Natural origin

- **Collagen**

Collagen, specially type I scaffolds, are increasingly being used in tissue repair applications.[93] Collagen is one of the most abundant proteins among ECM components and it plays a key role in maintaining the structural integrity of tissues and providing a biologically suitable environment for cells.[147] The merit of using collagen type I comes from its low immunogenicity which provides a tissue-like environment for cell attachment and growth, facilitating host cell integration.[148] Biocompatibility, biodegradability and fibrous

contractile structure are it main attributes.[149] However, it was shown that solid porous collagen has a lower elastic modulus which can limit its mechanical integration to the cardiac tissue.[150] Other forms of collagen such as gelatin have shown good cardiac cell attachment and viability, but its tensile strength and degradation rates are inferior to collagen, making it a less attractive option for cardiac tissue implants.[93]

- **Hyaluronic acid**

HA is a natural linear polysaccharide found in the ECM of several tissues.[93] Its structure and ligand binding properties have been linked to angiogenesis[151] and tissue repair.[152] In cardiac tissue, HA has shown modest results for cardiac function recovery post MI.[93] The molecular weight of HA affects its regenerative potential in the myocardium with the lowest molecular weight having the most significant regeneration and function recovery of the infarcted myocardium.[153]

- **Alginate**

Alginate is an anionic polysaccharide showing high biocompatibility.[154] Its capacity for *in situ* gelation and non-thrombogenic properties makes it attractive for cardiac tissue applications.[93] Alginate hydrogels have showed improving capability of cardiac function, reduced remodelling and increase neovascularization.[155] However, lack of integration between alginate and cardiac cells might be its major limitation for tissue regenerative applications.[93]

- **Chitosan**

Chitosan is a cationic hydrophilic polysaccharide derivate from chitin.[93] It has been extensively used in biomedical applications including wound healing,[156] drug delivery systems,[157] and surgical adhesives.[158] The porosity of this material can be controlled by freeze drying function, which is important for host cell migration and tissue integration.[159] However, chitosan alone is non-cell adhesive and has a high compressive modulus which requires its chemical modification and/or mixing with other biomaterials to obtain optimal mechanical and physiological properties for cardiac tissue.[93]

- **Fibrin**

Fibrin is a protein formed from the reaction of fibrinogen and thrombin in response to physiological injury such as bleeding.[160] The formation of the fibrin network plays an important role in various pathological processes like inflammatory responses, hemostasis, fibrinolysis and, as already mentioned, wound healing.[161] Polymerized fibrins are cooperative with fibronectin, factor XIII, angiogenic factors and platelets, which yields a hemostatic plug formation that enables them to anchor various cells at the site of injury. Scaffolds of this material have weak mechanical properties compared to other natural materials but a high degradability. Fibrin glue has been tested as an injectable scaffold or even a patch fixer for cardiac tissue repair.[162]

- **Decellularized extracellular matrix**

Decellularized ECMs are derived from biological tissues in which cells have been removed but the components of the ECM are preserved.[93] The main advantage of this kind of matrices is the preserved structure, size and components of native ECM without the presence of cellular antigens that could induce an immune reaction.[163] Although this material is an example of biologically inspired scaffolds close to native tissue, its use is limited by variations according to different donors and the availability of tissue.[164] In cardiac tissue studies, decellularized matrices have shown to promote cardiac cell infiltration due to their potential capacity to promote CM differentiation and/or migration, allowing the ventricular wall to approach its normal thickness, and finally resulting in improved mechanical function.[165]

5.3 Hybrid patches

The combination of biomaterials emerges to compensate limitations of the several materials, despite its origin. By analysis of the respective characteristics, synthetic materials normally show good mechanical proprieties but have limitations at biochemical levels. The opposite is found in natural materials where biochemical properties are strong but don't offer good mechanically capability.[162] Conjugation between synthetic and natural biomaterials is a possible way to overcome these problems but junction of materials from the same origin still providing good results too.

In hybridity between synthetic materials, the use of a patch made from PCL and PGS demonstrated higher mechanical properties compared to native human myocardial tissue which can be beneficial for a reduction in the infarct expansion and LV remodelling.[166] Another patch formed by a sheet of PLLA with a copolymer of lactide acid and poly(lactide-co-caprolactone) to make a longlasting polymeric patch showed an increase of collagen content on the scaffolds.[167] Among natural materials, a patch with collagen and chitosan showed an increase in compression modulus which makes it more suitable for the stabilization of the ventricular wall.[168] Other patch made from the same materials explain the combination of porous chitosan with lower compressive moduli and cell-adherent biomaterials, like collagen, may have the potential to increase tissue integration and therefore increase the mechanical stability of the ventricle post-infarction.[169]

In terms of combination of both types, a scaffold incorporating collagen and elastin into PCL fibers has proven to increase cellular attachment, proliferation, and elasticity. The addition of collagen and elastin even improved Young's modulus and tensile strength compared to the pure PCL scaffold ate certain point.[170] Alternatively, gelatin has also been used in a PCL based scaffold blend to improve cellular compatibility. The blended scaffold was capable of withstanding a greater strain than the pure PCL or pure gelatin scaffolds.[171] A complex patch involved a multi-layered patch with a core of PCL coated in a chitosan and ECM gel showed significant host tissue incorporation. The scaffold experienced a fast degradation of the gel portion while the PCL core had a much slower degradation rate. The multilayer patch induced significant muscular and vascular remodelling.[172] A PGS and fibrinogen scaffold seeded with bone marrow-derived MSCs were implanted in the infarct bed of the LV. This combination of materials increased the LV function, as opposed to the infarct-only control group. Additionally, the presence of cardiac marker proteins showed that this scaffold was instrumental in the differentiation and proliferation of the bone marrow-derived MSCs into cardiac cells.[173] Random and aligned nanofiber patches by using PLA, PEG and collagen were fabricated through electrospinning. A significant increase in electrical conductivity was observed after adding even a small amount of collagen to PLA and PEG. Cell viability before and after degradation test and proliferation studies displayed promising findings.[174] A cardia patch formed by a gelatin-chitosan hydrogel around a self-assembled PCL core discover that gelatin and chitosan ratios of 50:50 and 25:75 significantly improved cell adhesion while retaining the mechanical strength of PCL.[175] For natural

biomaterials, chemical modification of side chain groups is another option to improve mechanical properties.[93] One of this examples is the modification of gelatin with methacrylic anhydride giving rise to gelatin methacryloyl (GelMA) hydrogels which overcome physical limitations of gelatin.[176]

There are plenty of candidates for patch biomaterials and hybridization offers even more room for improvements. Even though biomaterials are only one of the components of cardiac patches, the variety of options in this matter supports the theory that there is not a single solution for cardiac regeneration scaffolds in terms of biomaterials with a lot of possible promising combinations between biomaterials and between biomaterials and other patch components.

6. Cellular component

6.1 Cellular cardiac patches

In recent years, the research on cellular cardiac patches took advantage the use of different cells and biomaterials. Abbasgholizadeh *et al.*[177] build a highly conductive three-dimensional (3D) cardiac patch made of fibrin with incorporated CMs spheroids derived from human adiposederived stem cells (ADSCs) using transcriptor factors and epinephrine. For the purpose of cardiac patch, a proposed range from 5 to 10 million of cells based on histological data and a total number of 10 million cells in terms of electrical conduction properties for a 2 cm x 2 cm patch was proposed as the best cell conditions showing uniformity and rhythmicity. In a long-term culture, with measuring changes in cell distribution and electrical impulse propagation, electrical impulses where recorded on culture with the 3D patch offering great stability and continuously increase in both electrical impulse amplitude and frequency in time. When treated with isoproterenol and epinephrine, an increase in cardiac function genes and electrical impulses amplitude and frequency was register. Their work offers the view of a clinical scenario where a small fat biopsy of the patient can create a cardiac patch with no immune-suppression therapy required. Reports of derived CMs for cardiac patches mostly include protocols using iPSCs.[178–181] In one of the studies, a pattern scaffold of chitosan and collagen was used in order to improve cellular attachment, spreading and orientation. The scaffold allowed CFs and myoblasts adhesion

and proliferation, thus being highly biocompatible. In an experiment with rat CMs it was observed an optimal preference for larger porosity patches with CMs showing favoured spreading, survival and intra-cellular connection. With this optimization, the pattern patch promoted attachment, spreading, and orientation of human CMs.[179]

Utilization of MSCs in patches is also very common (**Figure III.2**). Chang *et al.*[182] used MSCs in a decellularized porcine small intestinal submucosa ECM scaffold. A maximum loading density of 350 000 cells/cm^2 that can be supported on this biomaterial was determined before seeding of cells significantly modify the components and mechanical properties of the patch *in vitro*. For *in vivo* studies, MSCs significantly reduced T-cell infiltration and associated adaptive immune response in an epicardial location, thus showing being beneficial with reducing immune host response in a biomaterial that is already approved by the Food and Drug Administration (FDA). In another cardiac patch report, ADSCs where modified to express specific levels of vascular endothelial growth factor (VEGF). The present patch verified a high level of diffusion of VEGF and, after 14 days, showed a high vessel density from the borders to the centre of the scaffold when compared to control. Implanted cell survival can be significantly improved with this method, benefiting the patch healing capability.[183]

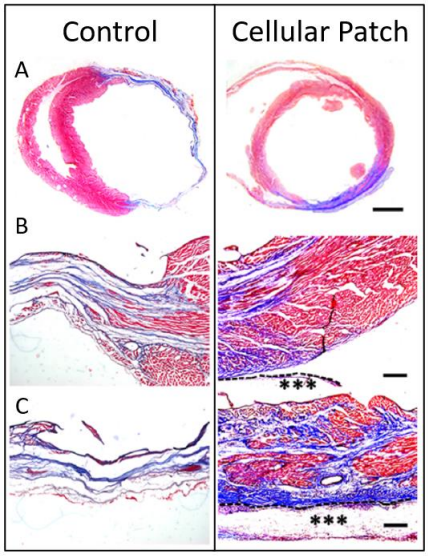

Figure III.2. (A) Transverse sections of the ventricles at the widest part of the infarct region in a rat MI model, 4 weeks after transplantation, with enhanced observation at (B) peri-infarcted area, (C) central infarcted area and (***) MSCs cellular patch position. (Adapted)[184]

Other types of cells showed interesting results to create cellular cardiac patches. Human coronary artery endothelial cells (HCAECs),[185] cardiac adipose tissue-derived progenitor cells (ATDPCs),[186] ADSCs[187] and human umbilical vein endothelial cells (HUVECs)[188] were also tested as cell cargo for cardiac tissue regeneration. For example, in the case of ATDPCs, these cells maintain their cardiomyogenic potential and here capable of migrate to the myocardium and scar in a MI model, improving cardiac function, and increase vessel density.[186] Myocyte regeneration, neovascularization and paracrine activity where pointed out as mechanisms of action of this cells.[189] The cardiac patch used was made of fibrin and cells were synchronous electromechanical conditioned before delivery onto infarcted heart for more efficient cardiac maturation.

Like material conjugation, cell co-cultures in a scaffold is also a research topic in cardiac TE.[190–192] Su *et al.*[190] demonstrate an easy to make fibrin patch including CSCs and encapsulated biomimetic microvessels of HUVECs to create a vascularized structure with cardiac application. In a model of acute MI, the patch induced profound mitotic activities of CM and significant increase in myocardial capillary density in the infarct region compared to controls, thus promoting CM proliferation and neovascularization. The encapsulation of HUVECS may be beneficial in nutrient diffusion for CSCs to facilitate their survival in the challenging infarct environment.

For last, not all cardiac patches use biomaterials. Recents studies also report biomaterial-free options. One report used a cell sheet of placental MSCs and tested their capacity to differenciate in CMs. The placental MSCs cardiac protein content was enhanced by differentiation media treatment. Althouth no beating cells were produced, undifferentiated cells benefit through encouraging migration and proliferation of surrounding cells. Mechanicaly, undifferentiated placental MSCs were formed and intact, aligned cell sheets were obtain.[193] Like cells sheets, spheroids are also used to form patches. A different study used 3D-bioprinting technology to create a structure of spheroids from a co-culture of derived CMs, CFs and ECs. The patch was tested in a MI model where even the survival rate of the group who received the treatment was higher than control. The spheroids reduce the potential for an inflammatory response and the risk of infection induced by scaffold materials. More interesting, cell retention within implanted patches, 4 weeks after surgery, was found to be much greater compared with prior studies, average vessel

counts within the infarcted area were higher and scar area was significantly smaller than control group. By echocardiography, a trend of improvement of cardiac function was observe related to increased patch production of extracellular vesicles.[194]

Kashiyama *et al.*[187] who studied the action of a hybrid patch made of poly(ester carbonate urethane) urea (PECUU) and porcine cardiac ECM with an ADSCs cell sheet by comparing with an acellular version patch and cell sheet patch of ADSCs. In an ischemic cardiomyopathy model, they demonstrated a higher engraftment of ADSCs, remodelling, contractility, preservation of thickness and minimized fibrosis with a PECUU and ECM patch combined with a ADSCs sheet than with a single application of the patch or the cell sheet. Besides these results, the fibrotic area was not significantly different between the patch with or without cells but the main difference was observed on the infiltrated cell number, vascular density and cardiac function, suggesting that the inclusion of cells could benefit these parameters (**Figure III.3**).

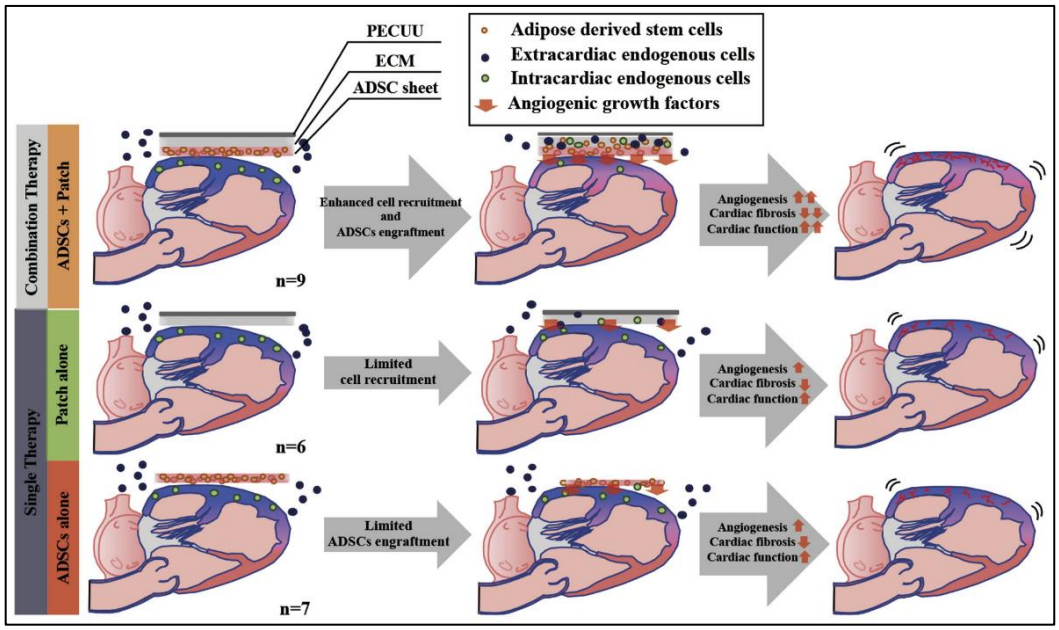

Figure III.3. Enhancement of cardiac function applying a combined therapy using PECUU/ECM patch with ADSCs sheet and single therapies with patch or ADSDs sheet alone. (Adapted)[187]

Another study used decellularized porcine cardiac ECM with MSCs in order to analyse if the addiction of cells could restore some of the original properties of this biomaterial. The main conclusion was the biological active plasticizer role that cells have.

From a biophysical perspective, cell presence results in tenability of the engineered construct. In addition to their space filling function, cells increase the overall protein density and remodelled patch construct according to their needs. These interactions result in increased stabilization of the reseeded construct (and also the native tissue) and hence an increased resistance to harsh external conditions such as denaturation.[195]

In resume, the addiction of cells opens a huge space of opportunity to increase regeneration capacity by the several amounts of different cells types and technologies, existing already substantial *in vitro* and *in vivo* data. Overall, the main requisites for functional cardiac patches with successful cardiac tissue improvements are the alignment of CMs (and stem cells) with the synchronous electromechanical contractile force and healing process, supportive allowed by the scaffolding structure to mimic the mechanical and biochemical properties of native tissue. Also, the generation of functional microvasculature to provide adequate nutrient and oxygen delivery for cells on the patch and on native tissue, not provoking immunogenic response on the host and suitable degree of cell maturation for successful implantation and host tissue integration.[8] **Table III.1** presents the main information on cardiac structures constructed on recent years with implied intentioned on having cellular content within patches in the field of cardiac regeneration research.

Table III.1. Cellular cardiac patches for tissue regeneration research in recent years.

Type of patch	Cell type	Origin of cells	Materials	Ref
Biomaterial Patch	Derived CMs spheroids	Human ADSCs	Fibrin	[177]
	Derived CMs	Human iPSC	PCL and Gelatin	[178]
			Chitosan and Collagen	[179]
			Decellularized human omental tissue	[180]
			Decellularized human amniotic membrane	[181]
	CMs	Neonatal Sprague-Dawley rat ventricle	PCL and Gelatin	[196]
	Human MSCs	-	Decellularized porcine small intestinal submucosa ECM	[182]

			Decellularized porcine cardiac ECM	[195]
			SOEA	[197]
			PCL	[198]
			Fibrin	[199]
	MSCs	Bone marrow of male Sprague-Dawley rat	PCL and Gelatin	[184]
		Cervical subcutaneous adipose tissue from a GFP-positive transgenic rat	Decellularized pericardia of white New Zealand rabbit	[200]
	VEGF expressing human ADSCs	-	Collagen	[183]
	Human MSC spheroids		Collagen	[201]
	HCAECs		Alginate and MeCol with carboxyl functionalized carbon nanotubes	[185]
	Human cardiac ATDPCs		Fibrin	[186]
	ADSCs	Inguinal subcutaneous adipose tissues of GFP transgenic Fischer 344 rat	PECUU and porcine decellularized cardiac ECM	[187]
	HUVECs	-	PCL and Collagen	[188]
	Human CSCs and encapsulated HUVECs		Fibrin	[190]
	Human MSCs and ECs		Decellularized human dermal fibroblast sheet	[191]
	HUVECs, CMs and CFs	Neonatal Sprague Dawley rat (CMs and CFs)	PELA	[192]
Spheroid patch	Derived CMs, human CFs and HUVECs spheroids	Human iPSCs (derived CMs)	-	[194, 202, 203, 204]
	Derived CMs spheroids	Human iPSCs		[205]

Cell sheet	MSCs	Human amnion and chorion placental tissue	-	[193]

SOEA: soybean oil epoxidized acrylate; GFP: green fluorescent protein; MeCol: methacrylated collagen; PELA: poly(ethylene glycol)-poly(DL-lactide)

6.2 Acellular cardiac patches

Although cellular patches provide much needed benefits for cardiac tissue regeneration, their limitations were the starting point for searching solutions for clinical application. Acellular versions or substitution of cells for other cardiac improving factors where the two main flows of research over the last years to address this problem.

In terms of acellular cardiac patches, results showed that, even with the absence of cells, scaffolds still improving cardiac function. D'Amore *et al*.[206] used an PECUU patch with decellularized porcine heart ECM to evaluate the incorporating of this natural material in a chronic MI model. The results showed alteration on progression of several keys aspects of maladaptive remodelling following MI. This included decreasing LV global mechanical compliance, inhibiting echocardiographically-measured functional deterioration, mitigating scar formation and LV wall thinning and promoting angiogenesis. The study demonstrates the benefit of a cardiac patch design that combines both ventricle mechanical support, through a biodegradable, fibrillary elastomeric component, and the incorporation of ECM based components, like review in the hybrid patches section. Another study developed a polypyrrole-chitosan conjugated patch that could mimic the mechano-electronic cardiac function for tissue healing. The scaffold demarking CMs maturation and integrity, reduced fibrosis, abundant angiogenesis and improved heart function when transplanted to a MI model.[207] Other study with a decellularized porcine pericardium ECM patch evaluate the decellularization process and biomechanical properties after the decellularization treatment. Histologically analysis showed the preservation of the ECM without any observable cellular remnants and mechanical tests showed no significant differences between native and decellularized tissues. In the biocompatibility assay, no toxic effects were noticed when human MSCs were attached on the patch. After implantation, the graft remained for 12 weeks without being rejected.[208] Francisco *et al*.[209] transplanted a decellularized amniotic membrane scaffold with the *in vivo* model having its pericardium excise and substituted by

the patch. The results showed preserved integrity of the patch, no calcification on the surface of the myocardium and thicker pericardium repair tissue when compared with control after 4 weeks. The patch induced cardiac protection and host cells organization with tissue fibrils and capillaries clearly identified and the host, virtue of the low immunogenicity, evoked minimal host versus graft reaction. Other ECM patch even used a decellularized porcine myocardium slice for this end. In a MI model, the graft was firmly attached to host myocardium after implantation, preventing thinning of the LV. The patch promoted infiltration of a large number of host cells and a significant number of vessel structures was observed in the patch and in the infarcted area. With that, contraction of the LV wall and cardiac functional parameters were improved after 4 weeks with a reduction of the infarcted area.[210]

The substitution of cells for components that also promote beneficial effects is a widely camp of research, especially when cardiac patches are capable of incorporate different substances. Nair *et al*.[211] produced a scaffold of decellularized porcine cholecystic ECM with gold nanoparticles for achieving homogeneity in surface architecture. The physical properties of the modified scaffold were similar to the acellular biomaterial patch and was found to be a suitable substrate for the growth and proliferation of the H9c2 cells, a cardiomyoblast cell line commonly used for cellular and molecular studies of cardiac cells. Further, the non-cytotoxic nature of the scaffold was established by direct contact cytotoxicity testing and live/dead staining. Another study using a PLLA patch incorporating granulocyte colony-stimulating factor (GCSF) was tested in a MI model. Functionalization of the scaffold with GCSF led to increased fibroblast-like vimentin-positive cellular colonization and reduced inflammatory cell infiltration. This graft induced an angiogenetic process with a significant increase in the number of neovessels and induced reorganization of the ECM architecture leading to connective tissue deposition and scar remodelling. These findings were coupled with a reduction in end-systolic and end-diastolic volumes, indicating a preventive effect of the scaffold on ventricular dilation, and an improvement in cardiac performance.[212] A patch with PCL and gelatin enriched with Salvianolic acid B and Magnesium L-ascorbic acid 2 phosphate (MAAP) showed sustained delivery of bioactive signals, improved cell adhesion, proliferation, migration and differentiation of H9c2 cell lines, increase expression of cardiac specific markers and expression of proteins, confirming cell to biomaterial interactions. Further, *in vivo* studies confirmed the efficacy of the

developed scaffold in inducing angiogenesis required for maintaining its viability after transplantation onto the infarcted zone.[213]

Patch material can also receive treatment to reduce limitations like antigenicity. One study used male Sprague–Dawley rats heart ECM treated to disassembly sarcomeres and remove antigens, which would produce a xenogeneic scaffold. The treated material showed unchanged component content, increase elasticity modulus and significantly decreased antigenicity, underscoring the notion that antigenic components might not be associated with the cellular components of the tissue.[214] A different strategy consist of build synthetic cells formed by encapsulated beneficial factors. Huang *et al*.[215] used a decellularized porcine myocardial ECM scaffold with synthetic CSCs generated by encapsulating secreted factors from isolated human CSCs. The objective is to mimic the therapeutic features of live stem cells, while overcoming their storage and survival problems and preserving the ECM structure and bioactivity. The synthetic cells were stable and maintain their therapeutic potency after 28 days of cryostorage. In two acute MI models, patch transplantation improved heart pump function, reduced fibrosis/infarct size, increased viable myocardial tissue and promoted angiomyogenesis.

Acellular versions of cardiac patches are also a viable option for tissue regeneration. Implanting important factors in patches can partial overcome cells limitations and mimic their beneficial effect in an easier way for commercialization, although the same results in terms of regeneration are not normally achieve. Like cellular patches, natural biomaterials dominate research. Apart from cell integration, requisites for acellular patches are similar to cellular patches with the scaffolds matching native heart elasticity, being mechanically stable, provide nutrient and oxygen diffusion and being nonimmunogenic to support tissue function and regeneration.[93] **Table III.2** presents the main information on acellular cardiac structures constructed on recent years in the field of cardiac regeneration research.

Table III.2. Acellular cardiac patches for cardiac tissue regeneration research in recent years.

Type of patch	Cardiac regeneration improving factors	Materials	Ref
Acellular patch	-	PECUU and decellularized porcine heart ECM	[206]

		Polypyrrole and chitosan	[207]
		Decellularized porcine pericardium ECM	[208]
		Decellularized amniotic membrane	[209]
		Decellularized porcine myocardium slice	[210]
		PU and siloxane	[216]
		Decellularized porcine cardiac ECM	[217,218]
		Decellularized porcine small intestinal submucosa ECM	[219]
		Decellularized bovine myocardium ECM and chitosan	[220]
		Ionically crosslinked hydrogel formed by reaction of $Ca(NO_3)_2$ $4H_2O$ with waxy starch	[221]
		PU, PEG and PVCL	[222]
		Chitosan	[223]
		PGS and PCL	[224]
		PCL	[225]
		P(3HO)	[226]
Acellular patch with cardiac regeneration improving factors	Gold nanoparticles	Decellularized porcine cholecystic ECM	[211]
	GCSFs	PLLA	[212]
	Salvianolic acid B and MAAP	PCL and Gelatin	[213]
	Sarcomere disassembly and antigen removal	Male Sprague-Dawley rats heart ECM	[214]
	Synthetic cardiac stromal cells	Decellularized porcine myocardial ECM	[215]
	Cerium oxide nanoparticles	PCL and Gelatin	[227]
	Titanium dioxide particles and basil oil	PU	[228]
	Selenium nanoparticles	Chitosan	[229]
	Extracellular vesicles	Collagen	[230]
	Porous silica nanoparticles with VEGFs and PDGFs	PLGA	[231]

	Gold nanorods	GelMA	[232]
	GelMA-polypyrrol nanoparticles	GelMA and PCL	[233]

PVCL: polyδ-valerolactone-cε-caprolactone; P(3HO): poly(3-hydroxyoctanoate); PDGF: platelet-derived growth factor

7. Cardiac patch architecture

Over the last years, besides the research on cellular, non-cellular and biomaterial content, the demanding better results for tissue regeneration promoted the optimization of cardiac patches. Details like patch architecture become interesting ways of promoting regeneration, which raised concerns in cellular spatial organisation and topography of the patch itself.

Many strategies for cellular spatial organisation have focused on generation of cellular spheroids or cell sheets for enhanced blood vessel growth, blood perfusion and cellular activity of the constructs *in vivo*.[234] At the macroscale, native heart contains elongated myofibers aligned in parallel enabling coordinated contraction of the ventricle and expulsion of blood. At the microscale, adult CMs are rod shaped and contain registries of sarcomeres that enable cell contraction in response to electrical signals. At the nanoscale, each sarcomere contains precisely organized sarcomeric proteins (for example, sarcomeric α-actin/α-actinin and myosin heavy chain) that enable coordinated contractions of sarcomeres.[235] In fibrotic disease, there are numerous changes in the alignment of CMs and in the composition and orientation of ECM proteins.[236] The response of cells to the changes in microenvironmental signals, substrate stiffness, surface or molecular composition is enabled by biochemical pathways via mechanotransduction mediated ligand receptor interactions which influences cell behaviour at the nano, micro and macroscale with respect to the expression of specific genes and proteins, cytoskeletal structure, morphology and functionality.[235] The main complexity involved in engineering functional myocardium is related to establishing appropriate structure-function correlation over different scales to induce controlled cellular responses like desired orientation and morphology that can benefit the infarct tissue[8,237] and induce the self-assembly of additional consistently organized layers of cells and ECM.[235]

7.1 Cellular spatial organisation

Given the recent patch information, two main cellular organisation types where used: spheroids and cell sheets. Spheroids are 3D multicellular models in which cells are aggregated in a spherical architecture.[162] The common method to form spheroids by aggregation is to utilize gravity by the hanging-drop method and the non-adhesive surface method.[238] They differ significantly from two-dimensional (2D) tissues in structure, function and morphology and, in case of CMs, also influences cardiac function and maturation.[239] Spheroids allow cell-to-cell junctions to form not only with the cells next to them but also with the cells around them. Furthermore, cardiac spheroids can be co-cultured with other types of cells such as CFs and ECs, which are components of native heart matrix, potentiating this way their use.[240] The gravity-assisted methods, however, can only regulate the number and type of cells, commonly yielding unsynchronized contraction. To overcome this limitation, electrically conductive materials can be added during the preparation of spheroids.[241] In another study, the effect of cell numbers on spheroids was evaluated, which suggests that a spheroid composed of 3 000 cells can form the best cell-to-cell junctions without core necrosis due to an insufficient oxygen supply.[242] These studies imply that cardiac spheroids can be improved by adding functional materials and modulating the number of cells per spheroid.

On the other hand, cell sheets are confluent layers of cells that are commonly used in engineering patches for cardiac tissue repair.[243] Cell sheets are formed by detachment of 2D cell monolayers using surface detachable polymers or magnetic particles.[93] In this type of tissues, CMs are mostly scattered and only a small portion of the adjacent cells form cell-to-cell junctions.[162] The stacking or rolling of monolayer cell sheets turns this configuration into a 3D structure.[238] However, due to poor vascularization, the thickest these sheets can be stacked is around three layers (< 300 μm).[244]

Cell spatial organisation with 3D spheroids or 2D/3D cell sheets are two different conformations for cell interaction, especially if differs from 3D to 2D. Nevertheless, the organisation of cells can be an improving factor for cardiac patches since cell-to-cell junctions are form and communication is promoted, which is an important subject in tissue regeneration previously reviewed.

7.2 Patch topography

The function of myocardial cells is tightly related to their structure and alignment, which includes the contractility and maturation of CMs.[245] The main outcomes of cell alignment studies refer parallel topography/ aligned fibers as the best conformation to obtain aligned CMs. The parallel topography gives better alignment if its constructed without interruptions since CMs prefers long parallel lines to the adding of spatial interruptions over topographical length.[246] Even using certain topographies as squares, CMs still demonstrated the correct adhesion, maintenance of function and alignment with mainly parallel features.[224] The distance between lines can also influence the alignment. If the space between lines is greater than cell size, the cells can fall into the grooves but also spread on the steep sidewalls on either side of the grooves, if the material allows, given rise to cells on different levels of high. If this space is reduced to less than cell size, cells don't fill the groove space and grow at the same high level. Cells can even be aligned in a certain shape. A material with the wanted shape can be added with parallel topographical patterns which allows cellular alignment. This can be used, for example, to fabricate a cardiac patch with the shape and needed alignment of the infarcted area (**Figure III.4**).[197] A study enhanced accentuated differentiation on aligned fibers which exhibited elevated expression of known cardiac markers such as cardiac actinin, cardiac troponin and myosin heavy chain, demonstrating that aligned nanofibrous scaffolds augment cardiomyogenic differentiation wherein topography plays a critical role in driving function.[198] However, the inherent weak mechanical properties of aligned fibers impeded the utilization on cardiac patch for TE. One of the solutions is the use of random fibers. Fabrication of a patch with a specific angle to mimic anisotropy of native cardiac muscle with central aligned nanofibers and edge random nanofibers enabled alignment of CMs in the central region and resistance owing to the edge region.[188] Another study with hybridization of random and aligned fibers also report the same mechanical reinforcement and alignment.[225]

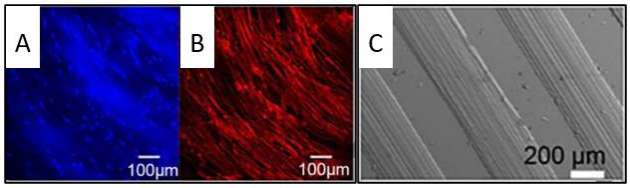

Figure III.4. (C) SEM image of a circular shape parallel micropattern scaffold seeded with MSCs and enhanced observation of the micropattern. (A) DAPI blue fluorescent dye stain cell nucleus and (B) Texas red fluorescent dye satin cell cytoskeleton. (Adapted)[197]

Advances in the development of microfabrication technologies allow us to generate highly organized microvascular networks to guide the formation of microvasculature in tissue constructs.[247] Su *et al*.[190] showed a patch having encapsulated preformed biomimetic microvessels formed by HUVECs. These vessels where constructed hoping to help the incorporated CSCs in the patch get nutrients from the heart to facilitate their survival in the challenging infarct environment, besides the interaction between these two types of cells. In an acute MI model, this patch could improve cardiac function as reviewed previously. Another study created an oriented and dense microvessel network with physiological myocardial microvascular features. Results demonstrate that the ECM topography could be translated to ECs, significantly improving crosstalk of ECs with the incorporated MSCs and vascular network formation. Also, the aligned ECM nanofibers of the patch enhanced the structure, length and density of microvascular networks compared to randomly organized nanofibrous ECM. The co-culture promoted secretion of pro-angiogenic growth factors and matrix remodelling which resulted in highly dense vascular network formation with intercapillary distance similar to the native myocardium.[191]

Topographical conformation can also interact with other factors to mitigate limitations on cardiac patches. One of these examples is the use of gold nanorods (GNRs) that provide electrical relevant myocardium function. On this study, parallel grooves still give alignment and enhanced cellular connectivity and, with GNRs, a more conductive material is created.[232] Also, the control of porosity could improve cardiac patches. Enhanced cell adhesion and proliferation properties are observed when porous and fibrous structures were incorporated to the patches.[226] It is important to mention that although porous structures provide more surface for cell residence, the number of porous structures that can be created are limited given the reduction of mechanical properties with high porosities.[248] Stiffness can increase the adhesion rate and development of actin filaments of CMs which affects

contract capability of this cells. The alignment of fibers increases stiffness but the biomaterial still has a huge impact on this parameter. Although cellular stiffness is partially related with cell-to-cell junctions and attachments, it suggests that biomaterial and cell attachment is also important for the mechanical properties of CMs. Therefore, coating with appropriate materials is highly necessary to mediate the maturation and function of CMs.[249] Discussion about biomaterials and cellular components have already been discussed as two main topics in cardiac patches but optimization allows better mimic of the cardiac native tissue which is why topography, and the related conductivity, porosity and stiffness, are positive features for improving tissue regeneration.

8. Cardiac patches in pre-clinical and clinical use

As cardiac patch research presents progressive positive results, tissue-engineered constructs are beginning their transition to clinical studies and commercially available products, with the target group reaching being the ultimate goal of science research.

The pathway to obtain this market approval can differ due to different regional and institutional regulations but there are some recommendations that should accompany this translational process to assure a better outcome. Since each cardiac patch can have different structural and functional demands when used as a treatment, specific performance criteria should be determined to predict how well the product will translate into the clinical trials and clinical use. Criteria to considered can include durability, connectivity and cell viability, proliferation and function if cells are present in the cardiac patch, with both *in vitro* and *in vivo* information included. All tests should also try to mimic, in the best way possible, the actual clinical circumstances in which the cardiac patch will be used, even using appropriate animal models' studies to mimic the biochemical and physiological interactions likely to occur in humans. This way, researchers can predict the patients' responses and product efficacy while performing the implantation guidelines used.[250]

For cardiac patches, there are three platforms of TE approaches: cellular cardiac patches, cellular biomaterial-free cardiac patches and acellular cardiac patches with each approach having different strengths and weaknesses.[251] With cellular cardiac patches, both cellular and biomaterial benefits are access with recent clinical trials and research showing potential safety, efficacy and cardiac tissue improvements. The weakness of this approach

relies on the more complex design, the potential weakness of the cells and biomaterials that compose the patch and the fact that current data does not show it as a superior product to cellular therapeutics. For cellular biomaterial-free cardiac patches, the cellular paracrine effect, the possibility of use autologous or allogenic cells and the cellular architecture design can promote the use of this technology, although problems with electrical synchronization, cell integration and survival, host rejection and the introduction of cell dosing may difficult their use. For last, acellular cardiac patches have strengths for their structural formation, possibility of choosing the biomaterial composition and enhanced efficiency for vascularization while still having risks for host rejection, host cellular integration and inflammatory and scar reactions.[252] In resume, the necessary information and research need to be adapt to the different benefits and problems that each technology offers.

If the cardiac patch meets the necessary criteria, necessity and potential as a cardiac patch product, these can move to clinical trials. Where, all the previous information will be tested in the human body complexity and confirm the safety, efficacy and durability of the product. Organizations that control products market approval have access different standards that tissue engineered products must fulfil to obtain this distinction. In order to be valid, clinical trials must be well prepared and controlled so the outcomes can truly determinate the healing capacity and user safety of the product and are taking in count by responsible organizations. Also, commercially available products should need information of shelf life and stability and taking in count production scale while maintaining quality and uniformity. By the end of this process, a valid idea of advantages and disadvantages of the product should be clear to establish the right conditions for proper application and, if the patch meet all the necessary criteria and regulations, it can be available for commercialization (**Table III.3**).[250]

Table III.3. Cardiac products with applications for cardiac regeneration or repair and the corresponding manufactures and materials registered on the United States Food and Drug Administration (FDA).[253]

Manufacturer	Product Name	Materials
Lemaitre Vascular, Inc.	CardioCel	Collagen
Aziyo Biologics, Inc.	ProxiCor For Cardiac Tissue Repair	Porcine Small Intestine Submucosa ECM
	ProxiCor For Pericardial Closure	
	Tyke	

Bard Peripheral Vascular, Inc.	ePTFE Cardiovascular Patch	ePTFE
Cook Biotech, Inc.	CorMatrix for Pericardial Closure	Porcine Small Intestine Submucosa ECM
	CorMatrix for Cardiac Tissue Repair	
CryoLife, Inc.	PhotoFix	Decellularized Bovine Pericardium
Edwards Lifesciences LLC	Edwards Bovine Pericardial Patch	Decellularized Bovine Pericardium
Glycar SA PTY., LTD.	St. Jude Pericardial Patch w/ EnCap AC Technology	Bovine pericardium with anti-calcification treatment
MAST Biosurgery, Inc.	Cardio-Wrap Bioresorbable Sheet	PLA
W. L. GORE & ASSOCIATES, INC.	GORE PRECLUDE	ePTFE
	GORE-TEX Cardiovascular Patch	

ePTFE: expanded Polytetrafluoroethylene

As seen by the current cardiac products approved, the quantity of different products stills very low and not focus on cardiac patch itself but more on products for suture the cardiac and vascular tissue. Also, the materials used are limited to animal and synthetic origin and do not include the use of cells. In terms of opportunities, a very small market can be appellative for the creation of new and promising products, together with the cardiac patch for MI treatment not exactly explored at the current state. Although, the commercialization of products with cells stills very challenging because of the previous mentioned reasons related to conservation and products lifetime problems. As research and clinical trials advance, some challenges need to be taken in count when developing future cardiac patches as the general nature of HF is represented as a geriatric disease,[254] there is a high frequency of diagnosed comorbidities in patients with HF,[255] and there is a disconnection between earlier studies involving preclinical animal models compared to the patient population requiring treatment[256].

9. Conclusion and future perspectives

Currently, the LV remodelling, dysfunction and hypertrophy after MI are some of the most significant clinical problems.[125] With developments on biomaterials, recent cellular and acellular approaches and patch architecture, TE increases the clinical relevance for functional cardiac patches to address solutions.

Proper biomaterial selection is an important option for the eventual success of the cardiac patch given the varying properties that may play a large role in how the patch performs. The common principle behind the use of biomaterials is their ability to function as potential mediators between the therapeutic agents and their target, while also having beneficial influence on their own.

There are two potential approaches for cardiac patches: cellular scaffolds that provide the combination of cells and biomaterial composition needed for increased biological activity and biophysical support, and acellular scaffolds that provide biological activity and biophysical support to the heart.[257] Recent patches of either strategy reveal promising results post-MI with improved regeneration and function of the cardiac tissue. Between the two types of patches, cellular scaffolds might have more limitations than acellular grafts but they demonstrate more capacity of regeneration because of cellular component factor[187] which enhances biochemical paths connected to cell communication and participation. This difference can be reduced on acellular patches by incorporation of various types of components.

In terms of optimization, cellular spatial organization with spheroids and cell sheets can be co-assembled with biomaterials to improve biological functions. Also, the parallel topography on patches mimics the aligned myocardial tissue of the heart and can influence cells function and performance. Considerations for conductivity, porosity and stiffness are too part of the cardiac ECM complexity and cardiac microenvironment, thus having influence on CMs function.[238]

To date, the clinical trials for some biomaterials showed their safety, encouraging results and implying improvement in cardiac function. There is a need to understand the functional integration and the signalling pathways that must be activated to achieve the proper inflammatory responses, inhibit tissue degradation and reduce adverse remodelling that leads to scar formation and most of them still not clear. These are all factors that must be considered when designing such treatment to reduce HF, so integration and healing ability is achieve.[126] As research continues to converge biomaterials, molecular biology and TE, cardiac patches will become an increasingly feasible option for the treatment of MI.[125]

In future, the approval of cardiac patches raises concerns on commercial production and storage of these TE constructs. The production of this technology must comply with industrial engineering ethics and standardization so that these patches can be produced with

efficiency and consistency and stored in a way that maintains a reasonable shelf-life.[258] With heart diseases affecting so many people world-wide and growing in prevalence every year,[126] regenerative therapies are at the forefront of research to improve the outcome for patients.

In conclusion, new discoveries and promising clinical outcomes in the field of cardiac regeneration give us optimism on finding suitable cardiac patches for tissue regeneration. The present knowledge for scaffolds construction has already defined some basic knowledge on how to create and optimize patches. However, in order to fulfil the true potential of this technology, the address limitations need to be overcome.

References

1. Virani, S. S. *et al.* Heart Disease and Stroke Statistics -2020 Update: A Report From the American Heart Association. *Circulation* **141**, e139–e596 (2020).
2. Khan, M. A. *et al.* Global Epidemiology of Ischemic Heart Disease: Results from the Global Burden of Disease Study. *Cureus* **12**, e9349 (2020).
3. Bui, A. L., Horwich, T. B. & Fonarow, G. C. Epidemiology and risk profile of heart failure. *Nat Rev Cardiol* **8**, 30–41 (2011).
4. He, L. & Chen, X. Cardiomyocyte Induction and Regeneration for Myocardial Infarction Treatment: Cell Sources and Administration Strategies. *Adv. Healthc. Mater.* **9**, 2001175 (2020).
5. Zhou, B. *et al.* Epicardial progenitors contribute to the cardiomyocyte lineage in the developing heart. *Nature* **454**, 109–113 (2008).
6. Bergmann, O. *et al.* Evidence for cardiomyocyte renewal in humans. *Science (80-.).* **324**, 98–102 (2009).
7. Cohn, J. N., Ferrari, R. & Sharpe, N. Cardiac remodeling--concepts and clinical implications: a consensus paper from an international forum on cardiac remodeling. Behalf of an International Forum on Cardiac Remodeling. *J. Am. Coll. Cardiol.* **35**, 569–582 (2000).
8. Thavandiran, N., Nunes, S. S., Xiao, Y. & Radisic, M. Topological and electrical control of cardiac differentiation and assembly. *Stem Cell Res. Ther.* **4**, 14 (2013).
9. Stehlik, J. *et al.* The Registry of the International Society for Heart and Lung Transplantation: Twenty-eighth Adult Heart Transplant Report--2011. *J Hear. Lung*

Transpl. **30**, 1078–1094 (2011).

10. Vollmer-Conna, U., Cvejic, E., Smith, I. G., Hadzi-Pavlovic, D. & Parker, G. Characterising acute coronary syndrome-associated depression: Let the data speak. *Brain. Behav. Immun.* **48**, 19–28 (2015).
11. Jensen, R. V., Hjortbak, M. V. & Bøtker, H. E. Ischemic Heart Disease: An Update. *Semin. Nucl. Med.* **50**, 195–207 (2020).
12. Kasprzyk, M., Wudarczyk, B., Czyz, R., Szarpak, L. & Jankowska-Polanska, B. Ischemic heart disease – definition, epidemiology, pathogenesis, risk factors and treatment. *Postępy Nauk Med.* **31**, 358–360 (2018).
13. Katz, P., Leiter, L. A., Mellbin, L. & Rydén, L. The clinical burden of type 2 diabetes in patients with acute coronary syndromes: prognosis and implications for short- and long-term management. *Diabetes Vasc. Dis. Res.* **11**, 395–409 (2014).
14. Wessler, J. D. & Kirtane, A. J. Patients who require non-cardiac surgery in acute coronary syndrome. *Curr. Cardiol. Rep.* **15**, 373 (2013).
15. Ferrari, R. & Fox, K. Heart rate reduction in coronary artery disease and heart failure. *Nat. Rev. Cardiol.* **13**, 493–501 (2016).
16. Jankowski, P. *et al.* Practice setting and secondary prevention of coronary artery disease. *Arch. Med. Sci.* **14**, 979–987 (2018).
17. Chaudhry, M. A. Heart Failure. *Curr. Hypertens. Rev.* **15**, 7 (2019).
18. Severino, P. *et al.* Diabetes Mellitus and Ischemic Heart Disease: The Role of Ion Channels. *Int. J. Mol. Sci.* **19**, 802 (2018).
19. Neumann, F. J. *et al.* 2019 ESC Guidelines for the diagnosis and management of chronic coronary syndromes. *Eur. Heart J.* **41**, 407–477 (2020).
20. Rayahin, J. E., Buhrman, J. S., Zhang, Y., Koh, T. J. & Gemeinhart, R. A. High and low molecular weight hyaluronic acid differentially influence macrophage activation. *ACS Biomater. Sci. Eng.* **1**, 481–493 (2015).
21. Kong, P., Christia, P. & Frangogiannis, N. G. The pathogenesis of cardiac fibrosis. *Cell. Mol. Life Sci.* **71**, 549–574 (2014).
22. Suthahar, N., Meijers, W. C., Silljé, H. H. W. & de Boer, R. A. From Inflammation to Fibrosis-Molecular and Cellular Mechanisms of Myocardial Tissue Remodelling and Perspectives on Differential Treatment Opportunities. *Curr. Heart Fail. Rep.* **14**, 235–250 (2017).

23. Lee, S. B. & Kalluri, R. Mechanistic connection between inflammation and fibrosis. *Kidney Int.* S22–S26 (2010). doi:10.1038/ki.2010.418
24. Wynn, T. A. & Ramalingam, T. R. Mechanisms of fibrosis: therapeutic translation for fibrotic disease. *Nat. Med.* **18**, 1028–1040 (2012).
25. Wilhelm, D. L. Mechanisms responsible for increased vascular permeability in acute inflammation. *Agents Actions* **3**, 297–306 (1973).
26. Zheng, W. *et al.* Role of osteopontin in induction of monocyte chemoattractant protein 1 and macrophage inflammatory protein 1β through the NF-κB and MAPK pathways in rheumatoid arthritis. *Arthritis Rheum.* **60**, 1957–1965 (2009).
27. Wight, T. N., Kang, I. & Merrilees, M. J. Versican and the control of inflammation. *Matrix Biol.* **35**, 152–161 (2014).
28. Litwiniuk, M., Krejner, A. & Grzela, T. Hyaluronic Acid in Inflammation and Tissue Regeneration. *Wounds* **28**, 78–88 (2016).
29. Ueha, S., Shand, F. H. W. & Matsushima, K. Cellular and molecular mechanisms of chronic inflammation-associated organ fibrosis. *Front. Immunol.* **3**, 71 (2012).
30. Bochaton-Piallat, M. L., Gabbiani, G. & Hinz, B. The myofibroblast in wound healing and fibrosis: answered and unanswered questions. *F1000Research* **5**, F1000 Faculty Rev-752 (2016).
31. Newby, A. C. Metalloproteinase expression in monocytes and macrophages and its relationship to atherosclerotic plaque instability. *Arterioscler. Thromb. Vasc. Biol.* **28**, 2108–2114 (2008).
32. Grabiec, A. M. & Hussell, T. The role of airway macrophages in apoptotic cell clearance following acute and chronic lung inflammation. *Semin. Immunopathol.* **38**, 409–423 (2016).
33. Fadok, V. A. *et al.* Macrophages that have ingested apoptotic cells in vitro inhibit proinflammatory cytokine production through autocrine/paracrine mechanisms involving TGF-beta, PGE2, and PAF. *J. Clin. Invest.* **101**, 890–898 (1998).
34. MacKinnon, A. C. *et al.* Regulation of alternative macrophage activation by galectin-3. *J. Immunol.* **180**, 2650–2658 (2008).
35. Madsen, D. H. *et al.* M2-like macrophages are responsible for collagen degradation through a mannose receptor-mediated pathway. *J. Cell Biol.* **202**, 951–966 (2013).
36. Van Linthout, S., Miteva, K. & Tschöpe, C. Crosstalk between fibroblasts and

inflammatory cells. *Cardiovasc. Res.* **102**, 258–269 (2014).

37. López, B. *et al.* Osteopontin-mediated myocardial fibrosis in heart failure: a role for lysyl oxidase? *Cardiovasc. Res.* **99**, 111–120 (2013).
38. Piek, A., de Boer, R. A. & Silljé, H. H. W. The fibrosis-cell death axis in heart failure. *Heart Fail. Rev.* **21**, 199–211 (2016).
39. Chan, J. K. *et al.* Alarmins: awaiting a clinical response. *J. Clin. Invest.* **122**, 2711–2719 (2012).
40. Nakaya, M. *et al.* Cardiac myofibroblast engulfment of dead cells facilitates recovery after myocardial infarction. *J. Clin. Invest.* **127**, 383–401 (2017).
41. Frangogiannis, N. G. The inflammatory response in myocardial injury, repair, and remodelling. *Nat. Rev. Cardiol.* **11**, 255–265 (2014).
42. Nah, D. Y. & Rhee, M. Y. The inflammatory response and cardiac repair after myocardial infarction. *Korean Circ. J.* **39**, 393–398 (2009).
43. Gabriel, A. S., Martinsson, A., Wretlind, B. & Ahnve, S. IL-6 levels in acute and post myocardial infarction: their relation to CRP levels, infarction size, left ventricular systolic function, and heart failure. *Eur. J. Intern. Med.* **15**, 523–528 (2004).
44. Hohensinner, P. J. *et al.* Monocyte chemoattractant protein (MCP-1) is expressed in human cardiac cells and is differentially regulated by inflammatory mediators and hypoxia. *FEBS Lett.* **580**, 3532–3538 (2006).
45. Yang, M., Chen, J., Zhao, J. & Meng, M. Etanercept attenuates myocardial ischemia/reperfusion injury by decreasing inflammation and oxidative stress. *PLoS One* **9**, e108024 (2014).
46. Durán, W. N. The double-edge sword of TNF-alpha in ischemia-reperfusion injury. *Am. J. Physiol. Heart Circ. Physiol.* **295**, H2221–H2222 (2008).
47. Gabay, C. Interleukin-6 and chronic inflammation. *Arthritis Res. Ther.* **8**, S3 (2006).
48. Fuchs, M. *et al.* Role of interleukin-6 for LV remodeling and survival after experimental myocardial infarction. *FASEB J.* **17**, 2118–2120 (2003).
49. Hartman, M. H. T. *et al.* Inhibition of Interleukin-6 Receptor in a Murine Model of Myocardial Ischemia-Reperfusion. *PLoS One* **11**, e0167195 (2016).
50. Frangogiannis, N. G. Regulation of the inflammatory response in cardiac repair. *Circ. Res.* **110**, 159–173 (2012).
51. Chen, W. *et al.* Endogenous IRAK-M attenuates postinfarction remodeling through

effects on macrophages and fibroblasts. *Arterioscler. Thromb. Vasc. Biol.* **32**, 2598–2608 (2012).

52. Meijers, W. C., Van Der Velde, A. R., Pascual-Figal, D. A. & De Boer, R. A. Galectin-3 and post-myocardial infarction cardiac remodeling. *Eur. J. Pharmacol.* **763**, 115–121 (2015).
53. Bujak, M. & Frangogiannis, N. G. The role of TGF-beta signaling in myocardial infarction and cardiac remodelin. *Cardiovasc. Res.* **74**, 184–195 (2007).
54. Tromp, J. *et al.* Fibrosis marker syndecan-1 and outcome in patients with heart failure with reduced and preserved ejection fraction. *Circ. Hear. Fail.* **7**, 457–462 (2014).
55. Lunde, I. G., Herum, K. M., Carlson, C. C. & Christensen, G. Syndecans in heart fibrosis. *Cell Tissue Res.* **365**, 539–552 (2016).
56. Talman, V. & Ruskoaho, H. Cardiac fibrosis in myocardial infarction - from repair and remodeling to regeneration. *Cell Tissue Res.* **365**, 563–581 (2016).
57. St. John Sutton, M. G. & Sharpe, N. Left ventricular remodeling after myocardial infarction: pathophysiology and therapy. *Circulation* **101**, 2981–2988 (2000).
58. Coletta, C. *et al.* Influence of contractile reserve and inducible ischaemia on left ventricular remodelling after acute myocardial infarction. *Heart* **89**, 1138–1143 (2003).
59. Hummel, A., Empen, K., Dörr, M. & Felix, S. B. De novo acute heart failure and acutely decompensated chronic heart failure. *Dtsch. Aerzteblatt Online* **112**, 298–310 (2015).
60. Boulogne, M. *et al.* Inflammation versus mechanical stretch biomarkers over time in acutely decompensated heart failure with reduced ejection fraction. *Int. J. Cardiol.* **226**, 53–59 (2017).
61. Heymans, S. *et al.* Inflammation as a therapeutic target in heart failure? A scientific statement from the Translational Research Committee of the Heart Failure Association of the European Society of Cardiology. *Eur. J. Heart Fail.* **11**, 119–129 (2009).
62. Dick, S. A. & Epelman, S. Chronic Heart Failure and Inflammation: What Do We Really Know? *Circ. Res.* **119**, 159–176 (2016).
63. Kameda, K. *et al.* Correlation of oxidative stress with activity of matrix metalloproteinase in patients with coronary artery disease: possible role for left

ventricular remodelling. *Eur. Heart J.* **24**, 2180–2185 (2003).

64. Paulus, W. J. & Tschöpe, C. A novel paradigm for heart failure with preserved ejection fraction: comorbidities drive myocardial dysfunction and remodeling through coronary microvascular endothelial inflammation. *J. Am. Coll. Cardiol.* **62**, 263–271 (2013).
65. Liu, L. *et al.* Up-regulated TLR4 in cardiomyocytes exacerbates heart failure after long-term myocardial infarction. *J. Cell. Mol. Med.* **19**, 2728–2740 (2015).
66. Zhi, H. *et al.* Effects of direct Renin inhibition on myocardial fibrosis and cardiac fibroblast function. *PLoS One* **8**, e81612 (2013).
67. Martínez-Martínez, E. *et al.* Galectin-3 blockade inhibits cardiac inflammation and fibrosis in experimental hyperaldosteronism and hypertension. *Hypertension* **66**, 767–775 (2015).
68. Mercola, M., Ruiz-Lozano, P. & Schneider, M. D. Cardiac muscle regeneration: Lessons from development. *Genes Dev.* **25**, 299–309 (2011).
69. Ruvinov, E., Sapir, Y. & Cohen, S. *Cardiac tissue engineering: principles, materials, and applications*. (Synth. Lect. Tissue Eng, 2012). doi:10.2200/S00437ED1V01Y201207TIS009
70. Bar, A. & Cohen, S. Inducing Endogenous Cardiac Regeneration: Can Biomaterials Connect the Dots? *Front. Bioeng. Biotechnol.* **8**, 126 (2020).
71. Torella, D., Ellison, G. M., Méndez-Ferrer, S., Ibanez, B. & Nadal-Ginard, B. Resident human cardiac stem cells: role in cardiac cellular homeostasis and potential for myocardial regeneration. *Nat. Clin. Pract. Cardiovasc. Med.* **3**, S8–S13 (2006).
72. Foglia, M. J. & Poss, K. D. Building and re-building the heart by cardiomyocyte proliferation. *Dev.* **143**, 729–740 (2016).
73. Li, F., Wang, X., Capasso, J. M. & Gerdes, A. M. Rapid transition of cardiac myocytes from hyperplasia to hypertrophy during postnatal development. *J. Mol. Cell. Cardiol.* **28**, 1737–1746 (1996).
74. Bergmann, O. *et al.* Dynamics of Cell Generation and Turnover in the Human Heart. *Cell* **161**, 1566–1575 (2015).
75. Urbanek, K. *et al.* Myocardial regeneration by activation of multipotent cardiac stem cells in ischemic heart failure. *Proc. Natl. Acad. Sci. U. S. A.* **102**, 8692–8697 (2005).
76. Broughton, K. M. *et al.* Mechanisms of Cardiac Repair and Regeneration. *Circ. Res.*

122, 1151–1163 (2018).

77. Garg, S., Narula, J. & Chandrashekhar, Y. Apoptosis and heart failure: clinical relevance and therapeutic target. *J. Mol. Cell. Cardiol.* **38**, 73–79 (2005).
78. Kolwicz, S. C., Purohit, S. & Tian, R. Cardiac metabolism and its interactions with contraction, growth, and survival of cardiomyocytes. *Circ. Res.* **113**, 603–616 (2013).
79. Ong, S. B. *et al.* Inflammation following acute myocardial infarction: Multiple players, dynamic roles, and novel therapeutic opportunities. *Pharmacol. Ther.* **186**, 73–87 (2018).
80. Frangogiannis, N. G. The extracellular matrix in myocardial injury, repair, and remodeling. *J. Clin. Invest.* **127**, 1600–1612 (2017).
81. Renault, M. A. & Losordo, D. W. Therapeutic myocardial angiogenesis. *Microvasc. Res.* **74**, 159–171 (2007).
82. Erbs, S. *et al.* Restoration of microvascular function in the infarct-related artery by intracoronary transplantation of bone marrow progenitor cells in patients with acute myocardial infarction: the Doppler Substudy of the Reinfusion of Enriched Progenitor Cells and Infa. *Circulation* **116**, 366–374 (2007).
83. Mohamed, T. M. A. *et al.* Regulation of Cell Cycle to Stimulate Adult Cardiomyocyte Proliferation and Cardiac Regeneration. *Cell* **173**, 104-116.e12 (2018).
84. Hatzistergos, K. E. & Hare, J. M. Murine Models Demonstrate Distinct Vasculogenic and Cardiomyogenic cKit+ Lineages in the Heart. *Circ. Res.* **118**, 382–387 (2016).
85. Alkass, K. *et al.* No Evidence for Cardiomyocyte Number Expansion in Preadolescent Mice. *Cell* **163**, 1026–1036 (2015).
86. Sluijter, J. P. G., Verhage, V., Deddens, J. C., Van Den Akker, F. & Doevendans, P. A. Microvesicles and exosomes for intracardiac communication. *Cardiovasc. Res.* **102**, 302–311 (2014).
87. Manabe, I., Shindo, T. & Nagai, R. Gene expression in fibroblasts and fibrosis: involvement in cardiac hypertrophy. *Circ. Res.* **91**, 1103–1113 (2002).
88. Bouzegrhane, F. & Thibault, G. Is angiotensin II a proliferative factor of cardiac fibroblasts? *Cardiovasc. Res.* **53**, 304–312 (2002).
89. Araszkiewicz, A. *et al.* Effect of impaired myocardial reperfusion on left ventricular remodeling in patients with anterior wall acute myocardial infarction treated with primary coronary intervention. *Am. J. Cardiol.* **98**, 725–728 (2006).

90. Boodhwani, M., Sodha, N. R., Laham, R. J. & Sellke, F. W. The future of therapeutic myocardial angiogenesis. *Shock* **26**, 332–341 (2006).
91. Di Franco, S., Amarelli, C., Montalto, A., Loforte, A. & Musumeci, F. Biomaterials and heart recovery: cardiac repair, regeneration and healing in the MCS era: A state of the 'heart'. *J. Thorac. Dis.* **10**, S2346–S2362 (2018).
92. Gordon, R. J., Quagliarello, B. & Lowy, F. D. Ventricular assist device-related infections. *Lancet. Infect. Dis.* **6**, 426–437 (2006).
93. Domenech, M., Polo-Corrales, L., Ramirez-Vick, J. E. & Freytes, D. O. Tissue Engineering Strategies for Myocardial Regeneration: Acellular Versus Cellular Scaffolds? *Tissue Eng. - Part B Rev.* **22**, 438–458 (2016).
94. Gaudron, P., Eilles, C., Ertl, G. & Kochsiek, K. Compensatory and noncompensatory left ventricular dilatation after myocardial infarction: Time course and hemodynamic consequences at rest and during exercise. *Am. Heart J.* **123**, 377–385 (1992).
95. Di Donato, M. *et al.* Akinetic versus dyskinetic postinfarction scar: relation to surgical outcome in patients undergoing endoventricular circular patch plasty repair. *J. Am. Coll. Cardiol.* **29**, 1569–1575 (1997).
96. Cooley, D. A., Collins, H. A., Morris, G. C. J. & Chapman, D. W. Ventricular aneurysm after myocardial infarction; surgical excision with use of temporary cardiopulmonary bypass. *J. Am. Med. Assoc.* **167**, 557–560 (1958).
97. Dor, V., Saab, M., Coste, P., Kornaszewska, M. & Montiglio, F. Left ventricular aneurysm: a new surgical approach. *Thorac. Cardiovasc. Surg.* **37**, 11–19 (1989).
98. Athanasuleas, C. L., Stanley, A. W. H. & Buckberg, G. D. Restoration of contractile function in the enlarged left ventricle by exclusion of remodeled akinetic anterior segment: surgical strategy, myocardial protection, and angiographic results. *J. Card. Surg.* **13**, 418 (1998).
99. Murry, C. E., Field, L. J. & Menasché, P. Cell-based cardiac repair: reflections at the 10-year point. *Circulation* **112**, 3174–3183 (2005).
100. Wang, J. S. *et al.* Marrow stromal cells for cellular cardiomyoplasty: feasibility and potential clinical advantages. *J. Thorac. Cardiovasc. Surg.* **120**, 999–1006 (2000).
101. Hutcheson, K. A. *et al.* Comparison of benefits on myocardial performance of cellular cardiomyoplasty with skeletal myoblasts and fibroblasts. *Cell Transplant.* **9**, 359–368 (2000).

102. Makino, S. *et al.* Cardiomyocytes can be generated from marrow stromal cells in vitro. *J. Clin. Invest.* **103**, 697–705 (1999).
103. Mangi, A. A. *et al.* Mesenchymal stem cells modified with Akt prevent remodeling and restore performance of infarcted hearts. *Nat. Med.* **9**, 1195–1201 (2003).
104. Nygren, J. M. *et al.* Bone marrow-derived hematopoietic cells generate cardiomyocytes at a low frequency through cell fusion, but not transdifferentiation. *Nat. Med.* **10**, 494–501 (2004).
105. Fraidenraich, D. *et al.* Rescue of cardiac defects in id knockout embryos by injection of embryonic stem cells. *Science (80-.).* **306**, 247–252 (2004).
106. Gnecchi, M. *et al.* Paracrine action accounts for marked protection of ischemic heart by Akt-modified mesenchymal stem cells. *Nature medicine* **11**, 367–368 (2005).
107. Murry, C. E. *et al.* Haematopoietic stem cells do not transdifferentiate into cardiac myocytes in myocardial infarcts. *Nature* **428**, 664–668 (2004).
108. Kajstura, J. *et al.* Bone marrow cells differentiate in cardiac cell lineages after infarction independently of cell fusion. *Circ. Res.* **96**, 127–137 (2005).
109. Hatzistergos, K. E. *et al.* Bone marrow mesenchymal stem cells stimulate cardiac stem cell proliferation and differentiation. *Circ. Res.* **107**, 913–922 (2010).
110. Chachques, J. C. *et al.* Cellular cardiomyoplasty: clinical application. *Ann. Thorac. Surg.* **77**, 1121–1130 (2004).
111. Teng, C. J., Luo, J., Chiu, R. C. J. & Shum-Tim, D. Massive mechanical loss of microspheres with direct intramyocardial injection in the beating heart: implications for cellular cardiomyoplasty. *J. Thorac. Cardiovasc. Surg.* **132**, 628–632 (2006).
112. Terrovitis, J. V., Smith, R. R. & Marbán, E. Assessment and optimization of cell engraftment after transplantation into the heart. *Circ. Res.* **106**, 479–494 (2010).
113. Robey, T. E., Saiget, M. K., Reinecke, H. & Murry, C. E. Systems approaches to preventing transplanted cell death in cardiac repair. *J. Mol. Cell. Cardiol.* **45**, 567–581 (2008).
114. Zhang, M. *et al.* Cardiomyocyte grafting for cardiac repair: graft cell death and anti-death strategies. *J. Mol. Cell. Cardiol.* **33**, 907–921 (2001).
115. Terrovitis, J. *et al.* Noninvasive quantification and optimization of acute cell retention by in vivo positron emission tomography after intramyocardial cardiac-derived stem cell delivery. *J. Am. Coll. Cardiol.* **54**, 1619–1626 (2009).

116. Radisic, M. & Christman, K. L. Materials science and tissue engineering: Repairing the heart. *Mayo Clin. Proc.* **88**, 884–898 (2013).
117. Chen, H. S. V., Kim, C. & Mercola, M. Electrophysiological challenges of cell-based myocardial repair. *Circulation* **120**, 2496–2508 (2009).
118. Rienks, M., Papageorgiou, A. P., Frangogiannis, N. G. & Heymans, S. Myocardial extracellular matrix: an ever-changing and diverse entity. *Circ. Res.* **114**, 872–888 (2014).
119. Yanamandala, M. *et al.* Overcoming the Roadblocks to Cardiac Cell Therapy Using Tissue Engineering. *J. Am. Coll. Cardiol.* **70**, 766–775 (2017).
120. Malliaras, K. *et al.* Safety and efficacy of allogeneic cell therapy in infarcted rats transplanted with mismatched cardiosphere-derived cells. *Circulation* **125**, 100–112 (2012).
121. Yeh, Y.-C. *et al.* Mechanically dynamic PDMS substrates to investigate changing cell environments. *Biomaterials* **145**, 23–32 (2017).
122. Khetan, S. *et al.* Degradation-mediated cellular traction directs stem cell fate in covalently crosslinked three-dimensional hydrogels. *Nat. Mater.* **12**, 458–465 (2013).
123. Muschler, G. F., Nakamoto, C. & Griffith, L. G. Engineering principles of clinical cell-based tissue engineering. *J. Bone Joint Surg. Am.* **86**, 1541–1558 (2004).
124. Jackman, C. P. *et al.* Engineered cardiac tissue patch maintains structural and electrical properties after epicardial implantation. *Biomaterials* **159**, 48–58 (2018).
125. Zhang, J., Zhu, W., Radisic, M. & Vunjak-Novakovic, G. Can We Engineer a Human Cardiac Patch for Therapy? *Circ. Res.* **123**, 244–265 (2018).
126. McMahan, S. *et al.* Current advances in biodegradable synthetic polymer based cardiac patches. *J. Biomed. Mater. Res. - Part A* **108**, 972–983 (2020).
127. Shin, M., Ishii, O., Sueda, T. & Vacanti, J. P. Contractile cardiac grafts using a novel nanofibrous mesh. *Biomaterials* **25**, 3717–3723 (2004).
128. Chen, W. L. & Kan, C. D. Using cell-seeded electrospun patch for myocardial injury: in-vitro and in rat model. *Annu Int Conf IEEE Eng Med Biol Soc* **2018**, 5338–5341 (2018).
129. Chen, M., Patra, P. K., Warner, S. B. & Bhowmick, S. Role of fiber diameter in adhesion and proliferation of NIH 3T3 fibroblast on electrospun polycaprolactone scaffolds. *Tissue Eng.* **13**, 579–587 (2007).

130. Yeong, W. Y. *et al.* Porous polycaprolactone scaffold for cardiac tissue engineering fabricated by selective laser sintering. *Acta Biomater.* **6**, 2028–2034 (2010).
131. Wang, Y., Ameer, G. A., Sheppard, B. J. & Langer, R. A tough biodegradable elastomer. *Nat. Biotechnol.* **20**, 602–606 (2002).
132. Kharaziha, M. *et al.* PGS:Gelatin nanofibrous scaffolds with tunable mechanical and structural properties for engineering cardiac tissues. *Biomaterials* **34**, 6355–6366 (2013).
133. Engelmayr, G. C. J. *et al.* Accordion-like honeycombs for tissue engineering of cardiac anisotropy. *Nat. Mater.* **7**, 1003–1010 (2008).
134. Joachim Loo, S. C. *et al.* Hydrolytic degradation characteristics of irradiated multi-layered PLGA films. *Int. J. Pharm.* **360**, 228–230 (2008).
135. Zhou, Q., Zhou, J.-Y., Zheng, Z., Zhang, H. & Hu, S.-S. A novel vascularized patch enhances cell survival and modifies ventricular remodeling in a rat myocardial infarction model. *J. Thorac. Cardiovasc. Surg.* **140**, 1383–1388 (2010).
136. Ahn, Y. & Jun, Y. In vivo evaluation of a porous, elastic, biodegradable patch for reconstructive cardiac procedures. *Early Hum. Dev.* **83**, 255–262 (2007).
137. Fujimoto, K. L. *et al.* An elastic, biodegradable cardiac patch induces contractile smooth muscle and improves cardiac remodeling and function in subacute myocardial infarction. *J. Am. Coll. Cardiol.* **49**, 2292–2300 (2007).
138. Hashizume, R. *et al.* Biodegradable elastic patch plasty ameliorates left ventricular adverse remodeling after ischemia-reperfusion injury: a preclinical study of a porous polyurethane material in a porcine model. *J. Thorac. Cardiovasc. Surg.* **146**, 391-399.e1 (2013).
139. Shah Mohammadi, M., Bureau, M. N. & Nazhat, S. N. 11 - Polylactic acid (PLA) biomedical foams for tissue engineering. in *Biomedical Foams for Tissue Engineering Applications* (ed. Netti, P. A.) 313–334 (Woodhead Publishing, 2014).
140. Farah, S., Anderson, D. G. & Langer, R. Physical and mechanical properties of PLA, and their functions in widespread applications — A comprehensive review. *Adv. Drug Deliv. Rev.* **107**, 367–392 (2016).
141. Wolf, M. T., Dearth, C. L., Sonnenberg, S. B., Loboa, E. G. & Badylak, S. F. Naturally derived and synthetic scaffolds for skeletal muscle reconstruction. *Adv. Drug Deliv. Rev.* **84**, 208–221 (2015).

142. Liu, Q. *et al.* Porous nanofibrous poly(L-lactic acid) scaffolds supporting cardiovascular progenitor cells for cardiac tissue engineering. *Acta Biomater.* **26**, 105–114 (2015).
143. Reid, B. *et al.* PEG hydrogel degradation and the role of the surrounding tissue environment. *J. Tissue Eng. Regen. Med.* **9**, 315–318 (2015).
144. Lin, C.-C. & Anseth, K. S. PEG hydrogels for the controlled release of biomolecules in regenerative medicine. *Pharm. Res.* **26**, 631–643 (2009).
145. Place, E. S., George, J. H., Williams, C. K. & Stevens, M. M. Synthetic polymer scaffolds for tissue engineering. *Chem. Soc. Rev.* **38**, 1139–1151 (2009).
146. Veronese, F. M. & Pasut, G. PEGylation, successful approach to drug delivery. *Drug Discov. Today* **10**, 1451–1458 (2005).
147. Aszódi, A., Legate, K. R., Nakchbandi, I. & Fässler, R. What mouse mutants teach us about extracellular matrix function. *Annu. Rev. Cell Dev. Biol.* **22**, 591–621 (2006).
148. Chevallay, B. & Herbage, D. Collagen-based biomaterials as 3D scaffold for cell cultures: applications for tissue engineering and gene therapy. *Med. Biol. Eng. Comput.* **38**, 211–218 (2000).
149. Wallace, D. G. & Rosenblatt, J. Collagen gel systems for sustained delivery and tissue engineering. *Adv. Drug Deliv. Rev.* **55**, 1631–1649 (2003).
150. Yang, Y.-L., Leone, L. M. & Kaufman, L. J. Elastic moduli of collagen gels can be predicted from two-dimensional confocal microscopy. *Biophys. J.* **97**, 2051–2060 (2009).
151. Peattie, R. A. *et al.* Stimulation of in vivo angiogenesis by cytokine-loaded hyaluronic acid hydrogel implants. *Biomaterials* **25**, 2789–2798 (2004).
152. Oksala, O. *et al.* Expression of proteoglycans and hyaluronan during wound healing. *J. Histochem. Cytochem.* **43**, 125–135 (1995).
153. Yoon, S. J. *et al.* Differential regeneration of myocardial infarction depending on the progression of disease and the composition of biomimetic hydrogel. *J. Biosci. Bioeng.* **118**, 461–468 (2014).
154. Augst, A. D., Kong, H. J. & Mooney, D. J. Alginate hydrogels as biomaterials. *Macromol. Biosci.* **6**, 623–633 (2006).
155. Yu, J. *et al.* The effect of injected RGD modified alginate on angiogenesis and left ventricular function in a chronic rat infarct model. *Biomaterials* **30**, 751–756 (2009).

156. Dai, T., Tanaka, M., Huang, Y.-Y. & Hamblin, M. R. Chitosan preparations for wounds and burns: antimicrobial and wound-healing effects. *Expert Rev. Anti. Infect. Ther.* **9**, 857–879 (2011).
157. Bhattarai, N., Gunn, J. & Zhang, M. Chitosan-based hydrogels for controlled, localized drug delivery. *Adv. Drug Deliv. Rev.* **62**, 83–99 (2010).
158. Dhandayuthapani, B., Krishnan, U. M. & Sethuraman, S. Fabrication and characterization of chitosan-gelatin blend nanofibers for skin tissue engineering. *J. Biomed. Mater. Res. B. Appl. Biomater.* **94**, 264–272 (2010).
159. Madihally, S. V & Matthew, H. W. Porous chitosan scaffolds for tissue engineering. *Biomaterials* **20**, 1133–1142 (1999).
160. Chiti, M. C., Dolmans, M. M., Donnez, J. & Amorim, C. A. Fibrin in Reproductive Tissue Engineering: A Review on Its Application as a Biomaterial for Fertility Preservation. *Ann. Biomed. Eng.* **45**, 1650–1663 (2017).
161. Mosesson, M. W. Fibrinogen and fibrin structure and functions. *J. Thromb. Haemost.* **3**, 1894–1904 (2005).
162. Jang, Y., Park, Y. & Kim, J. Engineering biomaterials to guide heart cells for matured cardiac tissue. *Coatings* **10**, 925 (2020).
163. Badylak, S. F., Freytes, D. O. & Gilbert, T. W. Extracellular matrix as a biological scaffold material: Structure and function. *Acta Biomater.* **5**, 1–13 (2009).
164. Hoshiba, T., Lu, H., Kawazoe, N. & Chen, G. Decellularized matrices for tissue engineering. *Expert Opin. Biol. Ther.* **10**, 1717–1728 (2010).
165. Kochupura, P. V *et al.* Tissue-engineered myocardial patch derived from extracellular matrix provides regional mechanical function. *Circulation* **112**, I144–I149 (2005).
166. Vogt, L. *et al.* Poly(ε-caprolactone)/poly(glycerol sebacate) electrospun scaffolds for cardiac tissue engineering using benign solvents. *Mater. Sci. Eng. C* **103**, 109712 (2019).
167. Ichihara, Y., Shinoka, T., Matsumura, G., Ikada, Y. & Yamazaki, K. A new tissue-engineered biodegradable surgical patch for high-pressure systems. *Interact. Cardiovasc. Thorac. Surg.* **20**, 768–776 (2015).
168. Deng, C. *et al.* A collagen–chitosan hydrogel for endothelial differentiation and angiogenesis. *Tissue Eng. Part A* **16**, 3099–3109 (2010).
169. Ahmadi, A., Vulesevic, B., Ruel, M. & Suuronen, E. J. A Collagen-Chitosan

Injectable Hydrogel Improves Vascularization and Cardiac Remodeling in a Mouse Model of Chronic Myocardial Infarction. *Can. J. Cardiol.* **29**, S203–S204 (2013).

170. Liu, Y. *et al.* Electrospun nanofibrous sheets of collagen/elastin/polycaprolactone improve cardiac repair after myocardial infarction. *Am. J. Transl. Res.* **8**, 1678–1694 (2016).
171. Zhang, Y., Ouyang, H., Lim, C. T., Ramakrishna, S. & Huang, Z.-M. Electrospinning of gelatin fibers and gelatin/PCL composite fibrous scaffolds. *J. Biomed. Mater. Res. B. Appl. Biomater.* **72**, 156–165 (2005).
172. Pok, S. *et al.* Full-Thickness Heart Repair with an Engineered Multilayered Myocardial Patch in Rat Model. *Adv. Healthc. Mater.* **6**, 10.1002/adhm.201600549 (2017).
173. Ravichandran, R., Venugopal, J. R., Mukherjee, S., Sundarrajan, S. & Ramakrishna, S. Elastomeric core/shell nanofibrous cardiac patch as a biomimetic support for infarcted porcine myocardium. *Tissue Eng. Part A* **21**, 1288–1298 (2015).
174. Cesur, S. *et al.* Production and characterization of elastomeric cardiac tissue-like patches for Myocardial Tissue Engineering. *Polym. Test.* **90**, 106613 (2020).
175. Pok, S., Myers, J. D., Madihally, S. V & Jacot, J. G. A multilayered scaffold of a chitosan and gelatin hydrogel supported by a PCL core for cardiac tissue engineering. *Acta Biomater.* **9**, 5630–5642 (2013).
176. Sun, M. *et al.* Synthesis and Properties of Gelatin Methacryloyl (GelMA) Hydrogels and Their Recent Applications in Load-Bearing Tissue. *Polymers (Basel).* **10**, 1290 (2018).
177. Abbasgholizadeh, R. *et al.* A Highly Conductive 3D Cardiac Patch Fabricated Using Cardiac Myocytes Reprogrammed from Human Adipogenic Mesenchymal Stem Cells. *Cardiovasc. Eng. Technol.* **11**, 205–218 (2020).
178. Kumar, N. *et al.* Scalable Biomimetic Coaxial Aligned Nanofiber Cardiac Patch: A Potential Model for "Clinical Trials in a Dish". *Front. Bioeng. Biotechnol.* **8**, 567842 (2020).
179. Benzoni, P. *et al.* Biomanufacturing of a Chitosan/Collagen Scaffold to Drive Adhesion and Alignment of Human Cardiomyocyte Derived from Stem Cells. *Procedia CIRP* **49**, 113–120 (2016).
180. Noor, N. *et al.* 3D Printing of Personalized Thick and Perfusable Cardiac Patches and

Hearts. *Adv. Sci.* **6**, 1900344 (2019).

181. Parveen, S., Singh, S. P., Panicker, M. M. & Gupta, P. K. Amniotic membrane as novel scaffold for human iPSC-derived cardiomyogenesis. *Vitr. Cell. Dev. Biol. - Anim.* **55**, 272–284 (2019).
182. Chang, C. W. *et al.* Mesenchymal Stem Cell Seeding of Porcine Small Intestinal Submucosal Extracellular Matrix for Cardiovascular Applications. *PLoS One* **11**, e0153412 (2016).
183. Boccardo, S. *et al.* Engineered mesenchymal cell-based patches as controlled VEGF delivery systems to induce extrinsic angiogenesis. *Acta Biomater.* **42**, 127–135 (2016).
184. Wang, Q. L. *et al.* Mesenchymal stem cell-loaded cardiac patch promotes epicardial activation and repair of the infarcted myocardium. *J. Cell. Mol. Med.* **21**, 1751–1766 (2017).
185. Izadifar, M., Chapman, D., Babyn, P., Chen, X. & Kelly, M. E. UV-Assisted 3D Bioprinting of Nanoreinforced Hybrid Cardiac Patch for Myocardial Tissue Engineering. *Tissue Eng. - Part C Methods* **24**, 74–88 (2018).
186. Llucià-Valldeperas, A. *et al.* Electromechanical conditioning of adult progenitor cells improves recovert of cardiac function after myocardial infarction. *Stem Cells Transl Med.* **6**, 970–981 (2017).
187. Kashiyama, N. *et al.* Adipose-derived stem cell sheet under an elastic patch improves cardiac function in rats after myocardial infarction. *J. Thorac. Cardiovasc. Surg.* S0022-5223(20)31139–9 (2020).
188. Mao, M., He, J., Li, Z., Han, K. & Li, D. Multi-directional cellular alignment in 3D guided by electrohydrodynamically-printed microlattices. *Acta Biomater.* **101**, 141–151 (2020).
189. Bai, X. & Alt, E. Myocardial regeneration potential of adipose tissue-derived stem cells. *Biochem. Biophys. Res. Commun.* **401**, 321–326 (2010).
190. Su, T. *et al.* Cardiac Stem Cell Patch Integrated with Microengineered Blood Vessels Promotes Cardiomyocyte Proliferation and Neovascularization after Acute Myocardial Infarction. *ACS Appl. Mater. Interfaces* **10**, 33088–33096 (2018).
191. Qian, Z. *et al.* Engineering stem cell cardiac patch with microvascular features representative of native myocardium. *Theranostics* **9**, 2143–2157 (2019).

192. Liu, Y., Xu, G., Wei, J., Wu, Q. & Li, X. Cardiomyocyte coculture on layered fibrous scaffolds assembled from micropatterned electrospun mats. *Mater. Sci. Eng. C* **81**, 500–510 (2017).
193. Roberts, E. G. *et al.* Evaluation of Placental Mesenchymal Stem Cell Sheets for Myocardial Repair and Regeneration. *Tissue Eng. - Part A* **25**, 867–877 (2019).
194. Yeung, E. *et al.* Cardiac regeneration using human-induced pluripotent stem cell-derived biomaterial-free 3D-bioprinted cardiac patch in vivo. *J. Tissue Eng. Regen. Med.* **13**, 2031–2039 (2019).
195. Chi Ting Au-Yeung, G. *et al.* Restoring the biophysical properties of decellularized patches through recellularization. *Biomater. Sci.* **5**, 1183–1194 (2017).
196. Feiner, R. *et al.* Engineered hybrid cardiac patches with multifunctional electronics for online monitoring and regulation of tissue function. *Nat. Mater.* **15**, 679–685 (2016).
197. Miao, S. *et al.* Photolithographic-stereolithographic-tandem fabrication of 4D smart scaffolds for improved stem cell cardiomyogenic differentiation. *Biofabrication* **10**, 035007 (2018).
198. Ghosh, L. Das, Jain, A., Sunderasan, N. R. & Chatterjee, K. Elucidating molecular events underlying topography mediated cardiomyogenesis of stem cells on 3D nanofibrous scaffolds. *Mater. Sci. Eng. C* **88**, 104–114 (2018).
199. Blondiaux, E. *et al.* Bone marrow-derived mesenchymal stem cell-loaded fibrin patches act as a reservoir of paracrine factors in chronic myocardial infarction. *J. Tissue Eng. Regen. Med.* **11**, 3417–3427 (2017).
200. Kameli, S. M. *et al.* Application of tissue-engineered pericardial patch in rat models of myocardial infarction. *J. Biomed. Mater. Res. - Part A* **106**, 2670–2678 (2018).
201. Joshi, J., Brennan, D., Beachley, V. & Kothapalli, C. R. Cardiomyogenic differentiation of human bone marrow-derived mesenchymal stem cell spheroids within electrospun collagen nanofiber mats. *J. Biomed. Mater. Res. - Part A* **106**, 3303–3312 (2018).
202. Ong, C. S. *et al.* Biomaterial-Free Three-Dimensional Bioprinting of Cardiac Tissue using Human Induced Pluripotent Stem Cell Derived Cardiomyocytes. *Sci. Rep.* **7**, 4566 (2017).
203. Yang, B. *et al.* A Net Mold-Based Method of Biomaterial-Free Three-Dimensional

Cardiac Tissue Creation. *Tissue Eng. - Part C Methods* **25**, 243–252 (2019).

204. Ong, C. S. *et al.* Creation of Cardiac Tissue Exhibiting Mechanical Integration of Spheroids Using 3D Bioprinting. *J. Vis. Exp.* 55438 (2017). doi:10.3791/55438
205. Mattapally, S. *et al.* Spheroids of cardiomyocytes derived from human-induced pluripotent stem cells improve recovery from myocardial injury in mice. *Am. J. Physiol. - Hear. Circ. Physiol.* **315**, H327–H339 (2018).
206. D'Amore, A. *et al.* Bi-layered polyurethane - Extracellular matrix cardiac patch improves ischemic ventricular wall remodeling in a rat model. *Biomaterials* **107**, 1–14 (2016).
207. Song, X. *et al.* In situ pPy-modification of chitosan porous membrane from mussel shell as a cardiac patch to repair myocardial infarction. *Appl. Mater. Today* **15**, 87–99 (2019).
208. Mallis, P., Michalopoulos, E., Dimitriou, C., Kostomitsopoulos, N. & Stavropoulos-Giokas, C. Histological and biomechanical characterization of decellularized porcine pericardium as a potential scaffold for tissue engineering applications. *Biomed. Mater. Eng.* **28**, 477–488 (2017).
209. Francisco, J. C. *et al.* Decellularized Amniotic Membrane Scaffold as a Pericardial Substitute: An In Vivo Study. *Transplant. Proc.* **48**, 2845–2849 (2016).
210. Shah, M., KC, P. & Zhang, G. In Vivo Assessment of Decellularized Porcine Myocardial Slice as an Acellular Cardiac Patch. *ACS Appl. Mater. Interfaces* **11**, 23893–23900 (2019).
211. Nair, R. S., Ameer, J. M., Alison, M. R. & Anilkumar, T. V. A gold nanoparticle coated porcine cholecyst-derived bioscaffold for cardiac tissue engineering. *Colloids Surfaces B Biointerfaces* **157**, 130–137 (2017).
212. Spadaccio, C. *et al.* Implantation of a Poly-L-Lactide GCSF-Functionalized Scaffold in a Model of Chronic Myocardial Infarction. *J. Cardiovasc. Transl. Res.* **10**, 47–65 (2017).
213. Shoba, E., Lakra, R., Kiran, M. S. & Korrapati, P. S. Strategic design of cardiac mimetic core-shell nanofibrous scaffold impregnated with Salvianolic acid B and Magnesium l-ascorbic acid 2 phosphate for myoblast differentiation. *Mater. Sci. Eng. C* **90**, 131–147 (2018).
214. Papalamprou, A. & Griffiths, L. G. Cardiac Extracellular Matrix Scaffold Generated

Using Sarcomeric Disassembly and Antigen Removal. *Ann. Biomed. Eng.* **44**, 1047–1060 (2016).

215. Huang, K. *et al.* An off-the-shelf artificial cardiac patch improves cardiac repair after myocardial infarction in rats and pigs. *Sci. Transl. Med.* **12**, eaat9683 (2020).
216. Baheiraei, N. *et al.* Electroactive polyurethane/siloxane derived from castor oil as a versatile cardiac patch, part II: HL-1 cytocompatibility and electrical characterizations. *J. Biomed. Mater. Res. - Part A* **104**, 1398–1407 (2016).
217. Sarig, U. *et al.* Natural myocardial ECM patch drives cardiac progenitor based restoration even after scarring. *Acta Biomater.* **44**, 209–220 (2016).
218. Efraim, Y. *et al.* 3D Structure and Processing Methods Direct the Biological Attributes of ECM-Based Cardiac Scaffolds. *Sci. Rep.* **9**, 5578 (2019).
219. Baker, R. S. *et al.* In Vivo Remodeling of an Extracellular Matrix Cardiac Patch in an Ovine Model. *ASAIO J.* **65**, 744–752 (2018).
220. Esmaeili Pourfarhangi, K., Mashayekhan, S., Asl, S. G. & Hajebrahimi, Z. Construction of scaffolds composed of acellular cardiac extracellular matrix for myocardial tissue engineering. *Biologicals* **53**, 10–18 (2018).
221. Lin, X. *et al.* A viscoelastic adhesive epicardial patch for treating myocardial infarction. *Nat. Biomed. Eng.* **3**, 632–643 (2019).
222. Xu, C. *et al.* Optimizing Anisotropic Polyurethane Scaffolds to Mechanically Match with Native Myocardium. *ACS Biomater. Sci. Eng.* **6**, 2757–2769 (2020).
223. Domengé, O. *et al.* Efficacy of epicardial implantation of acellular chitosan hydrogels in ischemic and nonischemic heart failure: impact of the acetylation degree of chitosan. *Acta Biomater.* **119**, 125–139 (2020).
224. Tallawi, M. *et al.* Novel PGS/PCL electrospun fiber mats with patterned topographical features for cardiac patch applications. *Mater. Sci. Eng. C* **69**, 569–576 (2016).
225. Eom, S., Park, S. M., Lim, J. & Kim, D. S. Electrospun random/aligned hybrid nanofiber mat for development of multi - layered cardiac muscle patch. *2018 IEEE Int. Conf. Cyborg Bionic Syst.* 177–180 (2018). doi:10.1109/CBS.2018.8612188
226. Bagdadi, A. V. *et al.* Poly(3-hydroxyoctanoate), a promising new material for cardiac tissue engineering. *J. Tissue Eng. Regen. Med.* **12**, e495–e512 (2018).
227. Jain, A., Behera, M., Mahapatra, C., Sundaresan, N. R. & Chatterjee, K.

Nanostructured polymer scaffold decorated with cerium oxide nanoparticles toward engineering an antioxidant and anti-hypertrophic cardiac patch. *Mater. Sci. Eng. C* **118**, 111416 (2021).

228. Mani, M. P., Jaganathan, S. K., Faudzi, A. A. & Sunar, M. S. Engineered Electrospun Polyurethane Composite Patch Combined with Bi-functional Components Rendering High Strength for Cardiac Tissue Engineering. *Polymers (Basel).* **11**, 705 (2019).
229. Kalishwaralal, K. *et al.* A novel biocompatible chitosan-Selenium nanoparticles (SeNPs) film with electrical conductivity for cardiac tissue engineering application. *Mater. Sci. Eng. C* **92**, 151–160 (2018).
230. Liu, B. *et al.* Cardiac recovery via extended cell-free delivery of extracellular vesicles secreted by cardiomyocytes derived from induced pluripotent stem cells. *Nat. Biomed. Eng.* **2**, 293–303 (2018).
231. Tsao, C. J. *et al.* Electrospun Patch Functionalized with Nanoparticles Allows for Spatiotemporal Release of VEGF and PDGF-BB Promoting in Vivo Neovascularization. *ACS Appl. Mater. Interfaces* **10**, 44344–44353 (2018).
232. Navaei, A. *et al.* Electrically conductive hydrogel-based micro-topographies for the development of organized cardiac tissues. *RSC Adv.* **7**, 3302–3312 (2017).
233. He, Y. *et al.* Mussel-inspired conductive nanofibrous membranes repair myocardial infarction by enhancing cardiac function and revascularization. *Theranostics* **8**, 5159–5177 (2018).
234. Takebe, T. *et al.* Vascularized and functional human liver from an iPSC-derived organ bud transplant. *Nature* **499**, 481–484 (2013).
235. Guillemette, M. D. *et al.* Combined technologies for microfabricating elastomeric cardiac tissue engineering scaffolds. *Macromol. Biosci.* **10**, 1330–1337 (2010).
236. Wei, S. *et al.* T-tubule remodeling during transition from hypertrophy to heart failure. *Circ. Res.* **107**, 520–531 (2010).
237. Bettinger, C. J., Orrick, B., Misra, A., Langer, R. & Borenstein, J. T. Microfabrication of poly (glycerol-sebacate) for contact guidance applications. *Biomaterials* **27**, 2558–2565 (2006).
238. House, A., Atalla, I., Lee, E. J. & Guvendiren, M. Designing Biomaterial Platforms for Cardiac Tissue and Disease Modeling. *Adv. NanoBiomed Res.* **1**, 2000022 (2020).
239. Soares, C. P. *et al.* 2D and 3D-organized cardiac cells shows differences in cellular

morphology, adhesion junctions, presence of myofibrils and protein expression. *PLoS One* **7**, e38147 (2012).

240. Zuppinger, C. 3D culture for cardiac cells. *Biochim. Biophys. Acta* **1863**, 1873–1881 (2016).
241. Tan, Y. *et al.* Silicon nanowire-induced maturation of cardiomyocytes derived from human induced pluripotent stem cells. *Nano Lett.* **15**, 2765–2772 (2015).
242. Tan, Y. *et al.* Cell number per spheroid and electrical conductivity of nanowires influence the function of silicon nanowired human cardiac spheroids. *Acta Biomater.* **51**, 495–504 (2017).
243. Masuda, S., Shimizu, T., Yamato, M. & Okano, T. Cell sheet engineering for heart tissue repair. *Adv. Drug Deliv. Rev.* **60**, 277–285 (2008).
244. Kubo, H., Shimizu, T., Yamato, M., Fujimoto, T. & Okano, T. Creation of myocardial tubes using cardiomyocyte sheets and an in vitro cell sheet-wrapping device. *Biomaterials* **28**, 3508–3516 (2007).
245. Nakane, T. *et al.* Impact of Cell Composition and Geometry on Human Induced Pluripotent Stem Cells-Derived Engineered Cardiac Tissue. *Sci. Rep.* **7**, 45641 (2017).
246. Wan, W. *et al.* Cardiac myocytes respond differentially and synergistically to matrix stiffness and topography. *bioRxiv* 682930 (2019). doi:10.1101/682930
247. Hasan, A. *et al.* Microfluidic techniques for development of 3D vascularized tissue. *Biomaterials* **35**, 7308–7325 (2014).
248. Goldstein, A. S., Juarez, T. M., Helmke, C. D., Gustin, M. C. & Mikos, A. G. Effect of convection on osteoblastic cell growth and function in biodegradable polymer foam scaffolds. *Biomaterials* **22**, 1279–1288 (2001).
249. Deitch, S., Gao, B. Z. & Dean, D. Effect of matrix on cardiomyocyte viscoelastic properties in 2D culture. *Mol. Cell. Biomech.* **9**, 227–249 (2012).
250. Taylor, D. A., Sampaio, L. C. & Gobin, A. Building new hearts: A review of trends in cardiac tissue engineering. *Am. J. Transplant.* **14**, 2448–2459 (2014).
251. Tomov, M. L. *et al.* Engineering Functional Cardiac Tissues for Regenerative Medicine Applications. *Curr. Cardiol. Rep.* **21**, 105 (2019).
252. Broughton, K. M. & Sussman, M. A. Cardiac tissue engineering therapeutic products to enhance myocardial contractility. *J. Muscle Res. Cell Motil.* **41**, 363–373 (2020).

253. Establishment Registration & Device Listing. *FDA* Available at: https://www.accessdata.fda.gov/scripts/cdrh/cfdocs/cfRL/rl.cfm. (Accessed: 15th November 2021)
254. Uchmanowicz, I. *et al.* Coexisting Frailty With Heart Failure. *Front. Physiol.* **10**, 791 (2019).
255. Mentz, R. J. *et al.* Noncardiac comorbidities in heart failure with reduced versus preserved ejection fraction. *J. Am. Coll. Cardiol.* **64**, 2281–2293 (2014).
256. Grigorian Shamagian, L. *et al.* Perspectives on Directions and Priorities for Future Preclinical Studies in Regenerative Medicine. *Circ. Res.* **124**, 938–951 (2019).
257. Stapleton, L., Zhu, Y., Woo, Y. ping J. & Appel, E. Engineered biomaterials for heart disease. *Curr. Opin. Biotechnol.* **66**, 246–254 (2020).
258. Gandhimathi, C., Muthukumaran, P. & Srinivasan, D. K. Nanofiber composites in cardiac tissue engineering. in *Nanofiber Composites for Biomedical Applications* (eds. Ramalingam, M. & Ramakrishna, S.) 411–453 (Elsevier, 2017).

Chapter IV

Human platelet lysate-based scaffolds as 3D culture platforms for cardiac regeneration

* This chapter is based on the following publication:

A. F. Lima, C. F. Monteiro, C. A. Custódio, J. F. Mano, *Human platelet lysate-based scaffolds as 3D culture platforms for cardiac regeneration*. (manuscript under preparation)

Human platelet lysate-based scaffolds as 3D culture platforms for cardiac regeneration

Abstract

Cardiovascular diseases are the leading cause of death in the world with myocardial infarction leading to heart failure and death of the victims. Since the current treatments do not restore the function of the cardiac tissue, tissue engineering aims to create cardiac patches to promote a better cardiac regeneration and outcome upon myocardial infarction. In this work, methacryloyl platelet lysates (PLMA) rehydrated hydrogels formed by freeze drying were evaluated for this purpose and to observe the impact of the freeze drying process on the hydrogel physical properties. The mechanical properties of the hydrogels increase with the freeze drying, not only in terms of Young's modulus, ultimate stress and ultimate strain, but also in durability. Although the top surface porosity was not different for all the PLMA concentrations used, PLMA scaffolds showed a high swelling ratio that decreases due to the release of protein from the scaffold matrix, a conductivity value that was on the same order of magnitude of the human heart and a rehydrated scaffold of 15% (w/v) PLMA that was able to be transported using a coronary catheter. To evaluate this scaffold as a three-dimensional (3D) culture platform, a successfully human umbilical vein endothelial cells assay was performed with PLMA concentration of 15% (w/v), showing, together with the physical properties results, promising results towards the use of these rehydrated hydrogels as cardiac patches for myocardial infarction regeneration.

1. Introduction

Cardiovascular diseases are the leading cause of death in the world with myocardial infarction (MI) being the main contributor for this statistic.[1] In most scenarios, MI is responsible for causing heart failure (HF) and death.[2] In a MI event, the cardiac tissue ceases to function properly due to the death of cardiomyocytes (CMs) and its extremely low healing capacity.[3] Without this capacity, the cardiac tissue is obligated to pass through a remodelling process, forming a scar tissue that promotes the degradation of the extracellular matrix (ECM), progressively worsening of heart function and finally leading to HF.[4]

Several pharmaceutical and surgical techniques have been exploited with the purpose of slowing down the progression of HF and are not capable of restore function of the damaged myocardium.[5] Thus, innovative therapeutic strategies should be developed to restore the function of infarcted myocardium.[6] This is where cardiac patches emerge as an innovate therapeutical approach using tissue engineering (TE) by recreating the heart microenvironment in order to facilitate cell assembly and build of functional tissue with the goal of providing replacement for damaged tissue after MI.[7] Engineered cardiac patch is fabricated to mimic the native ECM, offer mechanical support and promote cell engraftment into the region of infarction. Its application helps to limit left ventricle (LV) remodelling, prevent dilatation and thinning of the infarct zone, enhance mechanical properties of ventricle, and reduce CM apoptosis. Hence, the optimal properties of a scaffold involve high porosity, microenvironment similar to ECM, good mechanical properties, biodegradability, and biocompatibility.

Platelet lysates (PL) are an autologous source of grown factors, cytokines and several other proteins[8–10] that can locally promote wound[11–13] and tissue healing[14]. This material is obtained by a process of freeze/thaw cycles of platelet concentrates harvest from whole blood. As previously reported, chemically modified PL with methacrylic anhydride can form hydrogels by covalent photocrosslinking using ultraviolet (UV) light irradiation in the presence of a photoinitiator.[15] These hydrogels of methacryloyl platelet lysates (PLMA) have good mechanical and biochemical properties, supporting the adhesion and proliferation of encapsulated cells/spheroids while being an animal-free product approach for cell culture and biomedical applications.[16,17]

In this study, PLMA hydrogels were submitted to freeze drying, a known method for producing porous hydrogels.[18] With this, our goal is to evaluate the effects of the freeze drying process on the physical and biochemical properties of the rehydrated PLMA scaffolds when compared to the PLMA hydrogels and access these rehydrated scaffolds as three-dimensional (3D) culture platforms for the cardiac treatment of MI.

2. Materials and methods

2.1 Synthesis of methacryloyl platelet lysates

As previously reported, PL (STEMCELL Technologies, Canada) stored at -20 ºC and thawed at 37 ºC was chemically modified with methacrylic anhydride 94% (MA) (Sigma-Aldrich, USA) to form methacryloyl platelet lysate (PLMA) of low-degree of modification (PLMA100) for the purpose of this work.[15] Briefly, the reaction pH was maintained between 6 and 8 using 5 M sodium hydroxide (AkzoNobel, USA) solution, at room temperature (RT) and under constant stirring. The synthetized PLMA100 was then purified by dialysis with Float-A-Lyzer G2 Dialysis Device 3.5-5 kDa (Spectrum, USA) in deionized water for 24 hours, sterilized with a low protein retention 0.2 µm filter (Enzymatic S. A., Portugal), frozen in liquid nitrogen, freeze dried (LyoQuest Plus Eco, Telstar, Spain) and stored at 4 °C.

2.2 PLMA scaffold formation

The preparation of 10%, 15%, 20% or 30% (w/v) of lyophilized PLMA100 with 0.5% (w/v) 2-hydroxy-4'-(2-hydroxyethoxy)-2-methylpropiophenone (Sigma-Aldrich) in phosphate buffered saline (PBS) (Sigma-Aldrich) create a PLMA precursor solution that was pipetted to polydimethylsiloxane (PDMS) (Dow Corning, USA) molds with different shape and sizes. The hydrogels had an hight of approximately 1 mm and were photopolymerized for 60 seconds of UV exposure at 2.45 w/cm^2 in an 8 cm distance between the solution and the UV lamp. Hydrogels were placed at 4 ºC overnight in 5 mL PBS to achieve maximum absorption capacity and used in this state in all experiments. The shape and sizes of hydrogels used in the different experiments is specified in each one of them bellow. The prepared PLMA hydrogels were placed in Mr. Frosty^{TM} Freezing Container (ThermoFisher Scientific), for a cooling rate of -1 ºC/minute, at - 80 ºC for 2 hours. After that time, the frozen hydrogels where freeze dried (LyoQuest Plus Eco, Telstar, Spain) overnight and rehydrated in 5 mL of PBS also overnight to achieve maximum absorption capacity.

2.3 PLMA hydrogel characterization

2.3.1 Mechanical properties

PLMA hydrogels was tested using a Universal Mechanical Testing Machine Shimadzu MMT-101N (Shimadzu Scientific Instruments, Kyoto, Japan) equipped with a load cell of 100 N. A unidirectional tensile test was performed at RT on rectangular shaped hydrogels with a length of 2.5 cm, a width of 0.5 cm and using 75 µL of PLMA precursor solution. Samples of all four concentrations, from both freeze dried and non-freeze dried hydrogels, were used with an extension rate of 1 mm/minute. The Young's modulus was defined as the slope of the linear region of the strain/stress curve, corresponding from 0 to 45% strain. Ultimate stress and ultimate strain values were taken as the point where failure of the hydrogel occurred.

Preliminary cyclic tensile tests were also performed using the same spectrum of samples and equipment at a rate of 15.75 cm/minute for 45% of strain. The total cycle number obtained was the number of cycles each hydrogel support until failure and the maximum stress value was taken in count the of stress at 45% of strain within cycle number 5 to cycle number 10, the 5 cycles at half total cycle number and also the last 5 cycles discarding the last 5 total cycles obtained. The medium of these 15 cycles was the maximum stress value. All the samples were kept hydrated through all the tests.

2.3.2 Scanning electron microscopy

Scanning electron microscopy (SEM) analysis was obtained in a Hitachi TM4000 plus (Japan) equipment in order to analyse the scaffolds' structure and the surface porosity of the hydrogels for all concentrations by measuring the medium pore size using Image J software.

2.3.3 Swelling ratio

For a period of 24 hours and with circular scaffolds with 0.6 cm in diameter using 16.9 µL of PLMA precursor solution, hydrogels of all four different concentrations were freeze dried, with the value of the dry weight (W_d) measured in this state. The scaffolds were then hydrated in 10 mL of deionized water and, at each time-point, the value for the wet weight was measured (W_t). With the W_d and the W_t, the swelling ratio for that specific time

point was calculated using the following equation (**Equation 1**) and the process repeated for all time points:

$$Swelling\ Ratio = \frac{W_t - W_d}{W_t} \quad \textbf{(Equation 1)}$$

2.3.4 Conductivity

The conductivity analysis of hydrogels was performed in partnership with Dr. Paula Barbosa of CICECO – Aveiro Institute of Materials. For this work, a preliminary electrical conductivity of membranes was determined by impedance spectroscopy using an Agilent E4980A Precision LCR meter with measurements carried at 37 °C and 95% relative humidity after 20 minutes, in a climatic chamber (ACS DY 110). The impedance spectra was collected between 20 Hz and 2 MHz with a test signal amplitude of 100 mV. The electrodes were applied on a sample with an area of approximately 1.1 cm^2 by using a circular hydrogel with 0.6 cm in diameter, that was prepared from 16.9 µL of 20% (w/v) PLMA precursor solution, with 0.12 cm of thickness. The current collection was ensured by separate platinum wires for voltage and current. The sample holder was designed to ensure stable electrical contact while fully exposing the membrane surface to the surrounding atmosphere. The spectra was analyzed with ZView (Version 2.6b, Scribner Associates) to assess the ohmic R and the conductivity of the PLMA calculated using the following equation (**Equation 2**):

$$\sigma = L(RA)^{-1} \quad \textbf{(Equation 2)}$$

2.3.4 Cardiac patch transportation

A preliminary evaluation was performed using a rectangular shaped rehydrated scaffold with a length of 2.5 cm, a width of 0.5 cm and using 75 µL of solution of 15% (w/v) PLMA precursor solution using a FineCross® micro-guide microcatheter (Terumo, Japan). The construct was pulled in and out while submerse on PBS solution throughout the catheter extension and, after five rounds of transportation, the visual aspect of the rehydrated scaffold was access to see if there was any visible damage.

2.4 Cell culture

2.4.1 Scaffold seeding

Human umbilical veins endothelial cells (HUVECs) were isolated from human umbilical cord vein of newborn babies, under the approval of the Competent Ethics Committee (CEC), COMPASS Research Group and Hospital Infante D. Pedro, Aveiro, established a cooperation agreement to collect the human tissue. The consent declaration was obtained from all subjects and the handling of received human tissues was made in accordance with CEC guidelines. The samples were collected to a container with PBS supplemented with 1% (v/v) antibiotic/antimycotic (Thermo Fisher Scientific) and kept at 4°C until isolation procedure initiation. The samples were transferred to the laboratory within 24h after collection and immediately processed. Vein washing was performed with PBS, placing a catheter extender with side shunt (Vygon, Portugal) into the vein hole at one end of umbilical cord. The endothelial cells were released from vein walls by enzymatic digestion using 0.1% (w/v) collagenase type IA (MP Biomedicals, USA), under 37°C for 20-25 minutes. The HUVECs suspension was obtained rising the vein walls with M199 medium (Sigma-Aldrich) supplemented with 1% (v/v) of Endothelial Cell Growth Supplement (40 mg/mL, Merck, Germany), 10% (v/v) of Heparin (100 mg/mL, Sigma-Aldrich), 20% heat-inactivated fetal bovine serum (FBS, Thermo Fisher Scientific) and 1% antibiotic/antimycotic. The resultant cell suspension was plated in cell culture flasks previously coated with gelatin (0.7% (w/v), porcine skin type A, Sigma-Aldrich) for 20 minutes at 37 °C. Flow cytometry was then performed to confirm the successful isolation of HUVECs. HUVECs phenotypic profile was analyzed regarding CD31-APC (BioLegend, USA) positive surface marker and CD34-FITC (BioLegend) and CD90-Alexa Fluor 647 (BioLegend) negative surface markers for endothelial cells. The cells were harvested by TrypLE^{TM} Express solution (Thermo Fisher Scientific) at 37 °C for 5 min, centrifuged and resuspended in a PBS solution containing 2% (w/v) BSA and 0.1% (w/v) sodium azide (TCI Chemicals, Belgium). The antibodies were added at the dilutions recommended by the manufacture and incubated at 4 °C for 45 minutes, in the dark. After that, cell suspensions were washed with the above-mentioned PBS/BSA/sodium azide solution, centrifuged, fixed

in another PBS solution containing 1% (v/v) formaldehyde (Sigma-Aldrich) and 0.1% (w/v) sodium azide and then analyzed in a flow cytometer (Flow Citometer BD Accuri C6 Plus, BD Biosciences).

HUVEC cells were cultured in M199 medium (Sigma-Aldrich) supplemented with 1% (v/v) of Endothelial Cell Growth Supplement (40 mg/mL, Merck, Germany), 10% (v/v) of Heparin (100 mg/mL, Sigma-Aldrich), 20% (v/v) heat-inactivated FBS and 1% (v/v) antibiotic/antimycotic in T-flasks, maintained under 5% CO_2 atmosphere at 37 °C (standard cell culture conditions) and passaged at about 80% confluence. The medium was replaced every 2 to 3 days. Cells were detached with 0.25% trypsin/EDTA solution (Gibco, Thermo Fisher Scientific, USA) and resuspended in the same culture medium for application.

A 20 µL cell suspension containing 40 000 cells of HUVECs was applied on the top of scaffolds with a circular shape of 0.6 cm in diameter prepared from 16.9 µL of 15% (w/v) PLMA precursor solution. The cells were allowed to adhere for 4 hours and the culture was maintained for 14 days also in the described medium.

2.4.2 Cell viability

The live/dead assay of the rehydrated scaffolds was performed at days 3, 7 and 14 of culture in a solution of 1:1000 of Calcein AM 4mM solution in DMSO (Life Technologies, Thermo Fisher Scientific) and 1:2000 of 1 mg/mL PI (Thermo Fisher Scientific) in PBS at standard cell culture conditions (5% CO_2 at 37 °C) for 30 minutes. After three times washing with PBS, the samples were observed under a fluorescence microscope (Fluorescence Microscope Zeiss, Axio Imager 2, Zeiss, Germany), maintaining the same imaging parameters throughout all samples.

2.4.3 Cell morphology analysis

After 14 days of culture, the samples were washed with PBS and fixed in a solution of 4% (v/v) formaldehyde (Sigma-Aldrich) in PBS during at least 2 hours. After that, a phalloidin solution (Flash Phalloidin™ Red 594, 300U, Biolegend, USA) was diluted 1:40 PBS and the samples were incubated at 37 ºC for 1 hour. After 3 PBS washes, a DAPI (Thermo Fisher Scientific) solution was diluted in 1:1000 PBS, applied to the samples and

incubated at 37 ºC for 5 minutes. After 3 more washes with PBS, the samples were examined using a fluorescence microscope (Fluorescence Microscope Zeiss, Axio Imager 2, Zeiss, Germany).

2.5 Statistical analysis

All data were statistically analysed using the GraphPah Prism 8.4.2 software and, except for the preliminary tests, are expressed as mean ± standard deviation or mean ± standard error of the mean of at least 3 independent experiments. Statistical significance of unidirectional tensile test for both freeze dried and non-freeze dried samples was determined using two-way ANOVA analysis with Tukey's multiple comparison test and using one-way ANOVA analysis with Tukey's multiple comparison test for surface pore size.

3. Results and discussion

3.1 Hydrogel formation

For this work, hydrogels needed to have an heigh of about 1 mm for a better malleable capability. With this, we found out that using the correlation of 60 µL/cm^2 we were able to photopolymerize hydrogels that had around 1 mm of height, obtaining higher heights when increasing the concentration of PLMA on the hydrogels. For the second part, we developed a protocol for freeze drying hydrogels so they could keep their integrity without breaking throughout the process. One of the main concerns was the cooling rate and, by using an equipment that allows us to have a very slow cooling rate (-1 ºC/minute), we were able to freeze and then freeze dry the hydrogels to obtain scaffolds with their fully integrity.

3.2 PLMA hydrogel characterization

3.2.1 Mechanical properties

Elasticity is one the most important and necessary characteristics to follow the cardiac beat while keeping the integrity of the patch. To evaluate the effect that concentration and the freeze drying process had on the elasticity of PLMA hydrogels, unidirectional tensile tests (**Figure IV.1**) and also preliminary cyclic tensile tests (**Figure IV.2**) were performed.

When analysing the concentration profile on hydrogels where the freeze dried process was not carried out, the elasticity modulus, or Young's modulus (**Figure IV.1A**), of hydrogels with 10%, 15% and 20% (w/v) of PLMA is not significantly different. The only significant difference is between these values and the Young's modulus of the 30% (w/v) of PLMA hydrogels. When the freeze drying process is applied, the Young's modulus of all concentrations is increased significantly in all concentrations of PLMA hydrogels. The Young's modulus of 10% and 15% (w/v) PLMA is not significantly different but, when comparing to 20% and 30% (w/v), these values increase although not in a growing linear way since the value for 30% (w/v) PLMA is not higher than the value of 20% (w/v) PLMA. This means that not only the increase in concentration can create hydrogels with increase stiffness but the freeze drying process can also contribute to the increase of these values. The elasticity modulus of the human heart is said to be between 10 to 15 kPa.[19] When compared to the values presented on **Figure IV.1A**, 30% (w/v) PLMA rehydrated scaffolds are within this range, with 15% and 20% (w/v) PLMA rehydrated scaffolds being very close to the inferior and superior range, respectively.

In the case of the ultimate stress (**Figure IV.1B**), 10%, 15% and 20% (w/v) PLMA hydrogels without freeze drying are not significantly different, with an increase in value when increasing the PLMA concentration. Only the ultimate stress of 30% (w/v) PLMA hydrogels is significantly different from all other concentrations, with this analysis being very similar to the profile of the Young's modulus. When applying the freeze drying process, the only significant increase is observed on 20% (w/v) PLMA. Between rehydrated scaffolds, there is only significant difference between the 10% and 15% to the 20% (w/v) PLMA. This profile means that, besides the increase in stiffness, with increasing PLMA concentrations without freeze drying we can increase the ultimate stress. On the other half, the freeze drying process does not significantly increase the ultimate stress in the majority of the concentrations and the profile has two stabilizing values: one on 10% and 15% and the other on 20% and 30% (w/v).

The ultimate strain (**Figure IV.1C**) for non-freeze dried hydrogels starts with a low value for 10% (w/v) and then increases significantly for 15% and 20% (w/v) of PLMA. The value for 30% (w/v) PLMA hydrogels is lower than the previous concentrations and has no significance difference with the 10% (w/v) value. For the freeze dried samples, there is a significant decrease between the value for 10% (w/v) PLMA and the values of 20% and 30% (w/v) PLMA. Whitin concentrations, the freeze drying process significantly affects the ultimate strain of 15%, 20% and 30% (w/v) PLMA with a decrease of this statistic, meaning the observed increase in stiffness negatively affects the ultimate strain for these concentrations.

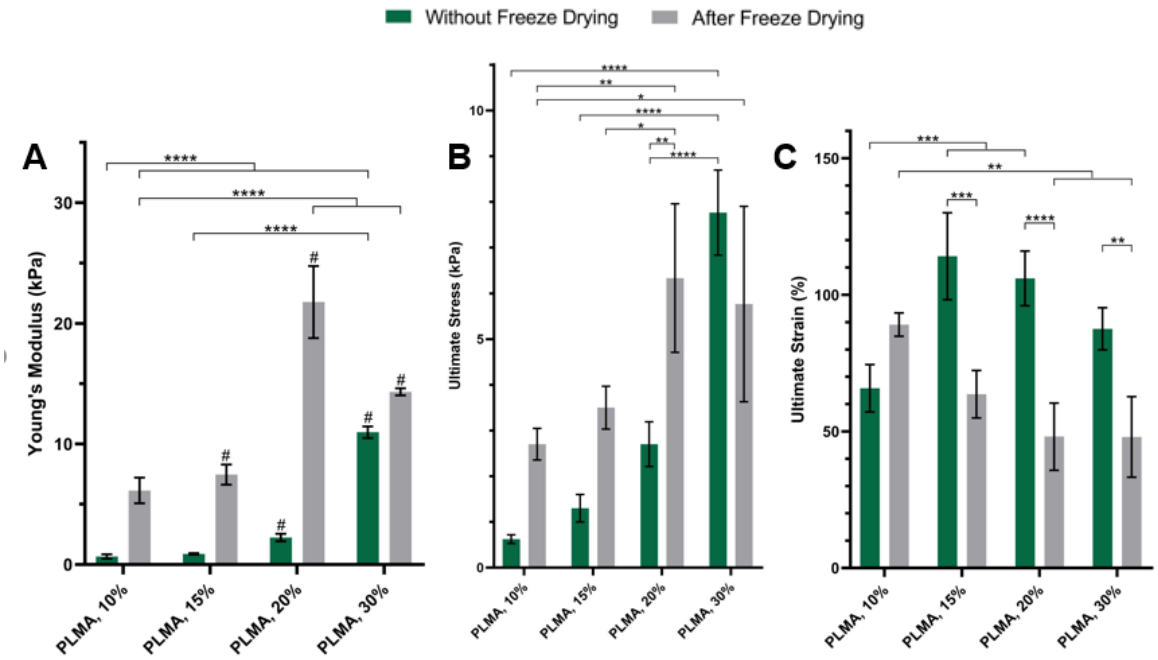

Figure IV.1. (A) Young's modulus, (B) ultimate stress and (C) ultimate strain obtained for PLMA hydrogels without or after freeze drying at 10%, 15%, 20% and 30% (w/v). Statistical analysis through two-way ANOVA with Tukey's multiple comparison test (*p<0.05, **p<0.005, ***p<0.0005, ****p<0.0001, # means significant differences with the groups on the right). Data is presented as mean ± standard deviation (n≥3).

Although as preliminary, a cyclic tensile test (**Figure IV.2**) was performed at 70 bpm with a 45% strain as maximum strain to replicate the human heartbeat at rest as close as possible. The 45% were chosen due to the heart longitudinal strain. While normal values for strain can be around 20%, in an injured heart these values can increse.[20] By using the given

strain, we assured to test the rehydrated scaffolds in conditions above the needed in MI. As seen above, the increase stiffness by freeze drying can be positive for low concentrations of PLMA but negative to higher concentrations. For total cycle count (**Figure IV.2A**), the increase in protein concentration decreases the number of cycles for PLMA hydrogels above 15% (w/v) of PLMA. With freeze drying, these values are lower for 10% and 30% (w/v) but increasing for 15% and 20% (w/v). In the profile, there is an increases from 10% to 15% and then a decrease until 30% (w/v), demonstrating that the increase in stiffness promotes a decrease in the total cycle number and that the freeze drying it has a negative impact for 10% and 30% but a positive one for 15% and 20% (w/v), elevating the number of cycles.

The tensile stress (**Figure IV.2B**) at the maximum strain for non-freeze dried hydrogels decrease from 10% to 20% (w/v) and then increase for 30% (w/v). As they are freeze dried, there is an increase at 15%, 20% and 30% (w/v) and a decrease for 10% (w/v). The profile for the freeze dried samples partially follows the same of total cycle number. Although this is only a preliminary test and more replicas are necessary, we can already observe that exist some differences in the behaviour of hydrogels between different concentrations and freeze drying process.

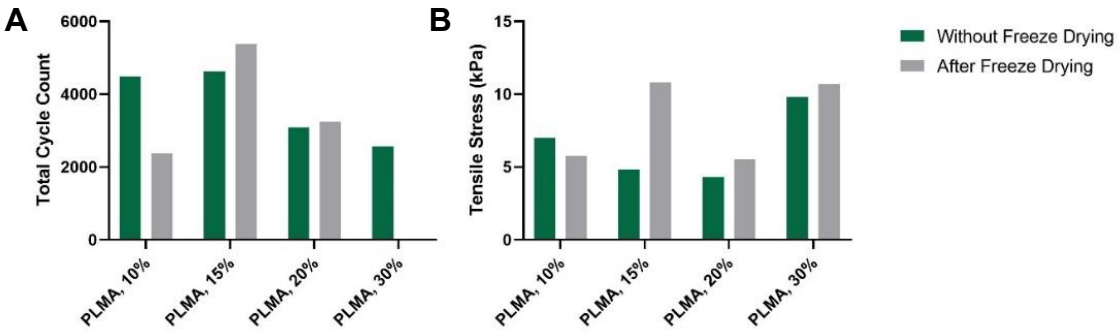

Figure IV.2. (A) Total cycle count and (B) tensile stress obtained for PLMA hydrogels without or after freeze drying at 10%, 15%, 20% and 30% (w/v) for the preliminary cyclic tensile test.

3.2.2 Pore size

In order to analyse the porous surface of the scaffolds, SEM was performed. The images obtained (**Figure IV.3A**) allowed the measurement of the diameter of the surface

pore (**Figure IV.3B**) and it was observed that the average length of the surface pore on PLMA scaffolds is not significantly different, being the average around 130 µm.

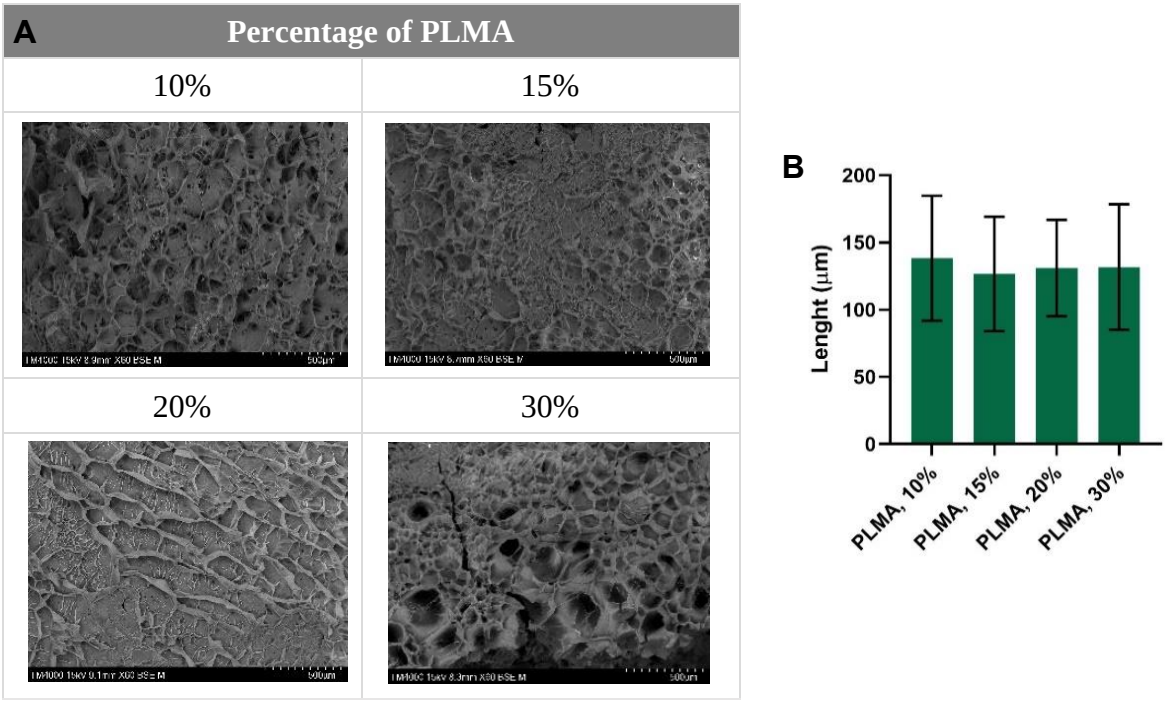

Figure IV.3. (A) Surface SEM images of PLMA-based scaffolds for the conditions of 10%, 15%, 20% and 30% (w/v) of PLMA. (B) Average length of the surface pore of PLMA-based scaffolds for the conditions of 10%, 15%, 20% and 30% (w/v) of PLMA. Statistical analysis through one-way ANOVA analysis with Tukey's multiple comparison test. Data is presented as mean ± standard deviation (n≥3).

3.2.3 Swelling ratio

With the use of scaffolds, it is important to know their swelling capacity and when these scaffolds reach their maximum of swealing, meaning they are ready for use.

On the first 30 minutes (**Figure IV.4A**), the swelling ratio rapidly increases and stabilizes on the first minutes by achieving the maximum swelling capacity within 10 to 15 minutes in all four concentrations of PLMA, being much higher for 10% and 15% then for 20% and 30% (w/v). After this time and throughout the assay (**Figure IV.4B**), the swelling ratio starts to decline, more accentually for 10% and 15% until it stabilizes again by 12 hours.

The swelling ratio experiment is done by calculations using the scaffolds weight over time and, giving the fact that the swelling ratio is decreasing, this means that the weight of the scaffolds is also decreasing over time. This phenomenon can be explained with the progressive protein release over time, which makes the scaffolds lose weight and decreases the swelling ratio.

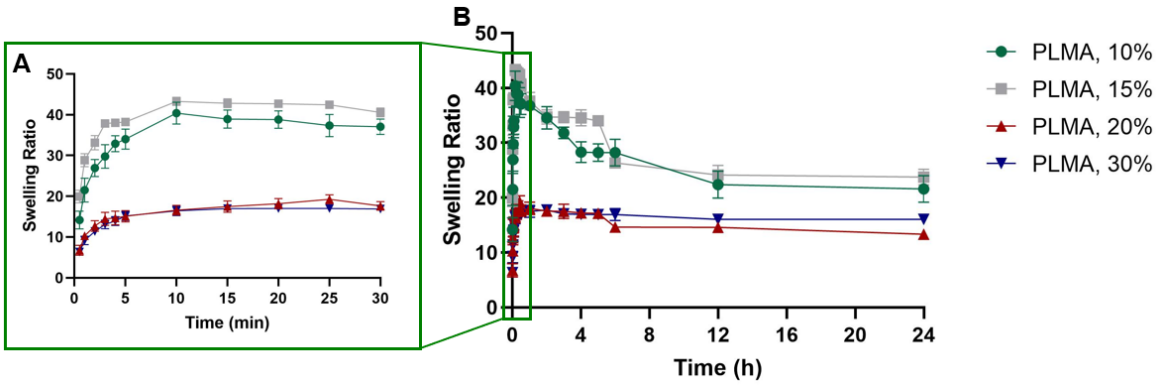

Figure IV.4. (B) Swelling capacity of PLMA-based scaffolds for the conditions of 10%, 15%, 20% and 30% (w/v) of PLMA thought out a period of 24 hours (A) with a close up of the first 30 minutes. Data is presented as mean ± standard deviation (n≥3).

3.2.4 Conductivity

For cardiac patches, conductivity is important feature to analyse due to the need of electrical capacity to produce muscle movement, especially in the cardiac tissue.[21] The measurement of the resistance results in a conductivity value of 3.46×10^{-3} Scm^{-1} for a 20% (w/v) PLMA hydrogel as a preliminary test. These results can be compared with the conductivity value for the human heart of 5.00×10^{-3} Scm^{-1},[22] meaning the values are on the same order of magnitude, which is a positive result since the patches are made from a human origin biomaterial that is not expected to have greater conductivity.

3.2.5 Cardiac patch transportation

Catheters are a commonly used medical equipment and can be used to deliver several substances to the body. Since minimal invasive techniques are an important feature, a rehydrated scaffold of 15% (w/v) PLMA was tested for transportation throughout a catheter

(**Figure IV.5)**. As observed, the scaffold was able to enter and exit the catheter while keeping fully visual integrity after 5 rounds, meaning that presents enough robustness to be delivered by using this method and can potentially prevent the use or more invasive techniques.

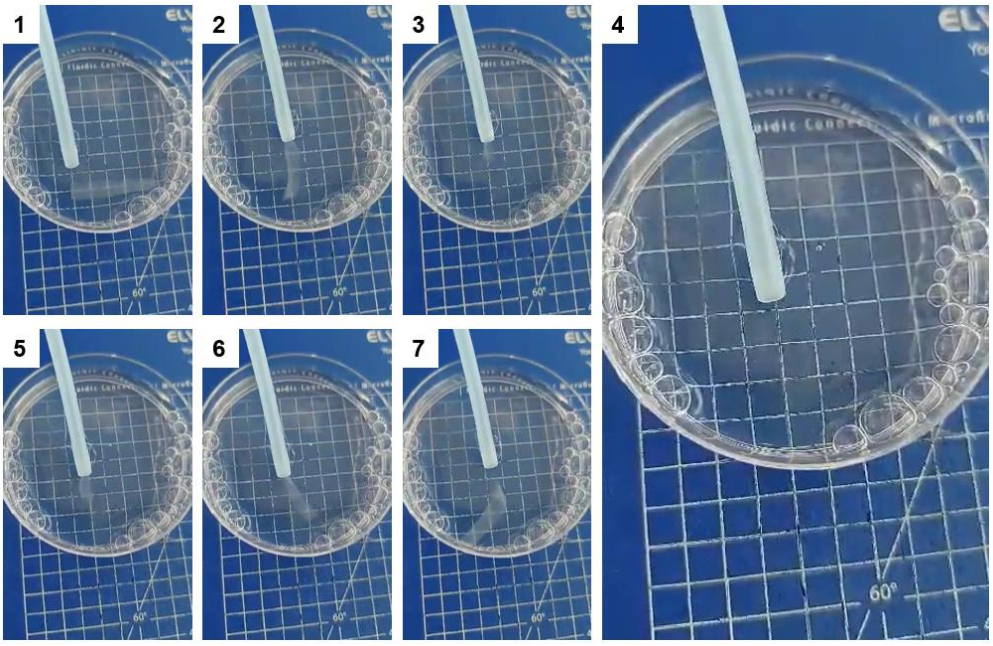

Figure IV.5. Transportation of a 15% (w/v) PLMA rehydrated scaffold with a coronary micro-guide catheter.

3.2 Cell culture

Taking all the previously information, the best performing concentration for cell culture in scaffolds was 15% (w/v) of PLMA due to their mechanical properties and swelling capacity. To assess these scaffolds as potential 3D cell culture platforms and potential application as cardiac patches, a cell assay was performed using HUVECs that are known to promote vascularization of the cardiac tissue.

HUVECs were seeded on the top surface of the hydrogel for 14 days. A live/dead assay was performed at day 3, 7 and 14 days and cell morphology were assessed at 14 days (**Figure IV.6**). The results of the fluorescence microscope showed that cells were able to adhere to the hydrated scaffolds and proliferate, exhibiting high viability and good morphology after 14 days, given the cell elongation by this time.

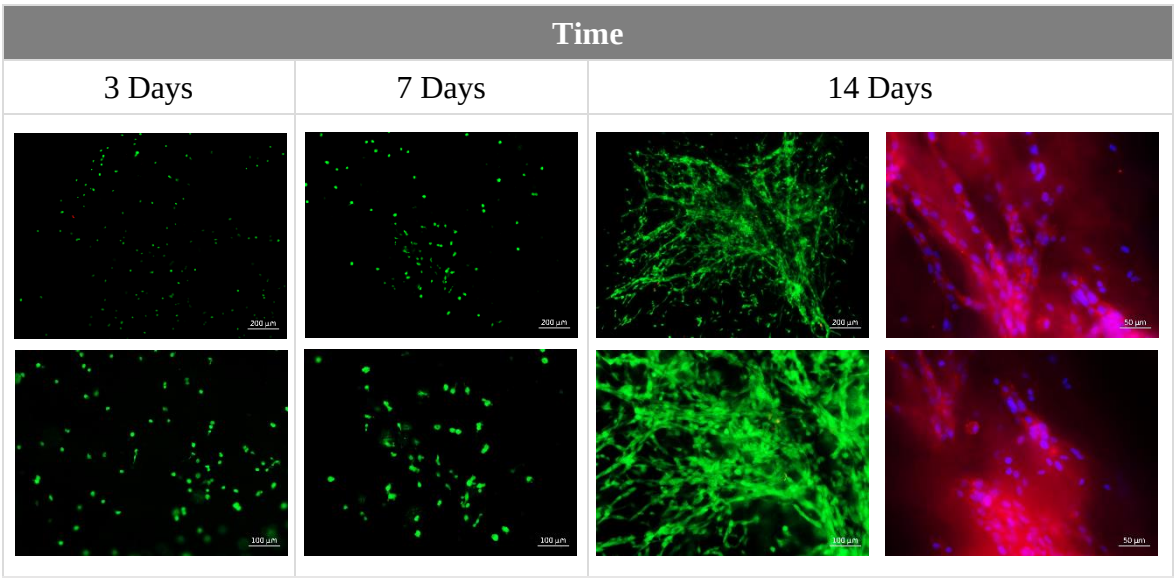

Figure IV.6. Fluorescence microscopy images of live/dead staining of the established HUVECs seeded on the top surface of rehydrated PLMA scaffolds. The green and red channels represent the Calcein-AM and PI staining of live and dead cells, respectively. The blue and red channels at day 14 represents DAPI/Phalloidin staining, respectively.

4. Conclusion

Given the current results for physical and biochemical properties of interest for cardiac application for regeneration after MI, the process of freeze drying can have a positive impact on the mechanical properties of the PLMA hydrogels, rising their stiffness to values close to the normal heart range for the elasticity modulus. This information is completed by the cyclic tensile test which demonstrates the durability of the hydrogels. Also, the scaffolds showed good swelling capability for their porous structure, that was not significantly different throughout all four concentrations of PLMA, a close value of conductivity to the human heart and that they can be transported using catheters. At a cellular level, HUVECs were seeded on the top surface of the rehydrated PLMA scaffolds, showing good adherence and interaction between cells. Comparing these results with the already reviewed conditions to use freeze dried PLMA scaffolds as cardiac patches, we can conclude that freeze drying is a process that can enhance the necessary properties for the use of PLMA hydrogels as a

cardiac patch, not only by their physical properties but also for their capability for cellular seeding with the best performing concentration of 15% (w/v) PLMA. Although, it is necessary to finish the current preliminary tests already mentioned and, furthermore, perform physical tests of degradation and protein release as well as cellular assays with CMs to prove the promising results and certify this strategy to produce better cardiac patches of PLMA.

References

1. Virani, S. S. *et al.* Heart Disease and Stroke Statistics -2020 Update: A Report From the American Heart Association. *Circulation* **141**, e139–e596 (2020).
2. Bui, A. L., Horwich, T. B. & Fonarow, G. C. Epidemiology and risk profile of heart failure. *Nat Rev Cardiol* **8**, 30–41 (2011).
3. Bergmann, O. *et al.* Evidence for cardiomyocyte renewal in humans. *Science (80-.).* **324**, 98–102 (2009).
4. Cohn, J. N., Ferrari, R. & Sharpe, N. Cardiac remodeling--concepts and clinical implications: a consensus paper from an international forum on cardiac remodeling. Behalf of an International Forum on Cardiac Remodeling. *J. Am. Coll. Cardiol.* **35**, 569–582 (2000).
5. Thavandiran, N., Nunes, S. S., Xiao, Y. & Radisic, M. Topological and electrical control of cardiac differentiation and assembly. *Stem Cell Res. Ther.* **4**, 14 (2013).
6. He, L. & Chen, X. Cardiomyocyte Induction and Regeneration for Myocardial Infarction Treatment: Cell Sources and Administration Strategies. *Adv. Healthc. Mater.* **9**, 2001175 (2020).
7. Radisic, M. & Christman, K. L. Materials science and tissue engineering: Repairing the heart. *Mayo Clin. Proc.* **88**, 884–898 (2013).
8. Altaie, A., Owston, H. & Jones, E. Use of platelet lysate for bone regeneration - are we ready for clinical translation? *World J Stem Cells* **8**, 47–55 (2016).
9. Wang, H. & Avila, G. Platelet Rich Plasma: Myth or Reality? *Eur J Dent* **1**, 192–194 (2007).
10. Araki, J. *et al.* Optimized preparation method of platelet-concentrated plasma and noncoagulating platelet-derived factor concentrates: Maximization of platelet concentration and removal of fibrinogen. *Tissue Eng. - Part C Methods* **18**, 176–185

(2012).

11. Gentile, P., Scioli, M. G., Bielli, A., Orlandi, A. & Cervelli, V. The Use of Adipose-Derived Stromal Vascular Fraction Cells and Platelet Rich Plasma in Regenerative Plastic Surgery. *Stem Cells* **35**, 117–134 (2017).
12. Backly, R. El *et al.* Platelet lysate induces in vitro wound healing of human keratinocytes associated with a strong proinflammatory response. *Tissue Eng. - Part A* **17**, 1787–1800 (2011).
13. Picard, F., Hersant, B., Bosc, R. & Meninguad, J.-P. Should we use platelet-rich plasma as an adjunct therapy to treat 'acute wounds', 'burns' and 'laser therapies': a review and a proposal of a quality criteria checklist for further studies. *Wound Repair Regen* **23**, 163–170 (2015).
14. Haleem, A. M. *et al.* The clinical use of human culture-expanded autologous bone marrow mesenchymal stem cells transplanted on platelet-rich fibrin glue in the treatment of articular cartilage defects: A pilot study and preliminary results. *Cartilage* **1**, 253–261 (2010).
15. Santos, S. C., Custódio, C. A. & Mano, J. F. Photopolymerizable Platelet Lysate Hydrogels for Customizable 3D Cell Culture Platforms. *Adv. Healthc. Mater.* **7**, e1800849 (2018).
16. Monteiro, C. F., Custódio, C. A. & Mano, J. F. Bioengineering a humanized 3D tri-culture osteosarcoma model to assess tumor invasiveness and therapy response. *Acta Biomater.* **134**, 204–214 (2021).
17. Monteiro, C. F., Santos, S. C., Custódio, C. A. & Mano, J. F. Human Platelet Lysates-Based Hydrogels: A Novel Personalized 3D Platform for Spheroid Invasion Assessment. *Adv. Sci.* **7**, 1902398 (2020).
18. Qian, L. & Zhang, H. Controlled freezing and freeze drying: A versatile route for porous and micro-/nano-structured materials. *J. Chem. Technol. Biotechnol.* **86**, 172–184 (2011).
19. Handorf, A. M., Zhou, Y., Halanski, M. A. & Li, W. J. Tissue stiffness dictates development, homeostasis, and disease progression. *Organogenesis* **11**, 1–15 (2015).
20. Voigt, J.-U. & Cvijic, M. 2- and 3-Dimensional Myocardial Strain in Cardiac Health and Disease. *JACC Cardiovasc. Imaging* **12**, 1849–1863 (2019).
21. House, A., Atalla, I., Lee, E. J. & Guvendiren, M. Designing Biomaterial Platforms

for Cardiac Tissue and Disease Modeling. *Adv. NanoBiomed Res.* **1**, 2000022 (2020).

22. Sovilj, S., Magjarević, R., Lovell, N. H. & Dokos, S. A simplified 3D model of whole heart electrical activity and 12-lead ECG generation. *Comput. Math. Methods Med.* **2013**, 134208 (2013).

Chapter V

Human platelet lysate-based hydrogels as 3D spheroids culture platforms for cardiac regeneration

* This chapter is based on the following publication:

A. F. Lima, C. F. Monteiro, C. A. Custódio, J. F. Mano, *Human platelet lysate-based hydrogels as 3D spheroids culture platforms for cardiac regeneration*. (manuscript under preparation)

Human platelet lysate-based hydrogels as 3D spheroids culture platforms for cardiac regeneration

Abstract

Cardiac spheroids are three-dimensional (3D) cellular architectures that can better mimic the cardiac environment than monolayer or two-dimensional (2D) approaches. Their incorporation on hydrogels not only supports them but also allows the use of these structures for therapeutic applications and control of their spatial organization on the patch. The purpose of this work is to directly generate cardiomyocytes (CMs) spheroids in specific position on methacryloyl platelet lysates (PLMA) hydrogels using a square feature with size-controlled wells. To optimize this system, MG-63 cells were used since they can easily form spheroids. From a physical point of view, PLMA hydrogels were evaluated for important properties for biomedical application and for the cardiac tissue more specifically. Mechanical properties of the hydrogels showed the increase in the elasticity modulus when increasing the PLMA concentration in the hydrogels. The water content evaluation demonstrated that all PLMA concentration hydrogels had a high content of water and a PLMA hydrogel was intact after holding overnight implanted to a chicken heart at constant rotation, showing a good capacity to resist to the cardiac environment. Using MG-63, the system was able to form spheroids although the system did not work properly due to technical issues. These spheroids were formed in the PLMA hydrogel wells and maintained in culture for 7 days. Besides the need of more information, the results showed that PLMA hydrogels have good characteristics for biomedical and cardiac application and that the optimization of this system can allow the formation of MG-63 spheroids and, potentially, CMs spheroids.

1. Introduction

Spheroids are three-dimensional (3D) culture system with a specialized architecture and cell organization that typically form from a self-assembling process.[1] These structures are significantly different from monolayer approaches in structure, function and morphology and, in case of cardiomyocytes (CMs), also influences cardiac function and maturation[2] to a

point where they become interesting for therapeutical cardiac application.[3] Cardiac spheroids are capable of better recapitulate the biological features of human cardiac tissue and more accurately mimic early-development of the heart than two-dimensional (2D) approaches.[4–7] Their composition allow the use of more than one cell type and can incorporate other types, which helps with the recapitulation of the native tissue[8–10], and their behaviour can be controlled through cell density, medium components and substrate that in contact with them.[11–13] With this, hydrogels are an interesting option not only to support the spheroids but also to delivered their therapeutic capacity to the cardiac tissue.

Platelet lysates (PL) are an autologous source of grown factors, cytokines and several other proteins[14–16] that can locally promote wound[17–19] and tissue healing[20]. This material is obtained by a process of freeze/thaw cycles of platelet concentrates harvest from whole blood. As previously reported, chemically modified PL with methacrylic anhydride (MA) can form hydrogels by covalent photocrosslinking using UV light irradiation in the presence of a photoinitiator.[21] These hydrogels of methacryloyl platelet lysates (PLMA) have good mechanical and biochemical properties, supporting the adhesion and proliferation of encapsulated cells/spheroids while being an animal-free product approach for cell culture and biomedical applications.[22,23]

For the purpose of this work, the goal is to create a cardiac patch with incorporated CMs spheroids in a squared feature using size-controlled wells to evaluate this biomaterial as a 3D culture platform for cardiac spheroids in the treatment of myocardial infarction (MI) events and interesting physical properties of this material for the cardiac tissue use. The first step would be the creation and optimization of a system that allows the formation of spheroids in the hydrogel and then use it with CMs to form the spheroids in the described configuration.

2. Materials and methods

2.1 Synthesis of methacryloyl platelet lysates

As previously reported, PL (STEMCELL Technologies, Canada) stored at -20 ºC and thawed at 37 ºC was chemically modified with methacrylic anhydride 94% (MA) (Sigma-Aldrich, USA) to form methacryloyl platelet lysate (PLMA) of low-degree of

modification (PLMA100) for the purpose of this work.[15] Briefly, the reaction pH was maintained between 6 and 8 using 5 M sodium hydroxide (AkzoNobel, USA) solution, at room temperature (RT) and under constant stirring. The synthetized PLMA100 was then purified by dialysis with Float-A-Lyzer G2 Dialysis Device 3.5-5 kDa (Spectrum, USA) in deionized water for 24 hours, sterilized with a low protein retention 0.2 µm filter (Enzymatic S. A., Portugal), frozen in liquid nitrogen, freeze dried (LyoQuest Plus Eco, Telstar, Spain) and stored at 4 °C.

2.2 PLMA hydrogel formation

The preparation of 10%, 15%, 20% or 30% (w/v) of lyophilized PLMA100 with 0.5% (w/v) 2-hydroxy-4'-(2-hydroxyethoxy)-2-methylpropiophenone (Sigma-Aldrich) in phosphate buffered saline (PBS) (Sigma-Aldrich) create a PLMA precursor solution that was pipetted to polydimethylsiloxane (PDMS) (Dow Corning, USA) molds with different shape and sizes. The hydrogels had an hight of approximately 1 mm and were photopolymerized for 60 seconds of UV exposure at 2.45 w/cm^2 in an 8 cm distance between the solution and the UV lamp. Hydrogels were placed at 4 ºC overnight in 5 mL PBS to achieve maximum absorption capacity and used in this state in all experiments. The shape and sizes of hydrogels used in the different experiments is specified in each one of them bellow.

2.3 PLMA hydrogel characterization

2.3.1 Mechanical properties

PLMA hydrogels was tested using a Universal Mechanical Testing Machine Shimadzu MMT-101N (Shimadzu Scientific Instruments, Kyoto, Japan) equipped with a load cell of 100 N. A unidirectional tensile test was performed at RT on rectangular shaped hydrogels with a length of 2.5 cm, a width of 0.5 cm and using 75 µL of PLMA precursor solution. Samples of all four concentrations, from both freeze dried and non-freeze dried hydrogels, were used with an extension rate of 1 mm/minute. The Young's modulus was defined as the slope of the linear region of the strain/stress curve, corresponding from 0 to

45% strain. Ultimate stress and ultimate strain values were taken as the point where failure of the hydrogel occurred.

2.3.2 Water content

Hydrogels of all concentrations in a circular shape with 0.6 cm in diameter, using 16.9 µL of PLMA precursor solution, where hydrated for 16 hours in 5 mL of deionized water at 4º C and 2 more hours at room temperate before the wet weight (W_w) was measured. After freeze drying of these hydrogels, the dry weight (W_d) was also measure and compared with the initial W_w using the following equation (**Equation 1**) that presents the water content value in percentage:

$$Water\ Content\ (\%) = \frac{W_w - W_d}{W_w} \times 100 \quad \textbf{(Equation 1)}$$

2.3.3 Cardiac patch implantation

A chicken heart, removed at the time of the chicken death and frozen at -20 ºC until defrost for use, was used to attach a square shaped hydrogel with a length and width of 0.5 cm and using 30 µL of solution of 15% (w/v) PLMA precursor solution. The hydrogel was fixed to the heart using 10 µL of the same prepared solution to reticulate the hydrogel pipetted around the limits of this and using the same protocol of photopolimerazation. The heart with the attached hydrogel was then submerse on 50 mL of PBS in a cup and placed at 350 rpm overnight in order to do a preliminary test to the hydrogel integrity but also to the capacity of PLMA to hold the hydrogel to the heart.

2.4 Cell culture

2.4.1 Preparation of micro-well PLMA hydrogels and spheroid encapsulation

MG-63 (European Collection of Authenticated Cell Cultures, ECACC) tumour cell line was cultured in Minimum Essential Medium Alpha (α-MEM, Thermo Fisher Scientific,

USA) supplemented with 2.2 g/L sodium bicarbonate (Sigma-Aldrich), 10% (v/v) heat-inactivated fetal bovine serum (FBS, Thermo Fisher Scientific) and 1% (v/v) antibiotic/antimycotic (Thermo Fisher Scientific) in T-flasks, maintained under 5% CO_2 atmosphere at 37 °C (standard cell culture conditions) and passaged at about 80% confluence. The medium was replaced every 2 to 3 days and cells were detached with 0.25% trypsin/EDTA (Gibco, Thermo Fisher Scientific, USA) and resuspended in the same culture medium for application.

At hydrogel formation, a PDMS mold was used to imprint 100 wells in a 1 cm length and 1 cm width hydrogel using 110 µL of 15% (w/v) PLMA precursor solution. The wells had 500 µm in diameter and 250 µm height arranged in a squared formation of 10 per 10 with a spacing between wells of 500 µm and 250 µm between the external wells and the limit of the hydrogel, respectively. This hydrogel was placed at another PDMS mold to support it for centrifugation at 500 G for 10 minutes with a MG-63 cell suspension of 150 µL containing 100 000 cells. This process is used to distribute in the most equally way the cells through all the wells in other to obtain 10 000 cells/well, approximately. The hydrogel culture was maintained for 7 days also in the described medium.

2.4.2 Cell viability

The MG-63 spheroids, the live/dead assay was performed after 7 days in culture, in a solution of 1:500 of Calcein AM 4mM solution in dimethyl sulfoxide (DMSO) (Life Technologies, Thermo Fisher Scientific) and 1:1000 of 1 mg/mL PI (Thermo Fisher Scientific) in PBS at standard cell culture conditions (5% CO_2 at 37 °C) for 1 hour, with the next steps being the same as the mentioned above. After three times washing with PBS, the samples were observed under a fluorescence microscope (Fluorescence Microscope Zeiss, Axio Imager 2, Zeiss, Germany), maintaining the same imaging parameters throughout all samples.

2.5 Statistical analysis

All data were statistically analysed using the GraphPah Prism 8.4.2 software and, except for the preliminary tests, are expressed as mean ± standard deviation of at least 3 independent experiments. Statistical significance of unidirectional tensile test and water

content was determined using one-way ANOVA analysis with Tukey's multiple comparison test.

3. Results and discussion

3.1 Hydrogel formation

To fulfil the necessary dimensions of the hydrogel for 3D cell culture platform of cardiomyocyte spheroids and assess this patch for cardiac regeneration, a system of PDMS mold was created to photopolymerize the hydrogel with a specific well topography and to sustain it during centrifugation. During the process of optimization, the appropriate quantity of solution of PLMA with photoinitiator in PBS was found to be 110 µL for the dimension already mentioned.

3.2 PLMA hydrogel characterization

3.2.1 Mechanical properties

The mechanical properties of the hydrogel are one of the important parameters of this complex structure. Since our goal is the cardiac tissue, elasticity takes a central role at the mechanical properties. With this, a unidirectional tensile test was performed on PLMA-based hydrogels of different concentrations (**Figure V.1**).

The main measure is their elasticity modulus, or Young's modulus (**Figure V.1A**), in which an increasing profile was observed throughout the concentrations with a significative increase at 20% and 30% (w/v) PLMA when compared with the close values of 10% and 15% (w/v). These results shown the increase of stiffness alongside the increase of PLMA concentration on the hydrogels. For the ultimate stress (**Figure V.1B**), the same profile is observed between the concentration and supports the information obtained using the elasticity modulus. For last, on the ultimate strain (**Figure V.1C**), the profile has two important parts. From the values of 10% to 15% (w/v), there is an increase in the ultimate strain which indicates that the increased stiffness has a positive effect on increasing the strain that hydrogels can support. At 20%, the value is not significantly different from the 15%

value and the 30% is not significantly different from the 10% (w/v) value, showing that the increasing in stiffness can potentiate a decrease in ultimate strain capacity. These results proved that the concentration of PLMA on hydrogels can have effects on their elasticity properties.

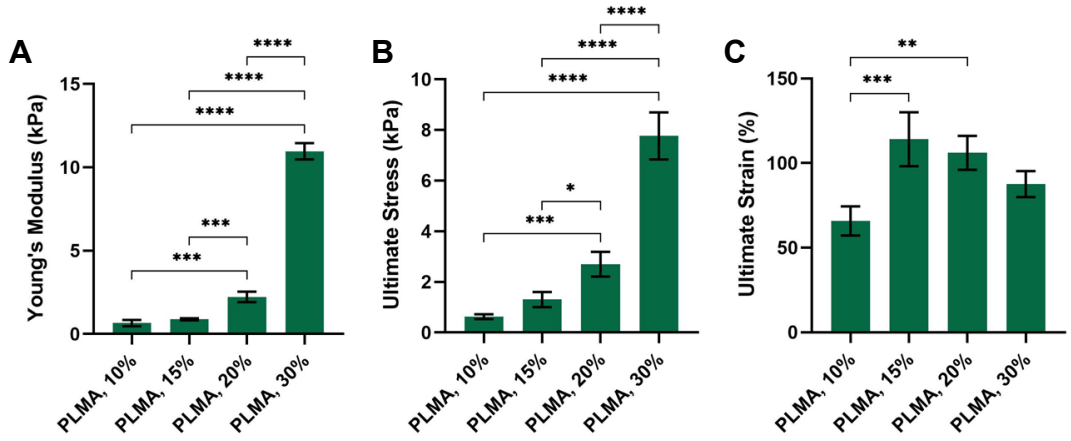

Figure V.1. (A) Young's modulus, (B) ultimate stress and (C) ultimate strain obtained for PLMA hydrogels at 10%, 15%, 20% and 30% (w/v). Statistical analysis through two-way ANOVA with Tukey's multiple comparison test (*$p<0.05$, **$p<0.005$, ***$p<0.0005$, ****$p<0.0001$). Data is presented as mean ± standard deviation ($n\geq3$).

3.2.2 Water content

Water is normally present in high quantities on hydrogels and it is an important aspect to quantify. In the case of all four concentration, all showed high values of water content above 90% (**Figure V.2**), with significant differences observed between all concentrations except for 10% and 15% (w/v) PLMA hydrogels.

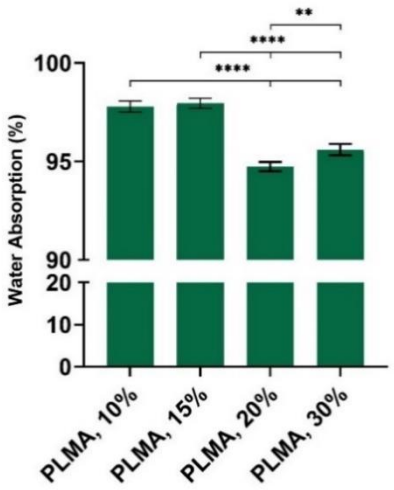

Figure V.2. Water absorption capacity of PLMA-based hydrogels of 10%, 15%, 20% and 30% PLMA after 16 hours. Statistical analysis through one-way ANOVA with Tukey's multiple comparison test. (**p<0.005, ****p<0.0001). Data is presented as mean ± standard deviation (n≥3).

3.2.3 Cardiac patch implantation

To try to reassemble a cardiac patch implantation and test the ability of PLMA to graft it to the heart, a chicken heart and a 15% (w/v) PLMA hydrogel were used (**Figure V.3**). After the implantation on the chicken heart and overnight rotation, the patch still attached to the heart and in full integrity meaning that PLMA hydrogels are capable of resisting to such environment and that PLMA can fix the patch onto the cardiac tissue and support it in the same environment.

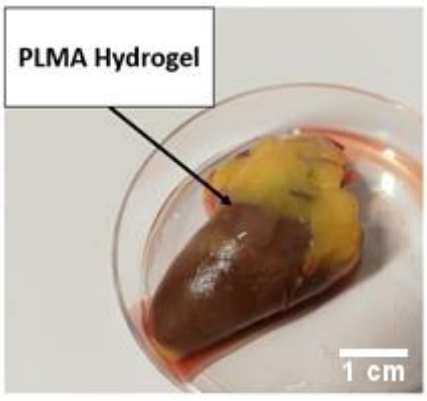

Figure V.3. 15% (w/v) PLMA hydrogel grafted with PLMA to a chicken heart.

3.2 Cell culture

To test if the created system was able to produce spheroids within the PLMA hydrogel and with centrifugation of a cell suspension, MG-63 cells were used as they are a cell line can easily form spheroids. The centrifugation system did not work perfectly as expected since the hydrogel moved out during centrifugation. However, as MG-63 cells were deposited inside some wells, we proceed with the experiment. After 7 days in culture, the live/dead assay confirmed the formation of spheroids within the wells (**Figure V.3**), although some cells that do not aggregate on the spheroid were dead. Also, almost no cells were at the top of the hydrogel which indicates that optimization of this process might work to distribute the cells within the wells.

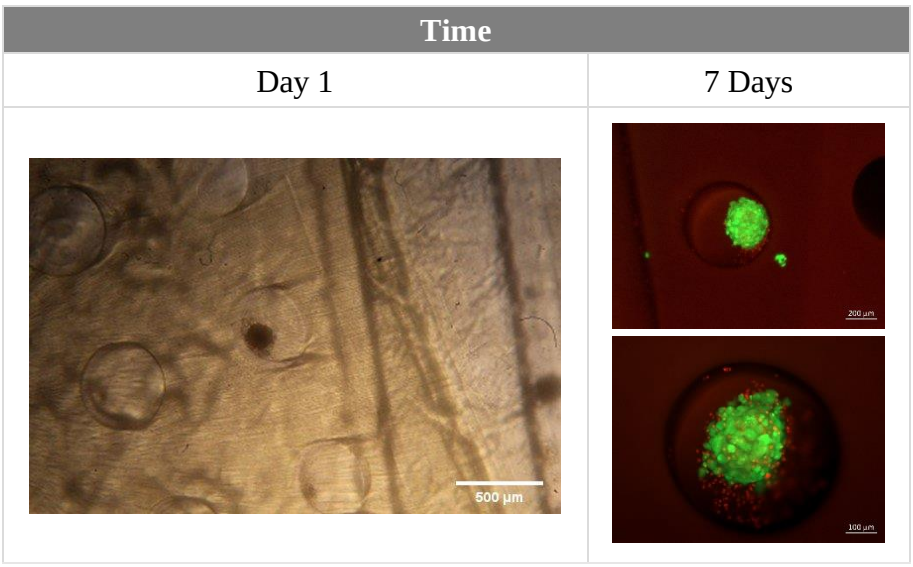

Figure V.4. Fluorescence microscopy images of live/dead staining of the established MG-63 spheroids on the 15% (w/v) PLMA hydrogel. The green and red channels represent the Calcein-AM and PI staining of live and dead cells, respectively.

4. Conclusion

Taking in consideration the physical results, mechanical properties of PLMA hydrogels increase when PLMA concentration is increased which allow to choose the needed concentration in function of the needed Young's modulus. Also, hydrogels have a high content in water, no matter the given PLMA concentration. These two factors indicate that

the mechanical properties of hydrogels can be modulated but the water content remains high, which are two important factors for cardiac patches. The ability of this hydrogels to be grafted with PLMA to heart tissue and be able to be keep his integrity after overnight rotation is also promising for their resistance to the cardiac environment. In the cellular assay, the goal of proving that the system could form spheroids using centrifugation was partially achieve since the system worked but needs more improvement to fully form the proposed spheroids.

In resume, the results already obtained are promising but the key process is to optimize the system to form spheroids within the hydrogel. After this, the spheroids behaviour and adaption can be monitored and that information used to form CM spheroids for cardiac patch application of MI regeneration.

References

1. Mazzola, M. & Di Pasquale, E. Toward Cardiac Regeneration: Combination of Pluripotent Stem Cell-Based Therapies and Bioengineering Strategies. *Front. Bioeng. Biotechnol.* **8**, 455 (2020).
2. Soares, C. P. *et al.* 2D and 3D-organized cardiac cells shows differences in cellular morphology, adhesion junctions, presence of myofibrils and protein expression. *PLoS One* **7**, e38147 (2012).
3. Edmondson, R., Broglie, J. J., Adcock, A. F. & Yang, L. Three-dimensional cell culture systems and their applications in drug discovery and cell-based biosensors. *Assay Drug Dev. Technol.* **12**, 207–218 (2014).
4. Richards, D. J. *et al.* Inspiration from heart development: Biomimetic development of functional human cardiac organoids. *Biomaterials* **142**, 112–123 (2017).
5. Tan, Y. *et al.* Cell number per spheroid and electrical conductivity of nanowires influence the function of silicon nanowired human cardiac spheroids. *Acta Biomater.* **51**, 495–504 (2017).
6. Nguyen, D. C. *et al.* Microscale generation of cardiospheres promotes robust enrichment of cardiomyocytes derived from human pluripotent stem cells. *Stem cell reports* **3**, 260–268 (2014).
7. Correia, C. *et al.* 3D aggregate culture improves metabolic maturation of human

pluripotent stem cell derived cardiomyocytes. *Biotechnol. Bioeng.* **115**, 630–644 (2018).

8. Polonchuk, L. *et al.* Cardiac spheroids as promising in vitro models to study the human heart microenvironment. *Sci. Rep.* **7**, 7005 (2017).
9. Hoang, P., Wang, J., Conklin, B. R., Healy, K. E. & Ma, Z. Generation of spatial-patterned early-developing cardiac organoids using human pluripotent stem cells. *Nat. Protoc.* **13**, 723–737 (2018).
10. Yan, Y. *et al.* Cell population balance of cardiovascular spheroids derived from human induced pluripotent stem cells. *Sci. Rep.* **9**, 1295 (2019).
11. Birket, M. J. *et al.* Expansion and patterning of cardiovascular progenitors derived from human pluripotent stem cells. *Nat. Biotechnol.* **33**, 970–979 (2015).
12. Song, L. *et al.* PCL-PDMS-PCL Copolymer-Based Microspheres Mediate Cardiovascular Differentiation from Embryonic Stem Cells. *Tissue Eng. Part C. Methods* **23**, 627–640 (2017).
13. Palpant, N. J. *et al.* Generating high-purity cardiac and endothelial derivatives from patterned mesoderm using human pluripotent stem cells. *Nat. Protoc.* **12**, 15–31 (2017).
14. Altaie, A., Owston, H. & Jones, E. Use of platelet lysate for bone regeneration - are we ready for clinical translation? *World J Stem Cells* **8**, 47–55 (2016).
15. Wang, H. & Avila, G. Platelet Rich Plasma: Myth or Reality? *Eur J Dent* **1**, 192–194 (2007).
16. Araki, J. *et al.* Optimized preparation method of platelet-concentrated plasma and noncoagulating platelet-derived factor concentrates: Maximization of platelet concentration and removal of fibrinogen. *Tissue Eng. - Part C Methods* **18**, 176–185 (2012).
17. Gentile, P., Scioli, M. G., Bielli, A., Orlandi, A. & Cervelli, V. The Use of Adipose-Derived Stromal Vascular Fraction Cells and Platelet Rich Plasma in Regenerative Plastic Surgery. *Stem Cells* **35**, 117–134 (2017).
18. Backly, R. El *et al.* Platelet lysate induces in vitro wound healing of human keratinocytes associated with a strong proinflammatory response. *Tissue Eng. - Part A* **17**, 1787–1800 (2011).
19. Picard, F., Hersant, B., Bosc, R. & Meninguad, J.-P. Should we use platelet-rich

plasma as an adjunct therapy to treat ‘acute wounds’, ‘burns’ and ‘laser therapies’: a review and a proposal of a quality criteria checklist for further studies. *Wound Repair Regen* **23**, 163–170 (2015).

20. Haleem, A. M. *et al.* The clinical use of human culture-expanded autologous bone marrow mesenchymal stem cells transplanted on platelet-rich fibrin glue in the treatment of articular cartilage defects: A pilot study and preliminary results. *Cartilage* **1**, 253–261 (2010).
21. Santos, S. C., Custódio, C. A. & Mano, J. F. Photopolymerizable Platelet Lysate Hydrogels for Customizable 3D Cell Culture Platforms. *Adv. Healthc. Mater.* **7**, e1800849 (2018).
22. Monteiro, C. F., Custódio, C. A. & Mano, J. F. Bioengineering a humanized 3D tri-culture osteosarcoma model to assess tumor invasiveness and therapy response. *Acta Biomater.* **134**, 204–214 (2021).
23. Monteiro, C. F., Santos, S. C., Custódio, C. A. & Mano, J. F. Human Platelet Lysates-Based Hydrogels: A Novel Personalized 3D Platform for Spheroid Invasion Assessment. *Adv. Sci.* **7**, 1902398 (2020).

Chapter VI

Conclusions and Future Perspectives

Conclusions and Future Perspectives

Cardiac tissue engineering (TE) differs from other strategies because their focus is not to minimize damage but to revert and regenerate the cardiac tissue. On this master thesis, we present two different approaches in order to create two different cardiac patches. One acellular approach created from the freeze drying process and other cellular approach using spheroids incorporated onto the patch. Both strategies have different limitations and benefits, but both biomaterial approval for these two situations would mean that methacryloyl platelet lysates (PLMA)-based hydrogels can be an efficient cardiac patch biomaterial for cardiac regeneration post-myocardial infarction (MI).

On the acellular approach, the freeze drying process had an impact on the mechanical properties of the hydrogel, increasing their capability to mimic the human heart stiffness and durability. These results, together with the swelling, conductivity and transportation on catheter results showed that freeze drying PLMA hydrogels can have a positive impact to achieve physical conditions closer to the original tissue and the theoretical ideals of what a patch might have. The cellular assays confirmed that rehydrated PLMA scaffolds can support the adhesion and proliferation of human umbilical vein endothelial cells (HUVECs), making them a promising three-dimensional (3D) cell culture platform. At the cellular approach, the tests performed with this type of hydrogel follow the same line of the work before, searching to know the essential characteristics of hydrogels for cardiac application. Although the system is not optimized, MG-63 cells were able to form spheroids.

In both cases it is important to choose the right PLMA concentration for the purpose. In the first study, 15% (w/v) PLMA hydrogels were the best performing concentration when having in count the mechanical properties, swelling capacity and catheter transportation. On the second study, the information given chooses the 30% (w/v) PLMA hydrogels based on the better mechanical properties. More tests for physical properties would help us to support the already obtained data and would allow to proceed for cell assays with cardiomyocytes (CMs). In resume, PLMA hydrogels and scaffolds are promising platforms for cardiac regeneration, assigning this biomaterial for cardiac application as an innovate alternative to common biomaterials.